



**Synthesis of Dopamine/Serotonin Receptor Ligands in Dual
Dopamine/Serotonin-Molecularly Imprinted Polymer Nanovessel**

Wanpen Naklua

**A Thesis Submitted in Partial Fulfillment of the Requirements for
the Degree of Doctor of Philosophy in Pharmaceutical Sciences**

Prince of Songkla University

2015

Copyright of Prince of Songkla University

Thesis Title Synthesis of Dopamine/Serotonin Receptor Ligands in Dual
Dopamine/Serotonin-Molecularly Imprinted Polymer Nanovessel

Author Miss Wanpen Naklua

Major Program Pharmaceutical Science

Major advisor

.....Chairperson
(Assoc. Prof. Dr. Roongnapa Srichana)

Examining Committee :

.....Committee
(Assoc. Prof. Dr. Wantana Reanmongkol)

..... Committee
(Assoc. Prof. Dr. Anuchit Plubrukarn)

..... Committee
(Dr. Neeranuch Phusunti)

..... Committee
(Prof. Dr. Peter Lieberzeit)

The Graduate School, Prince of Songkla University, has approved this
thesis as partial fulfillment of the requirements for the Doctor of Philosophy in
Pharmaceutical Sciences.

.....
(Assoc. Prof. Dr. Teerapol Srichana)

Dean of Graduate School

This is to certify that the work here submitted is the result of the candidate's own investigations. Due acknowledgement has been made of any assistance received.

.....Signature

(Assoc. Prof. Dr. Roongnapa Srichana)

Major Advisor

.....Signature

(Miss Wanpen Naklua)

Candidate

I hereby certify that this work has not been accepted in substance for any degree, and is not being currently submitted in candidature for any degree.

.....Signature

(Miss Wanpen Naklua)

Candidate

ชื่อวิทยานิพนธ์	การสังเคราะห์สารลิแกนด์ต่อโตนามีนและซีโรโตนินรีเซพเตอร์ในเบ้านาโนพอลิเมอร์ที่พิมพ์ ประทับด้วยโตนามีนและซีโรโตนิน
ผู้เขียน	นางสาววันเพ็ญ นาเกลือ
สาขาวิชา	เภสัชศาสตร์
ปีการศึกษา	2558

บทคัดย่อ

โตนามีนและซีโรโตนินรีเซพเตอร์เป็นโปรตีนที่สำคัญในการพัฒนาที่ใช้ในการรักษาโรคจิตเภท ในการศึกษานี้ได้ทำการสังเคราะห์พอลิเมอร์ที่มีรอยพิมพ์ประทับและนำไปใช้เสมือนโตนามีนและซีโรโตนินรีเซพเตอร์ ซึ่งเป็นเป้าหมายของยาโรคจิตเภท โดยหมู่ฟังก์ชันและรูปร่างในรอยพิมพ์ประทับด้วยโตนามีน หรือโตนามีนและซีโรโตนิน ในเบ้านาโนพอลิเมอร์ช่วยให้ปฏิกริยาระหว่างสารประกอบคลอโรบิฟิโรฟิโนกับสารประกอบเอมีนเกิดขึ้นที่แอคทิฟไซต์ของรอยพิมพ์และความสามารถในการจับของสารสังเคราะห์ที่ได้ถูกนำไปทดสอบกับโตนามีน (ดี1) รีเซพเตอร์ ให้ค่าคงที่การแตกตัวที่ 141-558 นาโนโมลาร์ มากกว่านั้นสารอนุพันธ์ของคลอซาปีนที่สังเคราะห์จากสารประกอบแอซิดคลอไรด์ที่มีหมู่แทนที่เมทอกซีอยู่ตรงตำแหน่งที่ 2 และ 3 ของเบนซีนก็สามารถสังเคราะห์ได้จากเบ้านาโนนี้แต่ไม่พบในปฏิกริยาควบคุม จากการใช้คอมพิวเตอร์จำลองการจับกันของลิแกนด์กับโตนามีน (ดี3) และซีโรโตนิน (2บี) รีเซพเตอร์ สารผลิตภัณฑ์จากเบ้านาโนพอลิเมอร์แสดงการจับและค่าพลังงานอิสระใกล้เคียงกับค่าที่ได้จากยาโรคจิตเภทที่รู้จักกันดี ดังนั้นเบ้านาโนพอลิเมอร์ที่มีรอยพิมพ์ประทับสามารถนำไปสังเคราะห์สารที่มีหมู่ฟังก์ชันและฤทธิ์ทางชีวภาพสอดคล้องกับสารที่เป็นแม่พิมพ์ นอกจากนี้พอลิเมอร์ที่พิมพ์ประทับด้วยโตนามีน หรือโตนามีนและซีโรโตนินยังถูกนำไปใช้เพื่อศึกษาการเปลี่ยนแปลงพลังงานการเปลี่ยนแปลงพลูออเรสเซนซ์ของยาเมื่ออยู่ในเบ้าพอลิเมอร์ในสถานะที่แตกต่างของอุณหภูมิ ปริมาณสังกะสี (2+) ทั้งที่มีหรือไม่มีโปรตีนจากสมองหนูส่วนไฮโปทาลามัส ซึ่งการจับของคลอซาปีนบนตำแหน่งของการจับยาของรีเซพเตอร์ธรรมชาติมีบทบาทสำคัญต่อกลไกการออกฤทธิ์ของยาซึ่งอาจจะทำให้เกิดความเข้าใจรีเซพเตอร์ที่แสดงผลการเกิด

ความจำเพาะต่อโมเลกุลในการทำหน้าทีในสมองและสามารถบอกความแตกต่างของยาได้อย่างชัดเจน นอกจากนี้ได้ทำการสังเคราะห์พอลิเมอร์ที่พิมพ์ประทับด้วยโดปามีน (ดี1) รีเซพเตอร์ ที่แยกจากสมองหนู เพื่อเคลือบบนอิเล็กโทรดของควอตซ์คริสตัลไมโครบาลานซ์เซ็นเซอร์ จากการวัดโดยเซ็นเซอร์ที่มีการเลียนแบบรูปร่างสามมิติของรีเซพเตอร์นี้ ส่งผลในการตอบสนองต่อสัญญาณความถี่ของโดปามีน (ดี1) รีเซพเตอร์ที่ความแตกต่างของความเข้มข้นของ โดปามีน (ดี1) รีเซพเตอร์ ในช่วง 5.9 ถึง 47.2 ไมโครโมลาร์ สำหรับการตรวจวัดโดยเซ็นเซอร์นี้ โดปามีน (ดี1) รีเซพเตอร์ที่จับอยู่กับพอลิเมอร์ ถูกนำไปใช้เพื่อทดสอบการจับกันของสารลิแกนด์ต่อโดปามีน (ดี1) รีเซพเตอร์ ได้แก่ โดปามีนไฮโดรคลอไรด์ ฮาโรเปอริดอล และ เอสซีเอส 23390 สามารถนำไปคำนวณค่าความเข้มข้นต่ำสุดที่สามารถจับกับรีเซพเตอร์ได้กึ่งหนึ่งของแต่ละสาร ได้ค่าสัมพรรคภาพ 517 ไมโครโมลาร์ 1.90 ไมโครโมลาร์ และ 0.283 นาโนโมลาร์ ตามลำดับ ยังสามารถนำไปพิจารณาความสามารถในการจับของสารเหล่านี้กับโปรตีนบนพอลิเมอร์สามารถสรุปได้ว่า ข้อดีของการใช้พอลิเมอร์ที่มีรอยพิมพ์ประทับที่เตรียมสำหรับ แอคทิฟไซต์ของโดปามีนและซีโรโตนินรีเซพเตอร์และการใช้เทคนิคการยึดโครงสร้างสามมิติของรีเซพเตอร์บนผิวสัมผัสดูดซับให้คุณสมบัติการเลือก ความจำเพาะสูง และการนำมาใช้ใหม่

Thesis Title	Synthesis of Dopamine/Serotonin Receptor Ligands in Dual Dopamine/Serotonin-Molecularly Imprinted Polymer Nanovessel
Author	Miss Wanpen Naklua
Major Program	Pharmaceutical Science
Academic Year	2015

Abstract

Dopamine and serotonin receptors are two of the important proteins involved in the development of antipsychotic agents. In this study, artificial molecularly imprinted polymers (MIPs) were prepared and applied as dopamine/serotonin receptor that could be targeted as antipsychotic drug receptors based on the use of either a single dopamine (D-MIP) or a dual dopamine/serotonin-molecularly imprinted polymer (DS-MIP). In the MIP cavity, the coupling reaction of the molecules for a nucleophilic reaction between chlorobutyrophenone and amine compounds occurred. The binding affinity of the synthesized compounds, K_d , were determined using a competitive binding assay with a dopamine (D_1) receptor (D_1R) that gave a value of 141-558 nM. In addition, the clozapine derivatives archived from the *meta*- and *ortho*-monomethoxy substituted acid chloride and hydrazine could be synthesized only within these MIP nanovessels. This was not observed in the control polymer. For the molecular docking, the binding affinity of the four chlorobutyrophenone derivatives and two hydrazinoclozapine for the dopamine (D_3) and serotonin ($5HT_{1B}$) receptors were closely related to the $-\log K_d$ and the Gibb free energy of the binding protein for these known compounds. Highly crosslinked chains

were produced that induced the chemical reaction inside the binding site of the imprint cavity, containing the biologically relevant functionalities and affinity according to the original template. Furthermore, the imprinted cavity of both the MIPs could be used for measuring the kinetic energy of a fluorescent quencher within the imprint cavity when clozapine which is a dopamine antagonist fitted into the surface pores of the MIPs on the surface. At a different temperatures and in the presence of Zn(II), clozapine on the surface of MIPs exhibited different fluorescent behavior with or without the hypothalamus receptor. The binding of clozapine to the binding site of the artificial receptor played a major role to analyse the diverse mechanisms of action of the drug and make it possible to have a better understanding of receptor by the manipulation of specific molecular interactions in the MIP and for the function of the neural system. In addition, the MIP for recognition of the D₁R were produced on a quartz crystal microbalance (QCM) electrode using the D₁R as a template on the poly(acrylic acid-*N*-vinylpyrrolidone-dihydroxyethylene-bisacrylamide) layer. Measurements from the QCM sensor, resulted in the immobilization of a three dimensional D₁R frequency response of D₁R upon exposure to the D₁R-MIP in the concentration range of 5.9 to 47.2 μ M. For the receptor ligand binding assay, the EC_{50} for dopamine HCl, haloperidol, and (+)-SCH23390 at 517 μ M, 1.90 μ M and 0.283 nM, respectively, were formed and this helper to identify the binding affinity for these compound on the surface immobilized proteins as the result of the surface chemistry of the chemical functionality of the MIP layer. In summary, MIPs were successfully prepared for both the active site of the dopamine and serotonin receptors and the surface immobilized D₁R polymer that was highly useful for screening for the selectivity, specificity and reusability of the binding ligand.

ACKNOWLEDGEMENT

The work and thesis of Ph.D. were successfully prepared by the result of cooperation with many people. First of all, I would like to express my sincere thanks to my advisor, Assoc. Prof. Dr. Roongnapa Srichana, Faculty of Pharmaceutical Sciences, Prince of Songkla University, who supports me everything such as research methodologies, inspiration and positive thinking in my Ph.D. study period. This thesis would not have been completed without her teaching and advice. Second, I am deeply indebted to Prof. Dr. Peter Lieberzeit for academic knowledge, suggestion, writing manuscript on sensor and all his help when I worked at Department of Analytical Chemistry, Faculty of Chemistry, University of Vienna. Next, I would like to gratefully thank to Prof. Dr. Chen Yu Zhong and Chen Shangying, Department of Pharmacy, National University of Singapore who helped in computer modeling. I extend my thank to Assoc. Prof. Dr. Wantana Reanmongkol, Assoc. Prof. Dr. Anuchit Plubrukarn, Faculty of Pharmaceutical Sciences, and Dr. Neeranuch phusunti, Faculty of Science for suggestions about my thesis and Dr. Brian Hodgson for assistance with English. Also go to all staff from Prince of Songkla University for always supporting me.

I would like to thank (1) Molecular Recognition Materials Research Unit; (2) Department of Pharmaceutical Chemistry; (3) Drug Delivery System Excellence Center, and NANOTEC Center of Excellence, Faculty of Pharmaceutical Sciences, Prince of Songkla University; (4) Bioinformatics and Drug Design Group, Department of Pharmacy, National University of Singapore and (5) Department of

Analytical Chemistry, Faculty of Chemistry, University of Vienna, for supporting facilities.

In addition, I recognize that research would not be possible without the financial assistance. For granting financial support, I would like to acknowledge (1) the Strategic Scholarships Fellowships Frontier Research Networks (Specific for the Southern region, Office of the Higher Education Commission; (2) the Graduate School, Prince of Songkla University; (3) the ASEAN European Academic University Network (ASEA-UNINET) and (4) Faculty of Pharmaceutical Science, Prince of Songkla University. The grant of thesis included of thesis fund, salary and conference scholarship throughout a very long period of study.

The author alone assumes responsibility for discussion and conclusions of this thesis and any errors of it may contain.

Lastly, the most special thanks go to all readers.

Wanpen Naklua

CONTENTS

Approval page	ii
Certificate of original work	iii
Certificate of thesis for submit Ph.D. degree	iv
บทคัดย่อ	v
Abstract	vii
Acknowledgement	ix
Contents	xi
List of tables	xiii
List of figures	xiv
List of abbreviations and symbols	xvi
List of papers and proceeding	xviii
Reprints were made with permission from the publishers	xix
CHAPTER 1 General introduction & review literatures	1
CHAPTER 2 Objectives	19
CHAPTER 3 Significant results and discussion	22
CHAPTER 4 Conclusion	41
References	43
Appendices	56
Reprints of papers, manuscript and proceeding	57
Paper 1	58
Paper 2	79
Manuscript 3	96

CONTENTS (continued)

Proceeding 4	126
Vitae	131

LIST OF TABLES

Table 1	Characteristics of synthesized polymers.	23
Table 2	The precursor amines and resulting components of the mold reaction.	27
Table 3	Summary of synthesis of clozapine derivatives from the reaction between hydrazinoclozapine and various acid chlorides in the MIP nanovessel	30
Table 4	Predicted binding affinity of dopamine and serotonin receptor to various ligands by Surflex-DOCK and SVM.	33
Table 5	Biological activity of chlorobutyrophenone derivatives for D ₁ R ($R^2 > 0.990$).	35
Table 6	B_{max} , K_d and EC_{50} values for each compound were calculated by Sigma plot.	40

LIST OF FIGURES

- Figure 1** Illustration of generation of molecularly imprinted polymer formation of complexation between monomers and template (1), polymerization of functional monomers with cross-linkers around the template (2), and template removal, formation of the complementary binding sites (3). 4
- Figure 2** The principle of direct molding, two fragments bind at MIP cavities and it accelerates the covalent bond formation between the two fragments with the highest affinity. 6
- Figure 3** The structure of atypical antipsychotic drugs. 8
- Figure 4** Schematic view of a piezoelectric QCM crystal. 15
- Figure 5** Epitope approach to synthesize MIP film for the detection of human immunodeficiency virus type 1 related protein glycoprotein 41. 15
- Figure 6** Modeling of biological receptors, D₃ receptor (PDB ID: 3PBL) and 5HT_{1b} (PDB ID: 4IAR) receptor for (A) butyrophenone derivatives, *1a-5a*, and (B) clozapine derivatives, *7b* and *8b*. 31
- Figure 7** Fluorescence emission spectra of the clozapine in the presence of methacryloyl chloride and AIBN for D-MIP, DS-MIP and control polymer at excitation wavelength 341 nm. 36

LIST OF FIGURES (continued)

- Figure 8** The effect of temperature on fluorescent spectra ($\lambda_{\text{ex}} = 340 \text{ nm}$) of clozapine in the solution for MIPs and NIP in the presence of methacryloyl chloride; (A) without Zn(II), (B) with Zn(II), (C) the addition of protein (200 μg) without Zn(II), and (D) with Zn(II). 37
- Figure 9** Sensor signals for MIP and NIP containing different amounts of D₁R in PBS buffer. 39

LIST OF ABBREVIATIONS AND SYMBOLS

AA	acrylic acid
ACM	acrylamide
AFM	atomic force microscopy
AIBN	2,2'-azobis-(isobutyronitrile)
BET	Brunauer- Emmett-Teller
BJH	Barrett-Joyner-Halenda
BSA	bovine serum albumin
D ₁ R	dopamine (D ₁) receptor
D-MIP	dopamine imprinted polymer
DHEBA	<i>N,N'</i> -(1,2-dihydroxy-ethylene)-bis-acrylamide
DS-MIP	dual dopamine/serotonin imprinted polymer
ICP-OES	inductively coupled plasma-atomic emission spectroscopy
k_b	Boltzmann constant, 1.380×10^{-23} J/K
K_d	dissociation constant
K_i	binding affinity
MAA	methacrylic acid
MBAA	<i>N,N'</i> -methylene bisacrylamide
MIP	molecularly imprinted polymer
NIP	non-imprinted polymer
NVP	<i>N</i> -vinylpyrrolidone
PBS	Phosphate-buffered saline
PDB	protein data bank

LIST OF ABBREVIATIONS AND SYMBOLS (continued)

QCM	Quartz Crystal Microbalance
SEM	scanning electron microscopy
SVM	Support Vector Machine

LIST OF PAPERS AND PROCEEDING

This thesis is based on the following papers, referred to their order of experimental design in the text. The publications are attached as appendices at the end of the thesis. Reprinted are published with kind permission of respective journals.

Paper 1 Naklua, W., Mahesh, K., Aundorn, P., Tanmanee, N., Aenukulpong, K., Sutto, S., Chen, Y. Z., Chen, S. and Suedee, R., 2015. An imprinted dopamine receptor for discovery of highly potent and selective D₃ analogues with neuroprotective effects. *Process Biochemistry* 50: 1537-1556.

Impact Factor (2015): 2.516 /5-Year Impact Factor: 2.909

Paper 2 Naklua, W., Mahesh, K., Chen, Y. Z., Chen, S. and Suedee, R., 2016. Molecularly imprinted polymer microprobes for manipulating neurological function by regulating temperature-dependent molecular interactions. *Process Biochemistry* 51: 142-157.

Impact Factor (2015): 2.516 /5-Year Impact Factor: 2.909

Proceeding 1 Naklua, W. and Suedee, R., 2012. Synthesis of the dopamine analogs in molecularly imprinted polymer nanovessel. The 2nd Current Drug Development International Conference (CDD2012), 2nd - 4th May 2012, Phuket, Thailand.

**REPRINTS WERE MADE WITH PERMISSION FROM THE
PUBLISHERS**

Author: Naklua, W., Mahesh, K., Aundorn, P., Tanmanee, N., Aenukulpong,
K., Sutto, S., Chen, Y. Z., Chen, S. and Suedee, R.

Title: An imprinted dopamine receptor for discovery of highly potent and
selective D₃ analogues with neuroprotective effects.

Journal: Process Biochemistry

Publisher: Elsevier B.V.

Your Submission

From: Kazuyuki Shimizu (shimi@bio.kyutech.ac.jp)

20/6/2558

To: roongnapa.s@psu.ac.th

CC: shimi@bio.kyutech.ac.jp, shimi@ttck.keio.ac.jp, ting_344@hotmail.com,
maheshsk@hotmail.com, Phern.a@psu.ac.th, niwan.t@psu.ac.th,
Kannuttha@hotmail.com, salinla007@hotmail.com, phacyz@nus.edu.sg,
chen.shangying@nus.edu.sg

Ms. Ref. No.: PRBI-D-15-00481R1

Title: An imprinted dopamine receptor for discovery of highly potent and selective D₃
analogues with neuroprotective effects

Process Biochemistry

Dear Dr Suedee Roongnapa,

We are pleased to confirm that your paper "An imprinted dopamine receptor for
discovery of highly potent and selective D₃ analogues with neuroprotective effects"
has been accepted for publication in Process Biochemistry.

It may be further copy-edited for style and format; in the event that any significant
matters arise, we will be back in touch with you.

Comments from the last Reviewer can be found below.

When your paper is published on ScienceDirect, you want to make sure it gets the

attention it deserves. To help you get your message across, Elsevier has developed a new, free service called AudioSlides: brief, webcast-style presentations that are shown (publicly available) next to your published article. This format gives you the opportunity to explain your research in your own words and attract interest. You will receive an invitation email to create an AudioSlides presentation shortly. For more information and examples, please visit <http://www.elsevier.com/audioslides>.

Your accepted manuscript will now be transferred to our production department and work will begin on creation of the proof. If we need any additional information to create the proof, we will let you know. If not, you will be contacted again in the next few days with a request to approve the proof and to complete a number of online forms that are required for publication.

Thank you for submitting your work to this journal.

With kind regards,
Kazuyuki Shimizu
Associate Editor

Joseph M. Boudrant
Editor
Process Biochemistry

Comments from the Reviewer:

Reviewer #1: The authors have satisfactorily addressed the reviewer's comments.

Author: Naklua, W., Mahesh, K., Chen, Y. Z., Chen, S. and Suedee, R.
Title: Molecularly imprinted polymer microprobes for manipulating neurological function by regulating temperature-dependent molecular interactions.
Journal: Process Biochemistry
Publisher: Elsevier B.V.

Your Submission

From: Process Biochemistry

2/11/2558

To: roongnapa.s@psu.ac.th

CC: ting_344@hotmail.com, maheshskrishna@gmail.com, phacyz@nus.edu.sg, chen.shangying@nus.edu.sg

Ms. Ref. No.: PRBI-D-15-00891R1

Title: Molecularly imprinted polymer microprobes for manipulating neurological function by regulating temperature-dependent molecular interactions
Process Biochemistry

Dear Dr Suedee Roongnapa,

A final disposition of "Accept" has been registered for the above-mentioned manuscript.

Kind regards,
Process Biochemistry

Comments from the Editors and Reviewers:

Reviewer #1 : The manuscript has been revised accordingly in light of the comments. The authors have fully addressed the concerns of the reviewers and the main revisions have been given. Additionally, the total manuscript has been carefully checked, adjusted and polished for improvement. Overall, this manuscript is finely organized and well written, I think it can be accepted now.

Reviewer #2: Thanks for the careful addressing of all remarks made! The quality of the paper is significantly improved. The manuscript reports on molecularly imprinted polymer microprobes for manipulating neurological function by regulating temperature-dependent molecular interactions in my opinion the paper is suitable for publication.

Author: Naklua, W., Suedee, R, and Lieberzeit P. A.
Title: Dopaminergic receptor-ligand binding assays based on molecularly imprinted polymers on quartz crystal microbalance sensors.
Journal: Biosensors and Bioelectronics
Publisher: Elsevier B.V.

Your recent submission to BIOS

From: Biosensors and Bioelectronics (Biosensors@elsevier.com)
18/10/2558

To: ting_344@hotmail.com

Dear Dr. Wanpen Naklua,

You have been listed as a Co-Author of the following submission:

Journal: Biosensors and Bioelectronics

Corresponding Author: Peter Lieberzeit

Co-Authors: Wanpen Naklua; Roongnapa Suedee, PhD;

Title: Dopaminergic Receptor-Ligand Binding Assays based on Molecularly Imprinted Polymers on Quartz Crystal Microbalance Sensors

If you did not co-author this submission, please contact the Corresponding Author of this submission at Peter.Lieberzeit@univie.ac.at; do not follow the link below.

An Open Researcher and Contributor ID (ORCID) is a unique digital identifier to which you can link your published articles and other professional activities, providing a single record of all your research.

We would like to invite you to link your ORCID ID to this submission. If the submission is accepted, your ORCID ID will be linked to the final published article and transferred to CrossRef. Your ORCID account will also be updated.

To do this, visit our dedicated page in EES. There you can link to an existing ORCID ID or register for one and link the submission to it:

<http://ees.elsevier.com/bios/l.asp?i=171347&l=KGMIWPPR>

More information on ORCID can be found on the ORCID website,

<http://www.ORCID.org>, or on our help page:

http://help.elsevier.com/app/answers/detail/a_id/2210/p/7923

Like other Publishers, Elsevier supports ORCID - an open, non-profit, community based effort - and has adapted its submission system to enable authors and co-authors to connect their submissions to their unique ORCID IDs.

CHAPTER 1

GENERAL INTRODUCTION & REVIEW LITERATURES

The molecularly imprinted polymers (MIPs) are generated the selectivity for structurally organized cavities that contain different functionalities on the structured surface and functionality capable of incorporating complementary counterparts of the molecular template assembled into the polymerized cross-linker. The template can be either small molecule (Cela-Pérez *et al.*, 2011) or macromolecules such as proteins (Bonini *et al.*, 2007; Yola *et al.*, 2014). This is related to knowledge of the chemistry of the target molecule together with the functional groups present and the types of molecular interactions are possible. Imprinting technology has advantages due to process yields a mimic of an original molecule. The selectivity of MIPs is related to the same size, shape and functional groups of the print molecule as the original compound complementary functionality between the template and polymer derived both from the matching shape and from having the same arrangement of charges at defined positions. The molecular recognition of the mimics of biological molecules such as the enzyme catalytic site, antibodies, receptors and functionalized protein (Vasapollo *et al.*, 2011) that mimics the recognition of biological process. A MIP has been recently reported to serve as a small probe for evaluation on biomimetic materials to evaluate the properties of other structures in functional selectivity of target (Tung *et al.*, 2016). Therefore, the cavity of MIPs plays a crucial key of determination of physicochemical properties of the compounds and context of use (Workman and Collins, 2010). The procedure of MIPs can be controlled and reproduced by using the same procedures and reuse for several

times without any change of their respective physical structure and selective recognition. And the imprinted cavities of MIP can be considered to give for relatively selectivity to the template or the structure of target compound or even highly specificity. The characterization and testing of recognition material for physical structure and fluorescence imaging that present the pros for these synthetic probes.

The types of monomers chosen for the generation of biomimetic receptor are related to their ability to interact with the template molecule in a suitable porogen solvent. Three different imprinting approaches have been commonly used for the preparation of these recognition materials. The first approach relies on the non-covalent interaction between the target molecule and the interactive functional monomer and the assembly, which is given to the formation of multiple weak electrostatic, hydrophobic, and hydrogen-bonding interactions between the print molecule and the functional monomer prior to polymerization. This approach is the most widely used because it is easier preparation due to template and functional monomer assembly and template removing step (Ramström *et al.*, 1994). However, the solubility of template requires during pre-polymer generation which the excess amount of a polar solvent has been found to interfere the complexation of template. The second is covalent imprinting approach, the templates and functional monomers formed covalent bonds in the polymer matrix (Wulff, 1995) which the breakdown between the template and functional group of polymer required for the rebinding of template during the selectivity testing that is usually difficult. The last one is the semi-covalent procedure, covalent bonds are formed between the template and monomers in pre-polymerization step then the template has been removed from the MIPs.

However, the rebinding of the analyte to the MIPs was generated with non-covalent interactions. The selected functional monomer(s) mixed with the polymerized mixtures were proceeded for the polymerization which a cross-linker and initiator are admixed for inducing of a cure polymer. The use of different polymerization techniques like bulk, suspension, precipitation, emulsion polymerization are well-known for established procedure in the formation of as elective recognition material. The bulk polymerization is commonly used method for the production of the polymer matrix, required for grinding and sieving method and template removal that is easy and rapid and is advantageous of the synthesized material. However the imprinted site within the polymer matrix was considered to be destroyed during the synthesized procedure and the leaching out of template is often found. Nevertheless, there is the possibility of whole template molecule ensemble within the surrounding of the crosslinked chain, and this method produced high yield of polymer matrix. Stamping method can be used to form different configuration of the polymer on the surface with the imprint formed on the surface of the substrate after template removal. The polymerization process takes place, then the print molecule obtained the template molecules fixed within the surrounded polymer. After the template was separated from polymer matrix, with the remaining cavities in the cross-linked matrix. The self-assembly processes of producing a MIP is shown in **Figure 1**.

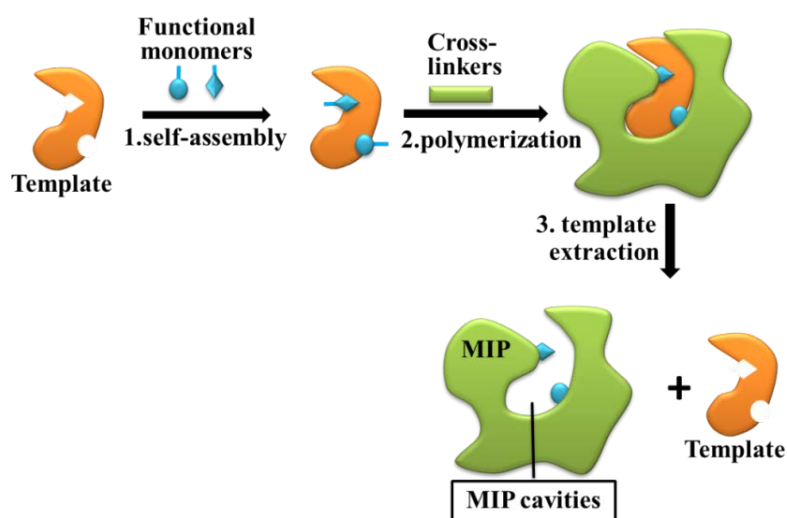


Figure 1 Illustration of generation of molecularly imprinted polymer formation of complexation between monomers and template (1), polymerization of functional monomers with cross-linkers around the template (2), and template removal, formation of the complementary binding sites (3).

The advantages of these synthetic recognition materials are easy preparation method and higher physical/chemical stability for a harsh condition such as pH, temperature and solvent. For this reason, MIPs have been usually used as selective materials for a wide range of applications such as artificial receptors (Cela-Pérez *et al.*, 2011; Alenus *et al.*, 2013; Mergola *et al.*, 2013; Karimian *et al.*, 2014; Kunath *et al.*, 2015), sensors (Sontimuang *et al.*, 2011; Kotova *et al.*, 2013; Latif *et al.*, 2014; Foguel *et al.*, 2015; Ratautaite *et al.*, 2015; Sharma *et al.*, 2015; Wackerlig and Lieberzeit, 2015), synthesis method (Alexander *et al.*, 2003; Zhang *et al.*, 2006; Wang *et al.*, 2007; Kirsch *et al.*, 2009; Sun *et al.*, 2013). Solid phase extractions have been often conducted with the use of MIPs as affinity phase for extraction of selected compounds (Xu *et al.*, 2004; Javanbakht *et al.*, 2010; Poma *et al.*, 2013; Díaz-Álvarez and Turiel, 2015; Li *et al.*, 2015). MIPs have also been used in pharmaceutical

application such as protein crystallization (Saridakis and Chayen, 2013), and drug development (Sellergren and Allender, 2005; Mohajeri *et al.*, 2012; Rostamizadeh *et al.*, 2012; Kempe *et al.*, 2015). From these applications by using the MIPs establish the generating of cavities is highly desirable for application in biological research giving rise to a unique biological response (Garcia-Serna and Mestres, 2011). In recent year, MIPs has been applied for coating then the target molecule or template used as fluorescent probes, that can be visualized by fluorescence microscope without the use of dye (Ren and Chen, 2015; Tang *et al.*, 2015). The complex of imprinted polymer and analyte, were analyzed and determine in thermodynamic activity and mobility of the targeted molecule by fluorescence spectroscopy. The number of recognition sites was determined by Boltzmann distribution which is a probability equation relating the entropy as shown in equation 1,

$$S = k_b \ln W \quad (1)$$

, where S is an entropy which related to stabilization energy (ΔH°), W is a weight, and k_b is Boltzmann constant, 1.380×10^{-23} J/K. The sum of the binding energies of the stability of a complex between ligand and receptor that is useful for the investigation of the binding properties between drug or ligand that mimics the biological process with natural receptor. The molecular imprinting is a process that exploits properties such as shape, size, and electronic features embedded in the known pharmaceutical compounds, can be used as a tool for the determination of chemical and physical property of the target or drug, or biological active entities (Mosbach *et al.*, 2001; Alexander *et al.*, 2003). We employed a biological molecule or the part of active site for generating a new biological compound in a nanovessel. **Figure 2** shows typical

synthesis procedure of generating a compound within the cavity formed with known biological substrate as the template during polymerization.

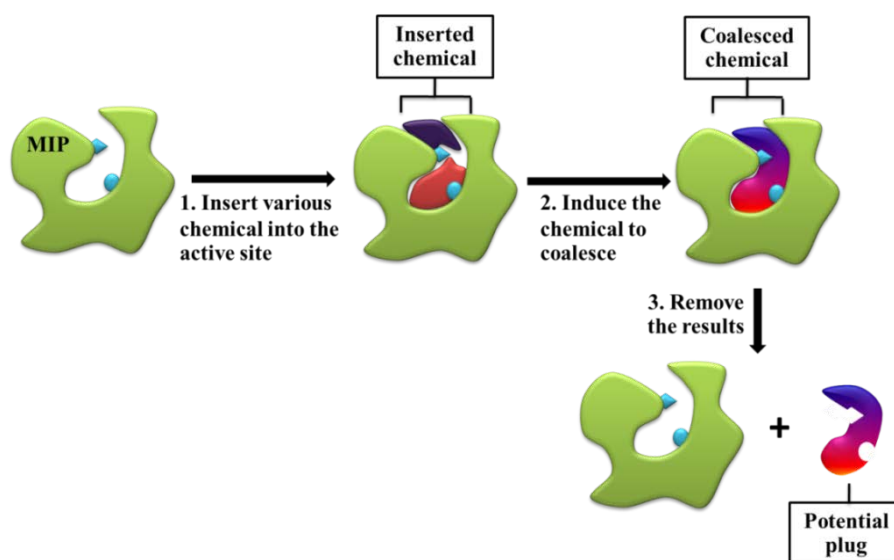


Figure 2 The principle of direct molding, two fragments bind at MIP cavities and it accelerates the covalent bond formation between the two fragments with the highest affinity.

When considering fabricating of molecular structures creating as nature to produce recognition materials, that the cavity created by pharmaceutically active counterparts that was assumed to produce biologically active compound when test further in biological evaluation or assay. This method includes the choice of chemical or the reagent that is known to be associated to the natural receptor to design ligands selective for receptor following by mixing and match the fragment in an imprint of original agent, resulting in the coupling product from the reaction of a series of reagent with selected chemicals. Then chemical is incorporated into the imprinted cavities, that was close proximity, near or at the active binding sites and induce the chemical merge or combined between encounters by an appropriate chemical reaction

into a structure before extraction of the final product. For example, the imprinting of the kallikrein inhibitor for generating new inhibitor have been previously reported, a similar dissociation K_d as the known template (Mosbach *et al.*, 2001). They pioneered the generation of several compounds within the selective recognition site based on the template-based method that the MIPs have also been applied as nanoreactors using Huisgen 1,3-dipolar cycloaddition of azides and alkynes by Zhang and coworkers. The synthesized products showed high regioselectivity and excellent kinetic rate of the reaction (Zhang *et al.*, 2006). Moreover, a metal-containing asymmetric heterogeneous catalyst that have been synthesized by molecular imprinting and methyl-(Z)- α -N-acetamido-cinnamate as the template showed a significant enantioselectivity of production of the (L)-enantiomeric product (Lee *et al.*, 2009). When the carboxypeptidase was chosen as template for preparation of the imprinted catalysts that led to imprinted cavity stabilized the tetrahedral transition state in the hydrolysis of carbonate (Wulff and Liu, 2011). Therefore, synthesis of different synthesized compounds and thus the particular entities is expected to contain the key recognition related to the template structure that was used to construct the MIP.

Dopamine and serotonin which are interested for this study were used as the templates that were single (dopamine) or mixed dopamine and serotonin. Dopamine and serotonin are important neurotransmitters that have the autonomous neuronal activities and can regulate the functional responses of neural activity. They are clinically relevant compounds and dopamine as well as serotonin is used as therapeutic. They are neurotransmitter, and hormone, which stimulate the receptors for the central nervous system response and function, with a multimodal reaction, this neurotransmitter receptor trigger and communicate each other within different

subtypes, or the other receptors for the regulation function of the body. One of advantageous approach of MIPs for direct molding is used in this study relevant to substances are used as the substrate for the reaction in both dopamine and serotonin MIP nanovessel. Subsequently, the characteristic and evaluation of recognition ability for the synthesized polymer materials were carried out by scanning electron microscope (SEM), Fourier transform infrared spectroscopy (FT-IR) and pore analysis.

Dopamine and serotonin receptors are targets in this study which the reason for this is that they offer the opportunities of the development and screening library of the dopamine mimics for the treatment of antipsychotics. The atypical antipsychotic agents are partial D₂ receptor agonist and also blockage dopamine D₁, D₃, D₄, and serotonin receptor (Roth *et al.*, 1997; Konradi and Heckers, 2001; Horacek *et al.*, 2006; Jafari *et al.*, 2012). **Figure 3** shows the chemical structure of some antipsychotic drugs used in this study. They were used as the substrate for testing the recognition in this study or verify the selectivity of MIPs.

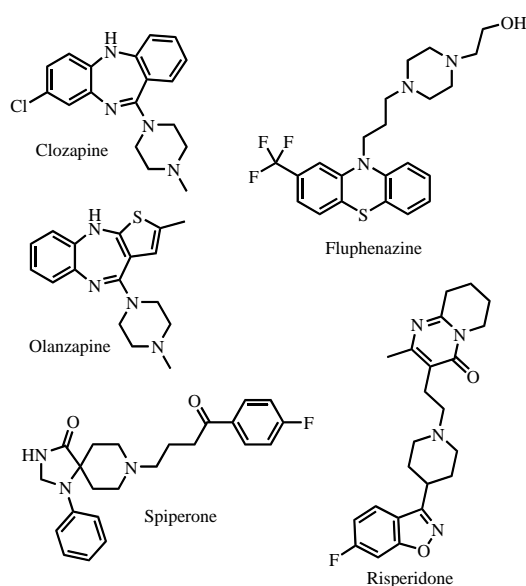


Figure 3 The structure of atypical antipsychotic drugs.

Normally, the purification and characterization of the natural brain receptor for assay and testing have many steps, time consuming, and cost effective. Accordingly, the synthetic artificial receptors based on imprinting technique provide the greater advantages of receptor mimics are less expensive to be synthesized than pure receptors by replacement of biological recognition system. In addition, they also storage and maintained their recognition cavities for several times (Vasapollo *et al.*, 2011). Previous work has shown that the biomimetic receptor using imprinting techniques such as artificial beta-adrenergic receptor prepared by a novel method such as reversible chain-transfer catalyzed polymerization (Bompart *et al.*, 2015) and photo initiated atom-transfer radical polymerization (Adali-Kaya *et al.*, 2015) and this employed the *S*-propranolol as a template. Latif and coworkers imprinted the estrogen receptor on polyurethane layer (Latif *et al.*, 2014). The previous studies of dopamine and serotonin receptor mimics natural dopamine/serotonin receptors have been reported that the polymer materials were tested for selective recognition properties and behavior in competitive binding assay using dopamine in fluorescence spectroscopy for ergot derivatives. The MIPs have potential to screen the compounds from natural products and drug candidate by the polymer with responsive properties (Suedee *et al.*, 2006; Suedee *et al.*, 2008). It is interesting to use these recognition cavities of MIPs for the synthesized dopamine analogs that show high affinity for both dopamine and serotonin MIPs. Moreover, each individual compound is tested for its ability to bind to a given biological molecule which could be replaced by a more stable artificial receptor. With MIP mimics, biological target have been developed, yielding a plug that fills the portion in the active sites or binding site of imprinted cavity.

Upon screening method, the variety of strategies that are usually used for evaluation of biological activity of new compounds such as, high throughput assay (Hughes *et al.*, 2011). In addition to biological assay, the screening without chemicals and fresh original target, virtual screening is well known in computer-based methods, molecular docking, for test large libraries of molecules of interest that complement targets of known structure with the receptors (Shoichet, 2004). A protein-ligand binding affinity is of greatly promising for study of the interaction between small molecule and ligand with their binding sites of protein via non covalent interactions. The information of affinity binding can help scientists screen of new lead compound that have the specificity to the protein such as receptor, enzyme, cell, *etc.* Therefore, protein-ligand binding affinity has become important for finding new drug and study the interaction between drug and target protein. These prediction using calculated binding free energies in detail Monte Carlo (MC) simulations (Michel *et al.*, 2006) combined with protein-ligand binding assay, allowed structure determination of inhibitors bound to *E. coli* recombinant dihydrodipicolinate reductase with SYBYL software package (Paiva *et al.*, 2001). The assay system with computer aid tools had a higher hit rate and allows the opportunity of screening potent compound to target. Moreover, the strategies of molecular screening can be model structure of potential synthesized compounds which had high affinity to the target by the MIPs for individual test compounds associated with the template binding to the natural receptor that reflected the structure similarity to the template. Furthermore, the biological testing of natural target protein has become an essential component of pharmacological screening, thus isolation and purification have to be carried out with care due to the stability and the perturbed active site. Activity of the selected

compounds for study of dopamine receptor or its binding site mimics the recognition ability, provided a template describing the shape and binding domains. The generation of candidate or drugs with biologically active properties is to describe the resulting from the interactions of drugs and other organic molecules with the binding site of proteins (i.e. receptor, channel, cellular organelles).

In this thesis, the mixture of building blocks for the synthesis procedure of the MIP used to screening the dopamine libraries and to create various compound-association dopamine and serotonin receptor; chlorobutyrophenone-type ligand, or clozapine-type ligands in the MIP nanovessel. Subsequently, we validate *situ* product formation into the binding site of MIP mimics by the competitive ligand binding assay using natural receptor isolated from the rat hypothalamus. Also the linking mechanisms of drug action at these receptors provide us the information of ligand binding reflected the dysfunctional biological and cellular processes of human diseases. The binding of imprinted polymer contains the active site for the assembly of candidate occurred from the agonist or antagonist are able to bind to these receptors mimicking the binding affinity of the natural one. The nucleophilic substitution between the ligands and the amine structure occurred in the MIPs with a high physical stability that have resistance in the harsh conditions. The energetic advantage of present method can prevent the site that is mimic the entities of biologically active compound formed for recognition during the polymerization, in turn to prevent the interacting with its usual substrate and the formation of by-products. Although the MIP nanovessels can give different conformational state or orientation, the synthesized compounds need to be screened in biological activity or the aids of

computer docking for study the binding properties of the obtained compounds from the molding in a nanovessel using crystal structure of protein.

The quantification of ligand binding to specific dopamine and serotonin receptors is a crucial key of drug finding research; therefore, receptor-ligand binding assays are necessary to measure binding affinity and ligand efficiency. In this study, we used the artificial receptor based on the biomimetic approach. Screening of biological activity as applied to D₁R ligand have been carried out by using of a dopamine binding site mimic that would be correlated with the physical and chemical properties of tested compound's structure. The previous studies of using of labeled ligand-binding assays, including fluorescent and radio ligand binding assays were mainly utilized to detect biological active compound to the binding site of a natural receptor. For competitive binding assays, the affinity of analyte for the receptor of interest can be determined from their ability to displace the marker, labeled ligands with radio-isotopes (Martres *et al.*, 1985; Alberto *et al.*, 1999; Lawler *et al.*, 1999), dyes or fluorophores (De *et al.*, 2005; Baker *et al.*, 2010), chemoluminescence (Macdonald *et al.*, 2000) and bioluminescence (Heils *et al.*, 1996).

Receptor–ligand binding technique by a labeled marker had major advantage is sensitivity (Lohse *et al.*, 2012). Solving problems of the actual compounds that have affinity for receptor instead of a labeled marker and detection of the eluted the free ligand by mass spectrometry (Jonker *et al.*, 2011). Previously, van Breemen and coworkers developed pulsed ultrafiltration by using the molecular weight cutoff membrane for pushes the unbound fraction to waste (van Breemen *et al.*, 1997). Then, the bound ligand was dissociated from the receptor, then eluted through the membrane, and measured and identified by LC-MS (Liu *et al.*, 2007).

Affinity screening method is also well-known in its ability that depends on possible binding of ligands to immobilize proteins on a solid support and the established procedure for binding ligands. Jonker and co-researcher produced protein-Co(II)-coated paramagnetic as affinity beads for isolation of the target biomolecule by using immobilized receptor on magnetic particles (Jonker *et al.*, 2009). Both Gellan beads and agarose were also used for the immobilization of bovine serum albumin (BSA) and Protein A as an affinity solid phase chromatography for target capturing of *IgG* (Ferrance, 2007). Also, Höfner and Wanner have reported the competitive binding assays with dopamine receptor-ligand and D₁R for the study of ligand binding in matrix solution that mixed ligands, native marker, and the addition of receptor (Höfner and Wanner, 2003), which selectivities similar to those of biological antibodies (Ansell *et al.*, 1996). In generally, artificial receptors based on molecularly imprinted technique were able to investigate the recognition selectivity for analytes or targets. This screening strategy employed the MIPs is beneficial about high affinity and specificity, although the shape of test compounds in the various binding sites of imprinted cavity may differ from the biological situation, the approach that speed up the searching candidates in discovery. The computer aids tool was employed for the determination of the binding affinity of recognition cavities generated by the bioactive template molecules. In the case of protein recognition, flexible structure and conformation can be easily affected by temperature and solvent upon the polymerization; therefore, the synthesized procedure needs to be control to prepare protein MIPs that have a biomolecule or protein as a template. However, the protein-imprinted polymers were successfully produced by stamping method. Because of the adsorption substrate for template proteins, such as mica surface with hydrophilic and

negatively charged, and sugar shell, that produced high selective recognition via surface imprinting. Immobilized sugars were used for fibrinogen-MIP production (Shi *et al.*, 1999). Immobilization techniques were developed to prepare MIP with selective recognition for the hemoglobin on silica surfaces by using covalently immobilized hemoglobin in polysiloxane networks (Shiomi *et al.*, 2005). The BSA-imprinted polymer with recognition polymer chains formed by using polyacrylamide that were studied for hold the form of the protein template in the surrounding polymer chains (Guo *et al.*, 2006).

Sensor is a device for detection of the analyte with several changes of signal, physical, chemical and electronic, and also mass in the process parameters or any stimulus. It includes three parts consisted of receiver, detector, and recorder. The transducer is a kind of detector that converts other form of energy such as electrical or electromagnetic to read out as shown in quartz crystal microbalance (QCM) sensor. The MIP thin films are used for coating on to QCM that are selective, simple and sensitive method. QCM sensors are well-known to measure small mass changes of the analyte by using the change in resonance frequency for the application in biosensor application (Bunde *et al.*, 1998; O'Sullivan and Guilbault, 1999). The QCM sensors include a thin quartz disc that sandwiched between a pair of metal electrodes and connected with oscillator circuit and frequency counter (**Figure 4**).

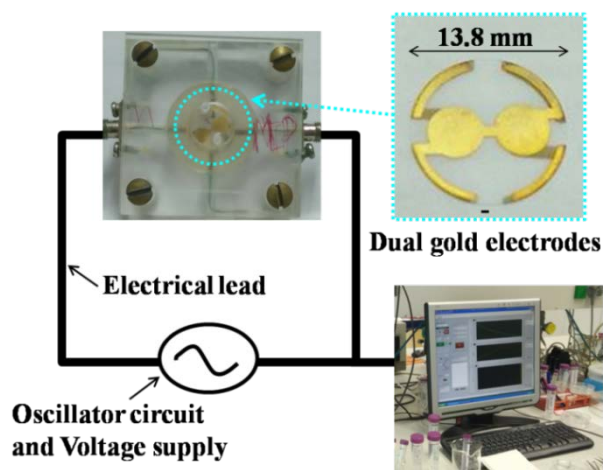


Figure 4 Schematic view of a piezoelectric QCM crystal.

Figure 5 shows illustration of the preparation MIP film on the QCM by using the synthesized peptide of gp41 fragment 579–613 as a template with epitope imprinting technique (Lu *et al.*, 2012). Then, this biomimetic sensor allowed for detection of human immunodeficiency virus type 1 (HIV-1) with a high selectivity and specificity to HIV-1.

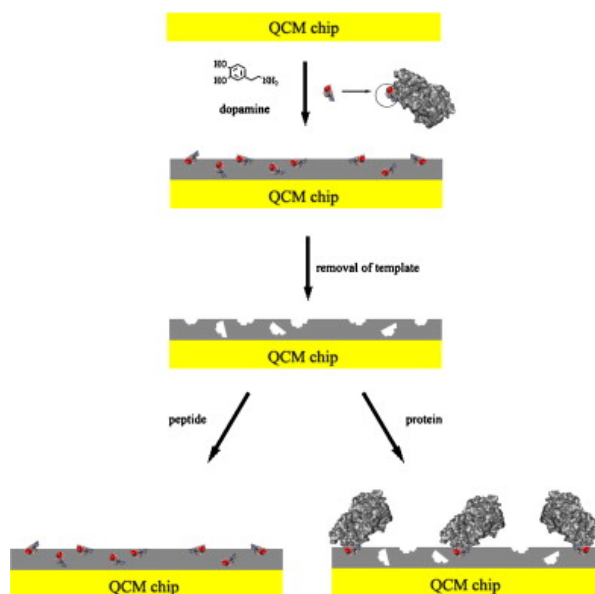


Figure 6 Epitope approach to synthesize MIP film for the detection of human immunodeficiency virus type 1 related protein glycoprotein 41.

Within this study, a three-dimensional structure of protein isolated from natural source receptor that was used as a template has been previously reported, new kind of the surface imprinting technique (Titirici *et al.*, 2003) was used for produced MIP material. The generation of MIPs using porcine serum albumin (PSA) as a template (Liu *et al.*, 2014). This strategy was also employed for the generation of recognition site for peptide biotoxin melittin, the major component of bee venom from *Apis mellifera* upon imprinting process and the measurement of QCM sensor after template removal (Hoshino *et al.*, 2008). One advantage of this technique for preparation molecular imprinting film is the epitope-mediated imprinting that recognized the dengue virus protein. A peptide containing Thr-Glu-Leu-Arg-Tyr-Ser-Trp-Lys-Thr-Trp-Gly-Lys-Ala-Lys-Met was selected as linear epitope template (Tai *et al.*, 2005). This method offers the proteins bound to the MIP that the pre-polymers were arranged in suitable orientation under the external conditions.

The change in mass of analytes on the quartz surface is related to the change in frequency of the oscillating crystal, as shown by the Sauerbrey equation (2) with high sensitivity and quick response.

$$\Delta f = -\frac{2f^2}{\sqrt{\rho_q u_q}} \Delta m = -C_f \Delta m \quad (2)$$

Δf is the different frequency resulting,

Δm is the mass change,

f is the intrinsic crystal frequency,

ρ_q is the density of the quartz, and

u_q is the shear modulus of the quartz film (Baltus *et al.*, 2007).

QCM sensors have been applied for study of interaction of organic compound or proteins of interest. The detection of both macro and small molecules such as human rhinovirus and the foot and mouth disease virus (Jenik *et al.*, 2009) has been previously reported, estrogen 17β -estradiol, as well as endocrine disrupting chemical (Latif *et al.*, 2014). Previous report on the MIP selective for racemic thalidomide and its (*R*)-enantiomer showed the selectivity of the enantiomer template other than the racemic mixture of thalidomide by using a polyurethane imprinted polymer (Suksuwan *et al.*, 2015). The selective recognition of lovastatin in red yeast rice with poly(2-hydroxy ethyl methacrylate methacryloylamido aspartic acid) nanofilms have been reported (Eren *et al.*, 2015). The themelphalan, an alkylating agent active against malignant diseases were analyzed via electropolymerized molecularly imprinted polythiophene films (Kumar Singh and Singh, 2015).

The goal of this thesis project as follows: first, MIPs were used as nanoreactors which have specific binding site to develop the target molecules to which dopamine analogs show binding affinity for dopamine and/or serotonin receptors. Second, MIP cavities were used as a probe for understanding of the specific molecular aspects of the dopamine receptor ligands. Third, MIP-based QCM sensor layers which non-covalent interaction is necessarily for the binding on the artificial receptors based on natural dopamine receptors as protein recognition that mimics biological process. On sensor measurement, MIP-based QCM in which analyte-MIP exhibits the sensor response and the binding sites of MIP allowed to trace back ligand selectivity of the natural receptor to overall structural changes in the known molecule. A dual electrode is advantageous to eliminate the effect of differences of conductivity, temperature and mechanical force, *etc.* That one electrode layered with sensor

element and another by non-imprinted control polymer that was prepared in the absence of template. The differences of substrates including either the agonist or antagonist of dopamine receptor have been studied through measurements of binding of the compounds using MIP-based QCM sensor. The test compounds associated to dopamine receptors which elicit a range of biological activities and the development of molecular structure for functional selectivity would be expected to be highly useful for antipsychotic therapy.

CHAPTER 2

OBJECTIVES

Choice of monomers and cross-linker

To prepare dual dopamine/serotonin molecularly imprinted polymer (DS-MIP), dopamine molecularly imprinted polymer (D-MIP), and control polymer (NIP) which dopamine and serotonin as template. The non-imprinted polymer which were used as control polymers were prepared the same as the polymerization of MIPs except in the absence of a template. Based on the structure of template, methacrylic acid (MAA) and acrylamide (ACM) were chosen as the functional monomers that have functional group of carboxylic acid and N-amide, respectively. A cross-linker, *N,N'*-methylene-bis-acrylamide (MBAA), was used in this study, it is also necessary in the formation of the selective material that play a key role of the formation of rigid polymer network for stabilized binding site that obtained from template. A thermal polymerization method involving free radical polymerization with 2,2'-azobis-(isobutyronitrile) (AIBN) was chosen for the synthesis of the obtained polymer. After the removal of template, MIPs and corresponding NIP were subsequently characterized by the examining of surface morphology and surface area by SEM and nitrogen adsorption/desorption using an automated gas sorption system, respectively. Surface areas were measured from Brunauer-Emmet-Teller (BET) plots. Moreover, pore volume and pore size were determined using the Barrett-Joyner-Halenda (BJH) method by nitrogen adsorption/desorption using an automated gas sorption system.

Objectives of this thesis

To apply the obtained artificial receptors of DS-MIP, D-MIP and corresponding non-imprinted polymer to synthesize a range of the dopamine analogs by nucleophilic reaction via molding method. This involved the reaction of butyrophenone derivatives by amine compounds, tyramine, phenylethylamine, benzylamine, phenylalanine methyl ester, 4-(3,4-dichlorophenyl)-*N*-methyl-1,2,3,4-tetrahydronaphthalen-1-amine and 2-(3-(4-(3-chlorophenyl)-piperazin-1-yl)propyl)-[1,2,4]triazolo[4,3-*a*]pyridin-3(2H)-one, with 1-chloro-(4'-fluorobutyrophenone). For modifying of clozapine derivatives, the reaction between the hydrazine derivative and eight acid halides, namely, 2-methoxybenzoyl chloride, 3-methoxybenzoyl chloride, 3-chlorobenzoyl chloride, 4-chlorobenzoyl chloride, phenylacetyl chloride, and 4-methoxy-phenylacetyl chloride. The synthesized compounds from the coupling reaction within the DS-MIP, D-MIP and the corresponding NIPs were compared and characterized by spectroscopic methods such as FT-IR, ¹H-NMR, ¹³C-NMR, liquid-chromatography and mass spectroscopy. Then, the synthesized compounds were screened for pharmacological activity to determine the binding affinity for isolated biological receptor from Wistar rat hypothalamus using label free competition binding assays with SCH23390 in ammonium formate buffer (pH 7.4) at room temperature following by LC-MS-MS method.

To determine the binding affinity of the products were also calculated by molecular docking, Surflex-Dock program, by using X-ray crystallographic structures of the D₃ receptor [Protein Data Bank entry 3PBL chain A] and the serotonin 5HT_{1b} receptor [Protein Data Bank entry 4IAR] that were removed the co-crystallized ligand and water molecules fixed, and that fixed side chains. For this, the

computer docking was used to determine the total score, $-\log(K_d)$, of hydrophobic, polar, repulsive, entropic and salvation for the binding affinities of the synthesized compounds with the simulated protein structure that was obtained from data bank. Also used to screen for active compounds with a binding affinity K_i and $IC_{50} < 1 \mu\text{M}$, the support vector machine (SVM) models.

To employ the dopamine and serotonin MIP binding sites for investigation function and photophysical properties of the hypothalamus proteins. In this work, the mixture of polymer particles (NIP, D-MIP or DS-MIP) along with clozapine were incubated for which the effect of probes or biomarker either with or without rat hypothalamus was examined using fluorescence spectroscopy and fluorescence imaging. A fluorescence decay and phase contrast microscopy for determination of temperature-dependent molecular interactions in the presence of the isolated rat hypothalamus, which allowed the relationship of energy and binding. Furthermore, the identification of drug achieved from the synthesis of a series of the chemical reagents and the precursor in MIP nanovessel were performed by $^1\text{H-NMR}$, SEM coupled microanalysis, and inductively coupled plasma-atomic emission spectroscopy (ICP-OES). To examine the binding properties of MIP and in the presence of D_1R agonist and antagonists by competitive binding assay. To establish the synthesizing procedure and differential binding of template on the optimal conditions to achieve the optimal MIP coated QCM. To investigate D_1R protein for their binding characteristics which is relevant to biological activity of small molecules on QCM sensors for analytical technique. To establish the binding affinity for ligand binding assays with MIP-base QCM sensor and to compare them to the previously reported that was achieved by radioimmunoassay.

CHAPTER 3

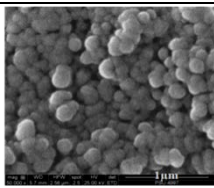
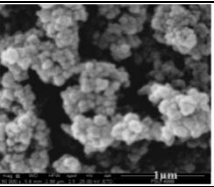
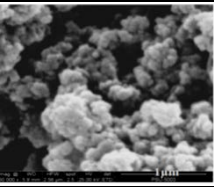
SIGNIFICANT RESULTS AND DISCUSSION

Synthesis and characteristic of MIPs

In this study, the MIPs, DS-MIP and D-MIP, were produced for the use in synthesis of a new entity of the dopamine as biological target for natural dopamine and serotonin receptors. These artificial receptors were obtained by the copolymerization of two functional monomers, MAA and ACM by thermal polymerization reaction, using MBAA as a cross-linking agent in the presence of mixture of dopamine and serotonin were the printed molecules for DS-MIP, single dopamine as template for D-MIP and non-template for NIP in 80% v/v methanol solution. This solvent was chosen because the dopaminergic and serotonergic agonist species of natural dopamine and serotonin receptors were soluble in polar solvents. For interaction in recognized sites, the carboxylic group or the amide group of functional monomers were capable of interacting with the hydroxyl and amino groups of dopamine and serotonin templates. Moreover, *N,N'*-methylene-bis-acrylamide would provide the flexibility and conformational adaptability to the polymer that partially mimicked the properties of the natural proteins.

Table 1 shows SEM image and physical properties of the imprinted polymers. The successful preparation of MIPs were confirmed by FT-IR spectra of imprinted and non-imprinted polymer materials that showed peak of O-H or N-H stretching vibration, C=O stretching vibration, -NH₂ bending, -CH₂-CO bending, -OH bending, and C-C-O stretching at 3422-3418, 1660-1657, 1532-1528, 1454-1452, 1388, and 1114 cm⁻¹, respectively.

Table 1 Characteristics of synthesized polymers.

Polymer	SEM micrograph ($\times 50,000$)	Pore volume ($\times 10^{-2} \text{ cm}^3/\text{g}$)	Pore size (\AA)	BET Surface area (m^2/g)	FT-IR (cm^{-1})
NIP		235.4	183.5	513.0	3421, 2945, 1657, 1532, 1452, 1388, 1212, 1114, 603
D-MIP		131.3	248.0	211.8	3418, 2943, 1660, 1531, 1452, 1388, 1211, 1114, 615
DS-MIP		252.1	259.0	389.4	3422, 2942, 1657, 1528, 1454, 1388, 1211, 1114, 619

The surface morphology of MIPs was observed by SEM. Imprinted polymers exhibited a rough surface of the particles in which the aggregation of both MIPs was higher than the NIP control polymer. The pore size, pore volume and total surface area of MIPs were characterized in the range of 248.0-259.0 \AA , 1.3-2.5 cm^3/g and 211.8-389.4 m^2/g , respectively. MIPs were found to have a larger pore size than NIP. The pore volume and BET surface area of corresponding NIP was larger than the porous material for dopamine imprinted polymer. The obtained MIPs had significantly enhanced surface area excellent template binding improved owing to an increased surface area, particularly in DS-MIP. The effect of pore sizes of MIP on absorption and the accessibility of the reagents or starting materials in imprinted cavity. A large portion of a surface area is associated with surface and smaller pore volume for D-MIP than the other polymers, the amine molecules will be unable to

reach these sites. The results confirmed that the recognition selectivity of MIP materials was successfully produced by molecular imprinting techniques. The MIP cavities were applied in the synthesis of chlorobutyrophenone-type ligand and clozapine derivatives for next study. Moreover, homogenous polymer chains containing of functional monomers, MAA and ACM distributed on the backbone were achieved in DS-MIP compared with D-MIP, and NIP, which led to higher affinity for rebinding of template and analogs.

Synthesis of dopamine analogues by self-assembly approach

-Butyrophenone derivatives

Compounds with several rotatable bonds have a number of equivalent low energy conformations that may gain access to imprinted cavity. The activated complex can be considered by the having one loose vibrational mode into the release bound molecules. In the case of transition state is much looser than the adsorbed phase, which conferred to the loose chemical entity that should have degrees of freedom that are more easily excited by temperature and the adsorption activation energy for the adsorbed phase. If the binding parameter (b) of the reagent-MIP obeys the Arrhenius equation:

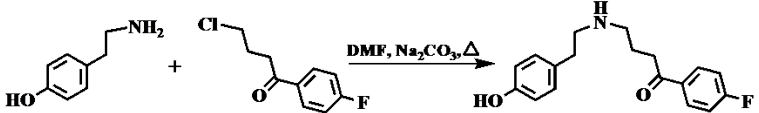
$$b = Ae \times p \left[\frac{-Ea}{RT} \right]$$

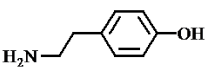
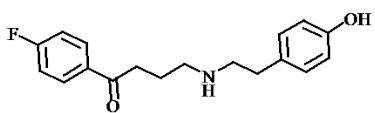
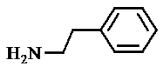
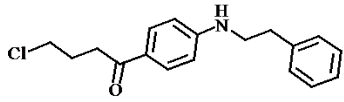
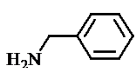
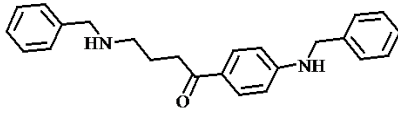
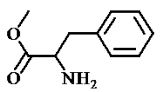
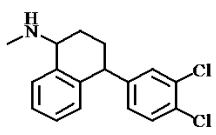
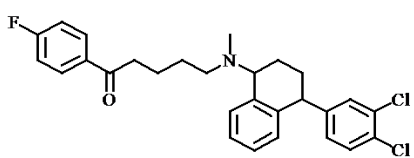
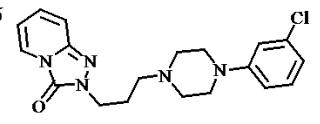
The activation energy derived from the Arrhenius type of temperature in the case of this MIP system may be associated with the imprinted polymer. The existence of a strong energy for driving the substrate or ligand into the reaction medium due to the difference in the parameter between the amine compounds. The postulate states that

the structure of a MIP-compound resembles that of the species nearest to it in free energy. From the current study, the chlorobutyrophenone merged to the other reagents at 60°C, and confirmed the structure of the MIPs resulted in its re-orientation and led to reversible binding of the chlorobutyrophenone and various amine precursors. This reversible binding of the bound species that the main driving force is non-covalent interactions between two partners and the ability of their functional groups, to react by nucleophilic substitution in a defined way. During the binding within the MIP binding site, the amino moiety changed orientation that entailed the molecule prefers to the most favorable conformation, or involving the lone pair electron on the nitrogen giving the attraction at the alkyl halide. A transition state from one type to other, was preassembly occurred, and selectivity dominantly in the nanovessel for the molding within the surrounded polymer chains. The structures of the assembled MIP and the reactants, then final reactant product in the binding sites as the template do. Thus, the preassembled template and functional monomer that formed crosslinked chain with a crosslinker, the forming of binding sites and the shape should be compliant to the structure of the intended product.

The nucleophilic substitution reaction in imprinted nanoreactors occurs only if there is a possibility of interaction between the precursor and binding site in recognition cavity. This reaction enabled the synthesis of new entities from a dopamine/serotonin receptor ligand by use of various amine structures as building blocks similar to the template. The characteristic of MIP binding site for molding reaction can be used to study the details by a systemic modification, for dopamine binding site mimics. This is in turn to gain the knowledge about the selectivity of biological process in the neural system. The process was used in this work that with

selections of amine precursors, tyramine (**1**), phenylethylamine (**2**), benzylamine (**3**), phenylalanine methyl ester (**4**), 4-(3,4-dichlorophenyl)-*N*-methyl-1,2,3,4-tetrahydro naphthalen-1-amine (**5**) and 2-(3-(4-(3-chlorophenyl)-piperazin-1-yl)propyl)-[1,2,4] triazolo[4,3-*a*]pyridin-3(2H)-one (**6**), as shown in **Table 2**, demonstrated for specific binding in area of the receptor binding site. Subsequently, the bound molecules may interact with the binding groups of functional monomers within the imprinted cavity, that direct the reagents to link covalently by a suitable alkylation reaction with 1-chloro-(4'-fluorobutyrophenone) confines within their binding pockets, which are important in forming of more favorable new ligand of the binding site of the receptor with a high degree of specificity. Sufficient time permitted the mold with reaction rates can be achieved for the chlorobutyrophenone-type ligands and the amine compounds. The results showed evidence supported that 1-chloro-(4'-fluorobutyrophenone) could bind into the MIP binding sites. The results from chemical synthesis in molecularly imprinted polymer nanovessel were obtained as can be seen in **Table 2**.

Table 2 The precursor amines and resulting components of the mold reaction.


R-NH ₂	Product in MIP cavities
	1a 
	2a 
	3a 
	4a
	5a 
	6a

The difference of nucleophilic substitution reaction in DS-MIP, D-MIP and NIP using the amine **1** and **5** to obtain **1a** and **5a**, respectively, depended upon their intrinsic nature of the reactive groups. This method is compatible with amino group of reagents under the controlled condition, which displaced the hetero atom on the chlorobutylphenone. The compound **2** formed a product **2a**, particularly in displacing only fluoride atom. In addition, the amine group of **3** displaced both halogen atoms of chlorobutylphenone gave **3a** in only the mold reactions. But the

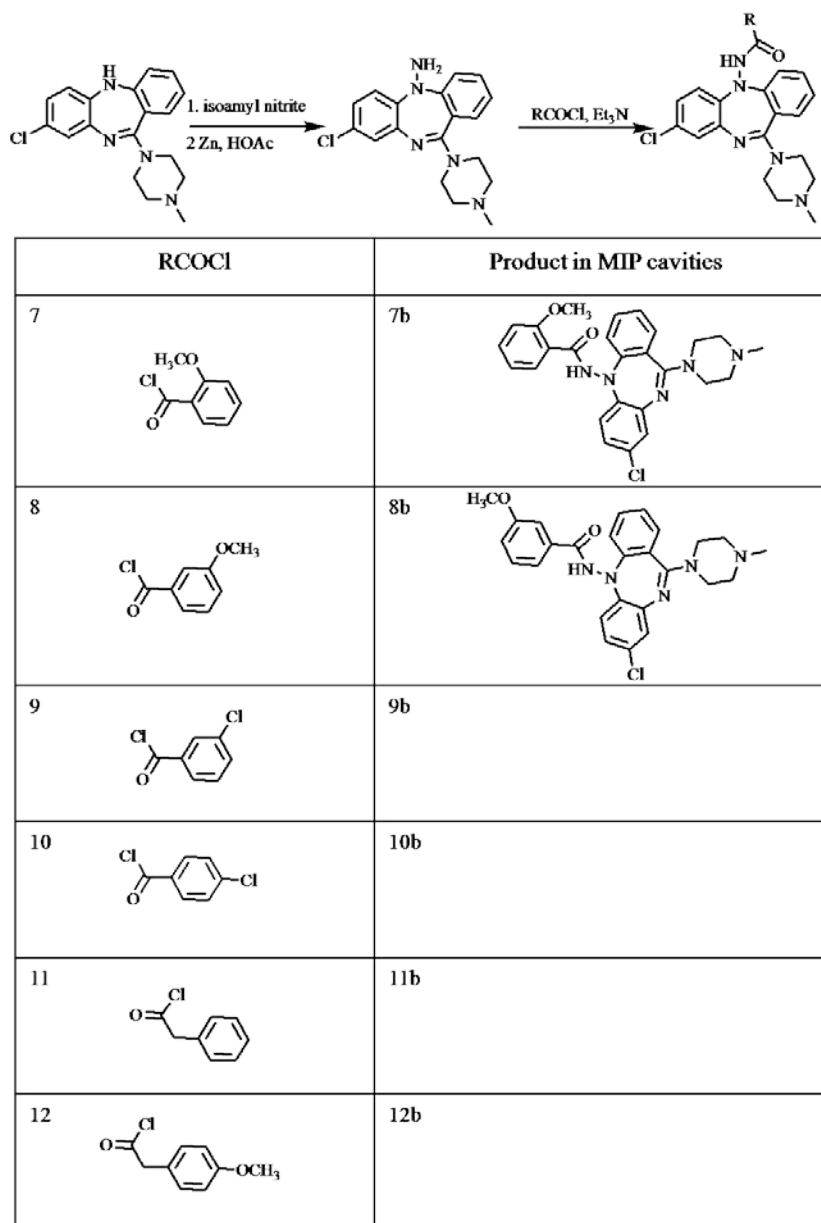
butyrophenone derivative was not obtained in MIP cavities when **4** and **6** acted as the reactants. The product from **4** and tertiary amine **6** were not observed because of steric effect of bulky amine. Moreover, the nucleophilic properties of nitrogen atom of amine reactants are important key in the nucleophilic substitution reaction but the molding reaction were controlled by MIP's cavity. Therefore, the nucleophilic substitution reaction in imprinted nanoreactors occurs only if there is possibility of interaction between the amine and binding site in the imprinted cavity, where the MIP was assessed with respect to the surface area and the accessibility. As the reaction should selectively generate the best synthesized compound for the imprinted polymer. The result demonstrates that the procedure used that imprinted with the MIP binding sites for product formation could be identified and enhanced a workable MIP system in which the binding site of MIPs and reactants and its reactivity is occurred. Note that, after washing the chemical product, the active binding sites in MIPs believed to remain stabilized functional groups can rebind to the other reactants for new cycle of the synthesis.

-Hydrazine derivatives

The hydrazine derivatives was produced to use for synthesis of clozapine derivatives because of the presence of hydrazine functional groups and the acid chlorides could be reacted easily that were capable of the formation of dopamine analogues in situ. In particular, the reaction between hydrazine and acid chloride are reactive toward carbonium ion are well suited for this study. As for the clozapine has the main structure can be reacted towards hydrazine derivative (Sasikumar *et al.*, 2006). First step, the intermediate step involved hydrazine reaction between of

clozapine with isoamyl nitrite obtained the hydrazine following by the diazotization with an acid chloride, as shown in **Table 3**. A series of acid halides, including 2-methoxybenzoyl chloride (**7**), 3-methoxybenzoyl chloride (**8**), 3-chlorobenzoyl chloride (**9**), 4-chlorobenzoyl chloride (**10**), phenylacetyl chloride (**11**) and 4-methoxyphenylacetyl chloride (**12**) were studied for the reaction of hydrazinoclozapine derivatives in mold reaction. In this modification, the resulted compounds (**7b** and **8b**) were obtained from the product from 2- or 3-methoxybenzoyl chloride only in MIP nanovessel (see **Table 3**). Comparing to all of the other acid chlorides (**9-12**) they did not react with the hydrazine compound in both the MIPs and control polymer such that on obtaining the conversion of these functional groups which is potential useful in the synthesis of these two clozapine derivatives in the MIP nanovessel. Also, the results from reaction of hydrazine with the acid chlorides in the triethylamine, indicating that the product may react in this solution but that the presence of drug impeded by the steric imposed by the binding site of MIPs occurred. The adsorption process of the imprinted materials may hydrogen bonding, van der Waals interaction, ion-dipole interaction and hydrophobic interaction.

Table 3 Summary of synthesis of clozapine derivatives from the reaction between hydrazinoclozapine and various acid chlorides in the MIP nanovessel.



The results from direct molding between butyrophenone and clozapine hydrazine derivatives indicated that MIP nanovessel can be induced a more favorable conformation of product that has high affinity to active site of artificial receptor by which the component of the reacted compound near or at the binding group of the

(B)

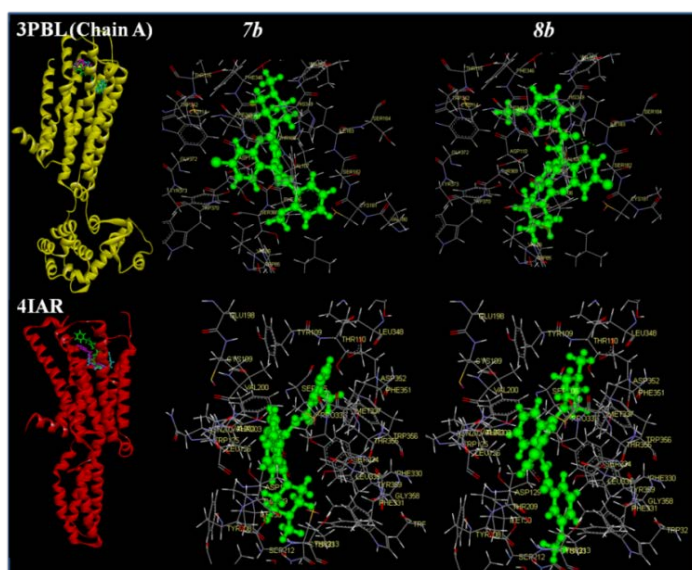


Figure 6 Modeling of biological receptors, D₃ receptor (PDB ID: 3PBL) and 5HT_{1B} (PDB ID: 4IAR) receptor for (A) butyrophenone derivatives, *1a-5a*, and (B) clozapine derivatives, *7b* and *8b*.

The computer docking for all the test compounds showed that the hydrogen bonds (1.78-2.75 Å) between the compounds and these receptors. The oxygen atom of carbonyl group of *1a*, *2a* and *8b* appeared to make one hydrogen bond with hydrogen atom of amide group of ILE183. *3a* also formed hydrogen bond with ILE183 and the NH- group of *3a* formed another hydrogen bond with oxygen atom on the benzene ring of TYR373. But *5a* and *7b* did not show hydrogen bonding interaction with this target. Moreover, the binding mode between the products and binding site of 4IAR is illustrated in **Figure 6**. *1a* was capable to form hydrogen bonding interactions with the CYS199 and ASP352 and GLN41. Hydrogen bond was formed between the amine group of *2a* and oxygen atom of hydroxyl group of THR134. And, the NH group of *3a* formed the hydrogen bond with ASP352. On the other hand, *5a*, *7b* and

8b did not hydrogen bonding with receptor. Apart from this, the Surflex–Dock scores gave the value of $-\log(K_d)$ and the free energy of binding (kJ/mol) of a ligand to a protein that present by total score and CHEMSCORE, respectively. In addition, Support Vector Machine (SVM) data for screening of active compounds by using D₂ ligands with binding affinity K_i and IC_{50} less than 1 μ M were collected from ChEMBLdb database (**Table 4**).

Table 4 Predicted binding affinity of dopamine and serotonin receptor to various ligands by Surflex-DOCK and SVM.

Compound	Surflex-DOCK D ₃ (PDB: 3PBL)		Surflex-DOCK 5HT _{2B} (PDB: 4IAR)		SVM*	
	$-\log(K_d)$	$\Delta G_{binding}$	$-\log(K_d)$	$\Delta G_{binding}$	D ₂	5HT
Dopamine	3.75	-19.58	4.99	-20.22	1	-1
Serotonin	5.28	-26.37	5.06	-26.00	1	1
1a	5.96	-28.90	6.88	-36.46	-1	-1
2a	6.24	-31.97	6.06	-40.54	-1	-1
3a	9.07	-41.46	7.66	-42.15	-1	-1
5a	5.94	-45.89	6.58	-30.57	-1	-1
7b	-0.50	-41.23	6.07	-25.77	1	-1
8b	3.44	-37.47	4.58	-34.13	1	-1
Aripiprazole	8.41	-39.02	8.88	-38.00	1	1
Bromocriptine	-1.19	-36.07	4.87	-32.73	1	-1
Clozapine	5.78	-33.33	3.87	-35.47	1	1
Fluphenazine	7.38	-38.87	8.02	-27.38	1	1
Haloperidol	7.84	-35.38	6.42	-30.45	1	1
Olanzapine	2.98	-25.66	5.29	-38.61	1	1
Risperidone	5.92	-29.84	7.75	-34.21	1	1
Spiperone	6.93	-36.17	6.78	-29.83	1	1
(S)(-)-Raclopride tartrate salt	4.13	-21.82	6.38	-26.75	-1	-1
(R)(+)- SCH23390	2.77	-31.97	3.92	-28.05	1	1

* For SVM ; 1 = active, -1 = inactive at $IC_{50} < 1 \mu$ M.

The reaction products from the MIP nanovessels that was achieved, produced Surflex-Dock scores and pK_d values, as shown in **Table 4** from chlorobutylphenone and the amine precursors more than 5.94 for both the dopamine D_3 and serotonin $5HT_{2B}$ receptors. The $\Delta G_{binding}$ of the synthesized compounds presented low binding energy. Both methacrylate derivatives of clozapine (**7b** and **8b**) were active for dopamine D_2 receptor and IC_{50} were less than 1 μ M. Moreover, the resulted compounds from mold reaction both the D-MIP and DS-MIP had binding affinities related to the well-known compounds used.

However, it is necessary to test biological activity with biological protein receptor. The biological receptors isolated from Wistar rat hypothalamus in ligand binding characteristics that represent the biological activity of the chemical compounds. The chlorobutylphenone-type ligands from mold reaction in the cavities as the template were determined by competitive ligand binding assay for D_1R with SCH23390 using LC-MS-MS method. **Table 5** shows the data of binding capacity and $\log ED_{50}$ of the test compounds for the natural D_1R from hypothalamus. The maximal binding affinity was obtained in order: **5a**>**2a**>**3a**>**1a**, while $\log ED_{50}$ of the compounds, **5a**>**1a**>**3a**>**2a**, was observed. The results of pharmacological screening indicated that MIP nanovessel is highly potential for creating dopamine-associated compounds that have biological activities related to the template.

Table 5 Biological activity of chlorobutyrophenone derivatives for D₁R ($R^2 > 0.990$).

Compound	B_{max} (μ M)	K_d (nM)	log ED_{50}
1a	0.423	141	6.26
2a	0.435	227	3.20
3a	0.437	207	5.02
5a	0.467	558	6.79

The investigation of function and photophysical properties of the hypothalamus proteins

The main objective of this study was to determine intrinsic properties of the ligand that a changed fluorescence spectral in an attached ligand via the use of dopamine and serotonin MIP binding sites either with or without the isolated rat hypothalamus. The difference of red-shift fluorescence spectra was obtained when the clozapine was adsorbed on the MIP with the addition of methacryloyl chloride that it is because of the clozapine enter the MIP binding sites and anchored part outside was within solution, as shown in **Figure 7**. This can be explained as that clozapine oriented and accessibility that resulted from deposition led to the observed spectral changes.

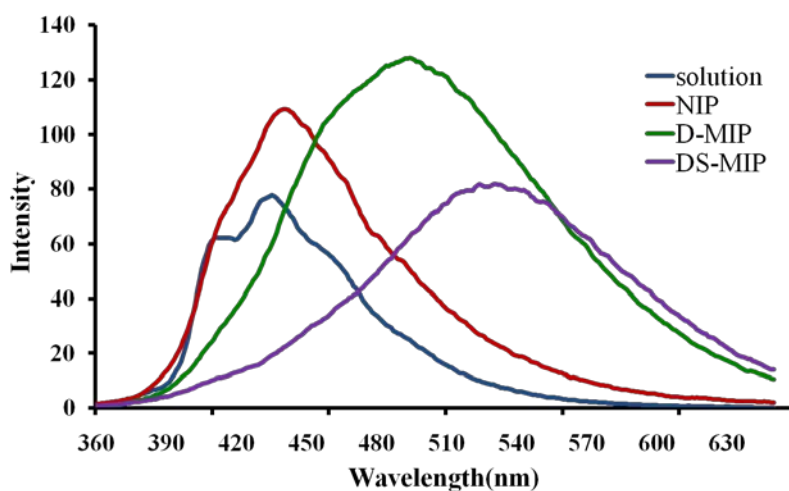


Figure 7 Fluorescence emission spectra of the clozapine in the presence of methacryloyl chloride and AIBN for D-MIP, DS-MIP and control polymer at excitation wavelength 341 nm.

Upon titration of a series of methacryloyl chloride concentrations with fluorescence assay where the MIP-bound clozapine were determined for the maximal wavelength in the region between 360-630 nm. For MIPs, the relative fluorescence intensity of clozapine rapidly increased but control polymer slightly increased with the relative fluorescence intensity. These results suggested that the orientation of clozapine in the presence of the methacryloyl chloride on the polymerization. The fluorescence of clozapine was examined at various methacryloyl chloride concentrations fluorescence spectroscopy have shown that the clozapine oriented different positions. These changes in the fluorescence spectra of the bound methacrylate derivative of clozapine reflect electron transition energies of the excited state. Furthermore, the effect of zinc gave the significantly different on fluorescence spectra. The results suggested that the differences of the clozapine fluorescence in the MIP binding site exhibited the overall kinetics of clozapine association with the

protein receptor, allows one to conduct extensive structure-activity studies and overall structural changes in the molecule. The change in fluorescence and quantum efficiency in the case of clozapine derivative in MIP cavities both with and without Zn(II) depended on temperature that obtained from DS-MIP in the addition of the hypothalamus protein, as shown in **Figure 8A** and **8B**. The surface area and a relatively small volume of D-MIP were shown but it provided different selectivity and temperature responses in the presence of Zn(II) with the protein.

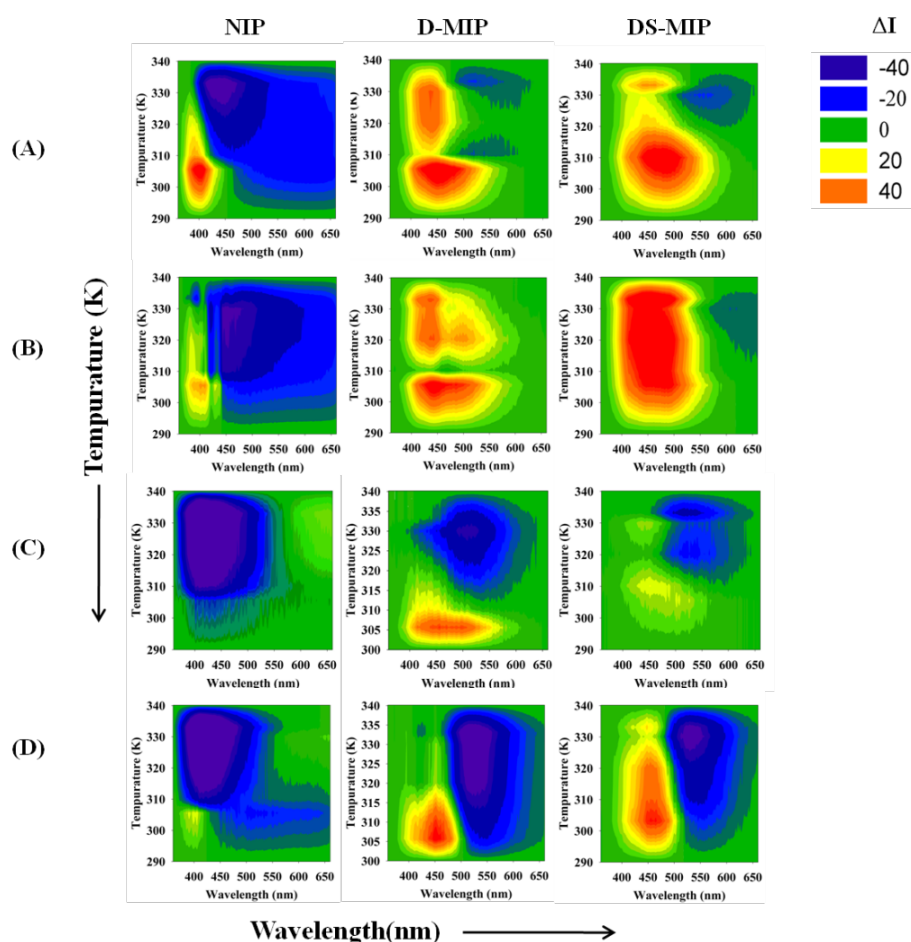


Figure 8 The effect of temperature on fluorescent spectra ($\lambda_{\text{ex}} = 340 \text{ nm}$) of clozapine in the solution for MIPs and NIP in the presence of methacryloyl chloride; (A) without Zn(II), (B) with Zn(II), (C) the addition of protein (200 μ g) without Zn(II), and (D) with Zn(II).

Figure 8C shows the behavior of clozapine fluorescence for both the MIPs in protein matrix. The results revealed that the hypothalamus protein affected the fluorescent intensity in the MIPs with increasing temperature by which the positions and organization of the reacted component in assemblies. Both the MIPs can be used as probe for the assembled dopamine receptors which the binding sites provided by prearrangement of the functionality of template complementary to functional monomers.

The development of D₁R-MIP based QCM sensor

The molecular imprinting technique was used to generate the recognition on the D₁R-imprinted polymer (D₁R-MIP) using D₁R as the template. D₁R-MIP has been prepared by stamping method. The generation of the D₁R-MIP on the QCM was carried out to mimic D₁R binding site by using two functional monomers, acrylic acid (AA) and *N*-vinylpyrrolidone (NVP), and *N,N'*-(1,2-dihydroxy-ethylene)-bisacrylamide (DHEBA) as the cross-linker. The optimal monomer ratio of AA:NVP:DHEBA was achieved at 2:3:12 molar ratio for preparation of thin film onto QCM electrodes due to the best binding site and excellent selectivity. AFM images showed the surface topographies of D₁R-MIP and NIP that were different although the same monomer mixture used but without a template. The surface of MIP with high pillars or column shape with D₁R was obtained, while NIP showed very low surface roughness.

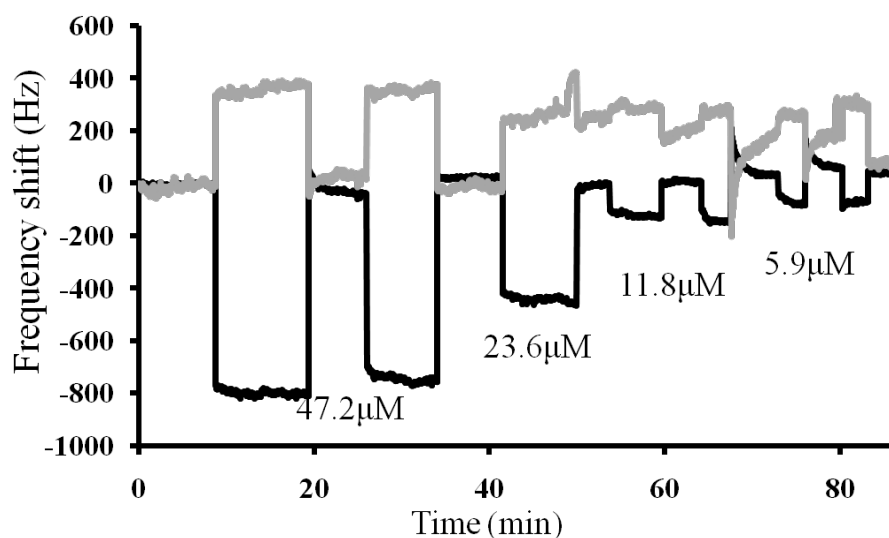


Figure 9 Sensor signals for MIP and NIP containing different amounts of D₁R in PBS buffer.

Figure 9 shows frequency response of D₁R at different concentrations on the D₁R-MIP on the QCM sensor. Strong adhesion between receptor and the imprinted cavities exhibited the properties of the imprinted polymers and the recognition selectivity toward the template protein and influence of D₁R in PBS both with and without stabilizer or BSA. This result confirmed that the signal response from D₁R obtained with the addition of the stabilizer and BSA, indicating that these compounds had no effect on sensor signal. The results revealed the imprinting effect due to the recognition by MIP to the template. The NIP showed positive frequency responses which suggested the mobility of analyte on the surface of the layer coating. An appreciable sensor characteristic was clearly shown with reversible signal is rapid within 30 min. The three-dimensional D₁R proteins deposited onto the MIP layer coating on the QCM that protein binding site was immobilized on the MIP, would be applied for sensor measurement in dopaminergic receptor-ligand binding assay. For this purpose, the agonist, dopamine HCl, and antagonists, haloperidol and SCH23390,

were tested which the frequency responses for these compounds produced IC_{50} and K_d values depending on the selectivity of D₁R-MIP. **Table 6** shows IC_{50} and K_d values correlated well with the value determined in previous study. The results showed that D₁R-MIP-QCM sensor can detect these compounds showing affinity to D₁R. However, the test compound with low affinity cannot be detected in lower concentration of dopamine HCl (< 9.4 μ M). The results suggested that D₁R-MIP on the QCM sensor provided the well-organized binding site of MIP and high efficiency of the MIP is due the surface chemistry the accessibility of the binding site, hence the possibility of receptor-ligand binding assay. The result also suggested that the stabilizer used preserved the active site of D₁R receptor on the MIP.

Table 6 B_{max} , K_d and EC_{50} values for each compound were calculated by Sigma plot.

Test compound	B_{max}	K_d (nM)	EC_{50} (nM)	IC_{50} or EC_{50} (ref.) (nM)
Dopamine	242	0.874	517×10^3	5000 (Mottola <i>et al.</i> , 1996), 39* (Risgaard <i>et al.</i> , 2014)
Haloperidol	242	25.7	1904	550 (Iorio <i>et al.</i> , 1987), 620 ⁺ (Höfner and Wanner, 2003)
(+)-SCH23390	43.0	0.004	0.283	0.57 (Brewster <i>et al.</i> , 1995), 0.60* (Sun <i>et al.</i> , 2013)

* D₁R from Homo sapiens

+ D₁R from Sus scrofa (pig)

CHAPTER 4

CONCLUSION

The development of MIPs was carried out to act as artificial dopamine and serotonin receptors and used as single dopamine and/or dual dopamine and serotonin templates that mimicked the binding sites of these receptors. The MIP nanosized cavities had properties that helped them to create dopamine analogs that had biological activity and were related to the printed molecule for recognition of the dopamine and serotonin receptors. Also, the cavity of the MIPs was used as a probe to tag the functions and photophysical properties of drugs. Changes of fluorescence for the drug clozapine occurred at higher temperatures, particularly with the MIP prepared by using mixed dopamine and serotonin. This indicated that the drug was oriented on the natural receptor with the additional small molecules or biomarkers for the MIP and this was highly useful for examining the activity of the drug at the target site. This alternative method may help to provide a better understanding of the binding characteristic of the neural receptor and function, and also the interactions between the subtypes or other receptors. This screening strategy made use of the high affinity and specificity of the MIPs, although the shape of the test compounds at the various binding sites of imprinted cavity may differ from the actual biological situation. However this approach can accelerate the search for candidates for new drugs. The computer aids tool would be employed for determination of the properties of the recognition cavities generated by the bioactive template molecules. Therefore, the imprinted cavities obtained from the dopamine and serotonin as templates can act as mimics for the natural active site of receptor. These bioanalogous receptors have a

more stable site of their predefined cavity than a natural receptor and they can be reused several times. In addition, the D₁R-MIP was prepared on a QCM to detect the recognition ability to the template protein as a result of the sensor measurement. This MIP had a high selectivity and provided a sensitive sensor signal towards the D₁R. The sensor measurement by the D₁R-MIP was examined during the D₁R receptor-ligand binding assay as well as for the binding site characteristics of the agonist and the antagonists on the D₁R. The computer docking information was combined with this method, although the crystal structure of the protein was obtained from the protein data bank, to help to screen for compounds that would be active with the natural neural receptor. The precise structure of the D₁R in the MIP-QCM sensor as well as those for the other receptors used should be examined by X-ray, protein crystallization *etc.*

The single dopamine- and dual dopamine/serotonin-molecularly imprinted polymer reflected the importance of the active site for the receptors for dopamine and serotonin. For future work, these imprinted binding sites will be applied to study other reactions of appropriate reagents on the binding sites in nanocavities of the MIP and the multiple sites for monitoring the interaction between other drugs and the natural neural receptor. This alternative method of using the protein-MIP-QCM sensor will be developed to measure the receptor-ligand binding and will be potentially useful for screening for the binding affinity of compounds that could be used to treat psychotic diseases.

REFERENCES

- Adali-Kaya, Z., Tse Sum Bui, B., Falcimaigne-Cordin, A. and Haupt, K. 2015. Molecularly imprinted polymer nanomaterials and nanocomposites: atom-transfer radical polymerization with acidic monomers. *Angewandte Chemie International Edition in English* 54: 5192-5195.
- Alberto, R., Schibli, R., Schubiger, A.P., Abram, U., Pietzsch, H.-J. and Johannsen, B. 1999. First Application of fac-[$^{99m}\text{Tc}(\text{OH}_2)_3(\text{CO})_3$]⁺ in bioorganometallic chemistry: design, structure, and in vitro affinity of a 5-HT_{1A} receptor ligand labeled with ^{99m}Tc . *Journal of the American Chemical Society* 121: 6076-6077.
- Alenus, J., Ethirajan, A., Horemans, F., Weustenraed, A., Csipai, P., Gruber, J., Peeters, M., Cleij, T. and Wagner, P. 2013. Molecularly imprinted polymers as synthetic receptors for the QCM-D-based detection of *L*-nicotine in diluted saliva and urine samples. *Analytical and bioanalytical chemistry* 405: 6479-6487.
- Alexander, C., Davidson, L. and Hayes, W. 2003. Imprinted polymers: artificial molecular recognition materials with applications in synthesis and catalysis. *Tetrahedron* 59: 2025-2057.
- Ansell, R.J., Kriz, D. and Mosbach, K. 1996. Molecularly imprinted polymers for bioanalysis: chromatography, binding assays and biomimetic sensors. *Current Opinion in Biotechnology* 7: 89-94.
- Baker, J.G., Middleton, R., Adams, L., May, L.T., Briddon, S.J., Kellam, B. and Hill, S.J. 2010. Influence of fluorophore and linker composition on the

- pharmacology of fluorescent adenosine A(1) receptor ligands. *British Journal of Pharmacology* 159: 772-786.
- Baltus, R.E., Carmon, K.S. and Luck, L.A. 2007. Quartz crystal microbalance (QCM) with immobilized protein receptors: comparison of response to ligand binding for direct protein immobilization and protein attachment via disulfide linker. *Langmuir* 23: 3880-3885.
- Bompart, M., Goto, A., Wattraint, O., Sarazin, C., Tsujii, Y., Gonzato, C. and Haupt, K. 2015. Molecularly imprinted polymers by reversible chain transfer catalysed polymerization. *Polymer* 78: 31-36.
- Bonini, F., Piletsky, S., Turner, A.P.F., Speghini, A. and Bossi, A. 2007. Surface imprinted beads for the recognition of human serum albumin. *Biosensors and Bioelectronics* 22: 2322-2328.
- Brewster, W.K., Nichols, D.E., Watts, V.J., Riggs, R.M., Mottola, D., Mailman, R.B., 1995. Evaluation of *cis*- and *trans*-9- and 11-hydroxy-5,6,6a,7,8,12b-hexahydrobenzo[a]-15phenanthridines as structurally rigid, selective D1 dopamine receptor ligands. *Journal of medicinal chemistry*, 38: 318-327.
- Bunde, R.L., Jarvi, E.J. and Rosentreter, J.J. 1998. Piezoelectric quartz crystal biosensors. *Talanta* 46: 1223-1236.
- Cela-Pérez, M.C., Castro-López, M.M., Lasagabáster-Latorre, A., López-Vilariño, J.M., González-Rodríguez, M.V. and Barral-Losada, L.F. 2011. Synthesis and characterization of bisphenol-A imprinted polymer as a selective recognition receptor. *Analytica Chimica Acta* 706: 275-284.

- De, S., Macara, I.G. and Lannigan, D.A. 2005. Novel biosensors for the detection of estrogen receptor ligands. *The Journal of Steroid Biochemistry and Molecular Biology* 96: 235-244.
- Díaz-Álvarez, M. and Turiel, E. 2015. Improved molecularly imprinted polymer grafted to porous polyethylene frits for the solid-phase extraction of thiabendazole from citrus sample extracts. *Molecular Imprinting* 2: 30-36.
- Eren, T., Atar, N., Yola, M.L. and Karimi-Maleh, H. 2015. A sensitive molecularly imprinted polymer based quartz crystal microbalance nanosensor for selective determination of lovastatin in red yeast rice. *Food chemistry* 185: 430-436.
- Ferrance, J.P. 2007. Gellan beads as a transparent media for protein immobilization and affinity capture. *Journal of Chromatography A* 1165: 86-92.
- Foguel, M.V., Ton, X.-A., Zanoni, M.V., Maria Del Pilar, T.S., Haupt, K. and Bui, B.T.S. 2015. A molecularly imprinted polymer-based evanescent wave fiber optic sensor for the detection of basic red 9 dye. *Sensors and Actuators B: Chemical* 218: 222-228.
- Garcia-Serna, R. and Mestres, J. 2011. Chemical probes for biological systems. *Drug Discovery Today* 16: 99-106.
- Guo, M.-J., Zhao, Z., Fan, Y.-G., Wang, C.-H., Shi, L.-Q., Xia, J.-J., Long, Y. and Mi, H.-F. 2006. Protein-imprinted polymer with immobilized assistant recognition polymer chains. *Biomaterials* 27: 4381-4387.
- Heils, A., Teufel, A., Petri, S., Stober, G., Riederer, P., Bengel, D. and Lesch, K.P. 1996. Allelic variation of human serotonin transporter gene expression. *Journal of Neurochemistry* 66: 2621-2624.

- Höfner, G. and Wanner, K.T. 2003. Competitive binding assays made easy with a native marker and mass spectrometric quantification. *Angewandte Chemie International Edition* 42: 5235-5237.
- Horacek, J., Bubenikova-Valesova, V., Kopecek, M., Palenicek, T., Dockery, C., Mohr, P. and schl, C. 2006. Mechanism of action of atypical antipsychotic drugs and the neurobiology of schizophrenia. *CNS Drugs* 20: 389-409.
- Hoshino, Y., Kodama, T., Okahata, Y. and Shea, K.J. 2008. Peptide imprinted polymer nanoparticles: a plastic antibody. *Journal of the American Chemical Society* 130: 15242-15243.
- Hughes, J.P., Rees, S., Kalindjian, S.B. and Philpott, K.L. 2011. Principles of early drug discovery. *British Journal of Pharmacology* 162: 1239-1249.
- Iorio, M.A., Reymer, T.P., Frigeni, V., 1987. Combined analgesic/neuroleptic activity in Nbutyrophenone prodine-like compounds. *Journal of medicinal chemistry*, 30, 1906-1910.
- Jafari, S., Fernandez-Enright, F. and Huang, X.-F. 2012. Structural contributions of antipsychotic drugs to their therapeutic profiles and metabolic side effects. *Journal of Neurochemistry* 120: 371-384.
- Javanbakht, M., Attaran, A.M., Namjumanesh, M.H., Esfandyari-Manesh, M. and Akbari-adergani, B. 2010. Solid-phase extraction of tramadol from plasma and urine samples using a novel water-compatible molecularly imprinted polymer. *Journal of Chromatography B* 878: 1700-1706.
- Jenik, M., Schirhagl, R., Schirk, C., Hayden, O., Lieberzeit, P., Blaas, D., Paul, G. and Dickert, F.L. 2009. Sensing picornaviruses using molecular imprinting

- techniques on a quartz crystal microbalance. *Analytical chemistry* 81: 5320-5326.
- Jonker, N., Kool, J., Irth, H. and Niessen, W.M.A. 2011. Recent developments in protein–ligand affinity mass spectrometry. *Analytical and Bioanalytical Chemistry* 399: 2669-2681.
- Jonker, N., Kretschmer, A., Kool, J., Fernandez, A., Kloos, D., Krabbe, J.G., Lingeman, H. and Irth, H. 2009. Online magnetic bead dynamic protein-affinity selection coupled to LC–MS for the screening of pharmacologically active compounds. *Analytical Chemistry* 81: 4263-4270.
- Karimian, N., Turner, A.P. and Tiwari, A. 2014. Electrochemical evaluation of troponin T imprinted polymer receptor. *Biosensors and Bioelectronics* 59: 160-165.
- Kempe, H., Pujolràs, A.P. and Kempe, M. 2015. Molecularly imprinted polymer nanocarriers for sustained release of erythromycin. *Pharmaceutical research* 32: 375-388.
- Kirsch, N., Hedin-Dahlström, J., Henschel, H., Whitcombe, M.J., Wikman, S. and Nicholls, I.A. 2009. Molecularly imprinted polymer catalysis of a Diels-Alder reaction. *Journal of Molecular Catalysis B: Enzymatic* 58: 110-117.
- Konradi, C. and Heckers, S. 2001. Antipsychotic drugs and neuroplasticity: insights into the treatment and neurobiology of schizophrenia. *Biological Psychiatry* 50: 729-742.
- Kotova, K., Hussain, M., Mustafa, G. and Lieberzeit, P.A. 2013. MIP sensors on the way to biotech applications: Targeting selectivity. *Sensors and Actuators B: Chemical* 189: 199-202.

- Kumar Singh, A. and Singh, M. 2015. QCM sensing of melphalan via electropolymerized molecularly imprinted polythiophene films. *Biosensors and Bioelectronics* 74: 711-717.
- Kunath, S., Panagiotopoulou, M., Maximilien, J., Marchyk, N., Sanger, J. and Haupt, K. 2015. Cell and tissue imaging with molecularly imprinted polymers as plastic antibody mimics. *Advanced healthcare materials* 4: 1322-1326.
- Latif, U., Qian, J., Can, S. and Dickert, F. 2014. Biomimetic receptors for bioanalyte detection by quartz crystal microbalances - from molecules to cells. *Sensors* 14: 23419.
- Lawler, C.P., Prioleau, C., Lewis, M.M., Mak, C., Jiang, D., Schetz, J.A., Gonzalez, A.M., Sibley, D.R. and Mailman, R.B. 1999. Interactions of the novel antipsychotic aripiprazole (OPC-14597) with dopamine and serotonin receptor subtypes. *Neuropsychopharmacology* 20: 612-627.
- Lee, J., Bernard, S. and Liu, X.C. 2009. Nanostructured biomimetic catalysts for asymmetric hydrogenation of enamides using molecular imprinting technology. *Reactive and Functional Polymers* 69: 650-654.
- Li, N., Zhao, L., Ng, T.B., Wong, J.H., Yan, Y., Shi, Z. and Liu, F. 2015. Separation and purification of the antioxidant compound hispidin from mushrooms by molecularly imprinted polymer. *Applied microbiology and biotechnology* 99: 7569-7577.
- Liu, D., Guo, J., Luo, Y., Broderick, D.J., Schimerlik, M.I., Pezzuto, J.M. and van Breemen, R.B. 2007. Screening for ligands of human retinoid x receptor- α using ultrafiltration mass spectrometry. *Analytical Chemistry* 79: 9398-9402.

- Liu, J., Deng, Q., Tao, D., Yang, K., Zhang, L., Liang, Z. and Zhang, Y. 2014. Preparation of protein imprinted materials by hierarchical imprinting techniques and application in selective depletion of albumin from human serum. *Scientific Reports* 4: 5487
- Lohse, M.J., Nuber, S. and Hoffmann, C. 2012. Fluorescence/bioluminescence resonance energy transfer techniques to study g-protein-coupled receptor activation and signaling. *Pharmacological Reviews* 64: 299-336.
- Lu, C.-H., Zhang, Y., Tang, S.-F., Fang, Z.-B., Yang, H.-H., Chen, X. and Chen, G.-N. 2012. Sensing HIV related protein using epitope imprinted hydrophilic polymer coated quartz crystal microbalance. *Biosensors and Bioelectronics* 31: 439-444.
- Macdonald, D., Murgolo, N., Zhang, R., Durkin, J.P., Yao, X., Strader, C.D. and Graziano, M.P. 2000. Molecular characterization of the melanin-concentrating hormone/receptor complex: identification of critical residues involved in binding and activation. *Molecular Pharmacology* 58: 217-225.
- Martres, M., Bouthenet, M., Sales, N., Sokoloff, P. and Schwartz, J. 1985. Widespread distribution of brain dopamine receptors evidenced with [¹²⁵I]iodosulpride, a highly selective ligand. *Science* 228: 752-755.
- Mergola, L., Scorrano, S., Del Sole, R., Lazzoi, M.R. and Vasapollo, G. 2013. Developments in the synthesis of a water compatible molecularly imprinted polymer as artificial receptor for detection of 3-nitro-*L*-tyrosine in neurological diseases. *Biosensors and Bioelectronics* 40: 336-341.

- Michel, J., Verdonk, M.L. and Essex, J.W. 2006. Protein-Ligand Binding Affinity Predictions by Implicit Solvent Simulations: A Tool for Lead Optimization? *Journal of Medicinal Chemistry* 49: 7427-7439.
- Mohajeri, S.A., Malaekheh-Nikouei, B. and Sadegh, H. 2012. Development of a pH-responsive imprinted polymer for diclofenac and study of its binding properties in organic and aqueous media. *Drug Development and Industrial Pharmacy* 38: 616-622.
- Mottola, D.M., Laiter, S., Watts, V.J., Tropsha, A., Wyrick, S.D., Nichols, D.E., Mailman, R.B., 1996. Conformational analysis of D₁ dopamine receptor agonists: pharmacophore assessment and receptor mapping. *Journal of Medicinal Chemistry*, 39: 285-296.
- Mosbach, K., Yu, Y., Andersch, J. and Ye, L. 2001. Generation of new enzyme inhibitors using imprinted binding sites: The anti-idiotypic approach, a step toward the next generation of molecular imprinting. *Journal of the American Chemical Society* 123: 12420-12421.
- O'Sullivan, C.K. and Guilbault, G.G. 1999. Commercial quartz crystal microbalances – theory and applications. *Biosensors and Bioelectronics* 14: 663-670.
- Paiva, A.M., Vanderwall, D.E., Blanchard, J.S., Kozarich, J.W., Williamson, J.M. and Kelly, T.M. 2001. Inhibitors of dihydrodipicolinate reductase, a key enzyme of the diaminopimelate pathway of *Mycobacterium tuberculosis*. *Biochimica et Biophysica Acta (BBA) - Protein Structure and Molecular Enzymology* 1545: 67-77.
- Poma, A., Guerreiro, A., Whitcombe, M.J., Piletska, E.V., Turner, A.P. and Piletsky, S.A. 2013. Solid-Phase synthesis of molecularly imprinted polymer

- nanoparticles with a reusable template–“Plastic Antibodies”. *Advanced Functional Materials* 23: 2821-2827.
- Ramström, O., Nicholls, I.A. and Mosbach, K. 1994. Synthetic peptide receptor mimics: highly stereoselective recognition in non-covalent molecularly imprinted polymers. *Tetrahedron: Asymmetry* 5: 649-656.
- Ratautaite, V., Plausinaitis, D., Baleviciute, I., Mikoliunaite, L., Ramanaviciene, A. and Ramanavicius, A. 2015. Characterization of caffeine-imprinted polypyrrole by a quartz crystal microbalance and electrochemical impedance spectroscopy. *Sensors and Actuators B: Chemical* 212: 63-71.
- Ren, X. and Chen, L. 2015. Quantum dots coated with molecularly imprinted polymer as fluorescence probe for detection of cyphenothrin. *Biosensors and Bioelectronics* 64: 182-188.
- Risgaard, R., Jensen, M., Jørgensen, M., Bang-Andersen, B., Christoffersen, C.T., Jensen, K.G., Kristensen, J.L., Püschl, A., 2014. Synthesis and SAR study of a novel series of dopamine receptor agonists. *Bioorganic & Medicinal Chemistry*, 22: 381-392.
- Rostamizadeh, K., Vahedpour, M. and Bozorgi, S. 2012. Synthesis, characterization and evaluation of computationally designed nanoparticles of molecularly imprinted polymers as drug delivery systems. *International journal of pharmaceutics* 424: 67-75.
- Roth, B.L., Meltzer, H.Y. and Khan, N. 1997. Binding of Typical and Atypical Antipsychotic Drugs to Multiple Neurotransmitter Receptors. *Advances in Pharmacology*. David S. Goldstein, G.E. and Richard, M., Academic Press 42: 482-485.

- Sasikumar, T.K., Burnett, D.A., Zhang, H., Smith-Torhan, A., Fawzi, A. and Lachowicz, J.E. 2006. Hydrazides of clozapine: A new class of D₁ dopamine receptor subtype selective antagonists. *Bioorganic & Medicinal Chemistry Letters* 16: 4543-4547.
- Saridakis, E. and Chayen, N.E. 2013. Imprinted polymers assisting protein crystallization. *Trends in Biotechnology* 31: 515-520.
- Sellergren, B. and Allender, C.J. 2005. Molecularly imprinted polymers: A bridge to advanced drug delivery. *Advanced Drug Delivery Reviews* 57: 1733-1741.
- Sharma, P.S., Iskierko, Z., Pietrzyk-Le, A., D'Souza, F. and Kutner, W. 2015. Bioinspired intelligent molecularly imprinted polymers for chemosensing: A mini review. *Electrochemistry Communications* 50: 81-87.
- Shi, H., Tsai, W.-B., Garrison, M.D., Ferrari, S. and Ratner, B.D. 1999. Template-imprinted nanostructured surfaces for protein recognition. *Nature* 398: 593-597.
- Shiomi, T., Matsui, M., Mizukami, F. and Sakaguchi, K. 2005. A method for the molecular imprinting of hemoglobin on silica surfaces using silanes. *Biomaterials* 26: 5564-5571.
- Shoichet, B.K. 2004. Virtual screening of chemical libraries. *Nature* 432: 862-865.
- Sontimuang, C., Suedee, R., Canyuk, B., Phadoongsombut, N. and Dickert, F.L. 2011. Development of a rubber elongation factor, surface-imprinted polymer-quartz crystal microbalance sensor, for quantitative determination of Hev b1 rubber latex allergens present in natural rubber latex products. *Analytica Chimica Acta* 687: 184-192.

- Suedee, R., Seechamnaturakit, V., Canyuk, B., Ovatlarnporn, C. and Martin, G.P. 2006. Temperature sensitive dopamine-imprinted (*N,N*-methylene-bis-acrylamide cross-linked) polymer and its potential application to the selective extraction of adrenergic drugs from urine. *Journal of Chromatography A* 1114: 239-249.
- Suedee, R., Seechamnaturakit, V., Sukswan, A. and Canyuk, B. 2008. Recognition properties and competitive assays of a dual dopamine/serotonin selective molecularly imprinted polymer. *International Journal of Molecular Sciences* 9: 2333-2356.
- Sukswan, A., Lomlim, L., Dickert, F.L. and Suedee, R. 2015. Tracking the chemical surface properties of racemic thalidomide and its enantiomers using a biomimetic functional surface on a quartz crystal microbalance. *Journal of Applied Polymer Science* 132: 42309
- Sun, H., Zhu, L., Yang, H., Qian, W., Guo, L., Zhou, S., Gao, B., Li, Z., Zhou, Y., Jiang, H., Chen, K., Zhen, X., Liu, H., 2013. Asymmetric total synthesis and identification of tetrahydroprotoberberine derivatives as new antipsychotic agents possessing a dopamine D₁, D₂ and serotonin 5-HT_{1A} multi-action profile. *Bioorganic & Medicinal Chemistry*, 21, 856-868.
- Sun, W., Tan, R., Zheng, W. and Yin, D. 2013. Molecularly imprinted polymer containing Fe(III) catalysts for specific substrate recognition. *Chinese Journal of Catalysis* 34: 1589-1598.
- Tai, D.-F., Lin, C.-Y., Wu, T.-Z. and Chen, L.-K. 2005. Recognition of dengue virus protein using epitope-mediated molecularly imprinted film. *Analytical Chemistry* 77: 5140-5143.

- Tang, Y., Gao, Z., Wang, S., Gao, X., Gao, J., Ma, Y., Liu, X. and Li, J. 2015. Upconversion particles coated with molecularly imprinted polymers as fluorescence probe for detection of clenbuterol. *Biosensors and Bioelectronics* 71: 44-50.
- Titirici, M.M., Hall, A.J. and Sellergren, B. 2003. Hierarchical imprinting using crude solid phase peptide synthesis products as templates. *Chemistry of Materials* 15: 822-824.
- Tung, Y.-T., Chang, C.-C., Lin, Y.-L., Hsieh, S.-L. and Wang, G.-J. 2016. Development of double-generation gold nanoparticle chip-based dengue virus detection system combining fluorescence turn-on probes. *Biosensors and Bioelectronics* 77: 90-98.
- van Breemen, R.B., Huang, C.-R., Nikolic, D., Woodbury, C.P., Zhao, Y.-Z. and Venton, D.L. 1997. Pulsed ultrafiltration mass spectrometry: a new method for screening combinatorial libraries. *Analytical chemistry* 69: 2159-2164.
- Vasapollo, G., Sole, R.D., Mergola, L., Lazzoi, M.R., Scardino, A., Scorrano, S. and Mele, G. 2011. Molecularly imprinted polymers: present and future prospective. *International Journal of Molecular Sciences* 12: 5908.
- Wackerlig, J. and Lieberzeit, P.A. 2015. Molecularly imprinted polymer nanoparticles in chemical sensing-synthesis, characterisation and application. *Sensors and Actuators B: Chemical* 207: 144-157.
- Wang, J., Chen, Z.Y., Zhao, M.P. and Li, Y.Z. 2007. Catalytical oxidation of styrene by molecularly imprinted polymer with phenylacetic acid as template and hemin as co-monomer. *Chinese Chemical Letters* 18: 981-984.

- Workman, P. and Collins, I. 2010. Probing the probes: Fitness factors for small molecule tools. *Chemistry & Biology* 17: 561-577.
- Wulff, G. 1995. Molecular imprinting in cross-linked materials with the aid of molecular templates- a way towards artificial antibodies. *Angewandte Chemie International Edition in English* 34: 1812-1832.
- Wulff, G.n. and Liu, J. 2011. Design of biomimetic catalysts by molecular imprinting in synthetic polymers: the role of transition state stabilization. *Accounts of Chemical Research* 45: 239-247.
- Xu, X., Zhu, L. and Chen, L. 2004. Separation and screening of compounds of biological origin using molecularly imprinted polymers. *Journal of Chromatography B* 804: 61-69.
- Yola, M.L., Uzun, L., Özaltın, N. and Denizli, A. 2014. Development of molecular imprinted nanosensor for determination of tobramycin in pharmaceuticals and foods. *Talanta* 120: 318-324.
- Zhang, H., Piacham, T., Drew, M., Patek, M., Mosbach, K. and Ye, L. 2006. molecularly imprinted nanoreactors for regioselective huisgen 1,3-dipolar cycloaddition reaction. *Journal of the American Chemical Society* 128: 4178-4179.

APPENDICES

Appendix 1 Reprints of papers, manuscript and proceeding

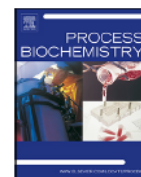
Appendix 2 Vitae

REPRINTS OF PAPERS, MANUSCRIPT AND PROCEEDING

PAPER 1

An Imprinted Dopamine Receptor for Discovery of Highly Potent and
Selective D₃ Analogues with Neuroprotective Effects.

(Published in *Process Biochemistry*)



An imprinted dopamine receptor for discovery of highly potent and selective D₃ analogues with neuroprotective effects

Wanpen Naklua^a, Krishna Mahesh^a, Phern Aundorn^a, Niwan Tanmanee^a,
Kannatha Aenukulpong^a, Salilla Sutto^a, Yu Zong Chen^b, Shangying Chen^b,
Roongnapa Suedee^{a,*}

^a Molecular Recognition Materials Research Unit, Drug Delivery System Excellence Center, and NANOTEC Center of Excellence, Department of Pharmaceutical Chemistry, Faculty of Pharmaceutical Sciences, Prince of Songkla University, Hatyai 90112, Songkhla, Thailand

^b Bioinformatics and Drug Design Group, Department of Pharmacy, National University of Singapore, Blk S16 Singapore, Singapore

ARTICLE INFO

Article history:

Received 23 April 2015

Received in revised form 15 June 2015

Accepted 20 June 2015

Available online 24 June 2015

This article is dedicated to Associate Prof. Dr. Chamnan Patarapanich the occasion of his 65th birthday.

Keywords:

Molecularly imprinted polymer

Bioassays

Biomimic receptor

Neurobiology

Regenerative medicine

Impulse control disorders

ABSTRACT

In this study, we have developed a novel molecular imprinting method for the cloning of a drug with multiple templates to achieve a broad selectivity, and then produce reactive dopamine analogs. The products were produced within selective recognition sites of the artificial system prepared against dopamine (D) and serotonin (S) as a single and a mixed template. As a consequence of the functionality of the anchoring sites being was able to make proximity changes that could promote changes in the nanosized space for surface access for the reactants but avoided the non-active center of the formed nanosized assembly. The most effective analogues had a B_{max} of the DS-MIP (1.0 M per g polymer) that was about twice that of the D-MIP. The receptor–ligand interaction studies revealed differences in the absorbance by the rat hypothalamus, and indicated that an additional potent hit was obvious. The dopamine analogs had a smaller space for receptor subtypes as determined by molecular docking and the implication of the selective D₃ receptor agonists as well as the 5HT_{1b} receptors, for the treatment of Parkinson's disease. The proposed model indicated a possible role from the desired fragments that had been inserted into a specific binding pocket of the protein near to the gorge rim as being the significant pharmacophore of this class. They showed good binding affinity for the 5-HT_{1b} receptors. The screening test with a natural D₁ receptor yielded a B_{max} of 0.44 μ M and the corresponding K_d values were 100–500 nM. Thus, this process that occurred in an artificial dopamine-imprinted receptor allowed for preclinical testing to identify possible neuroleptic agents and their neuroprotective effects hopefully with reduced side effects.

© 2015 Elsevier Ltd. All rights reserved.

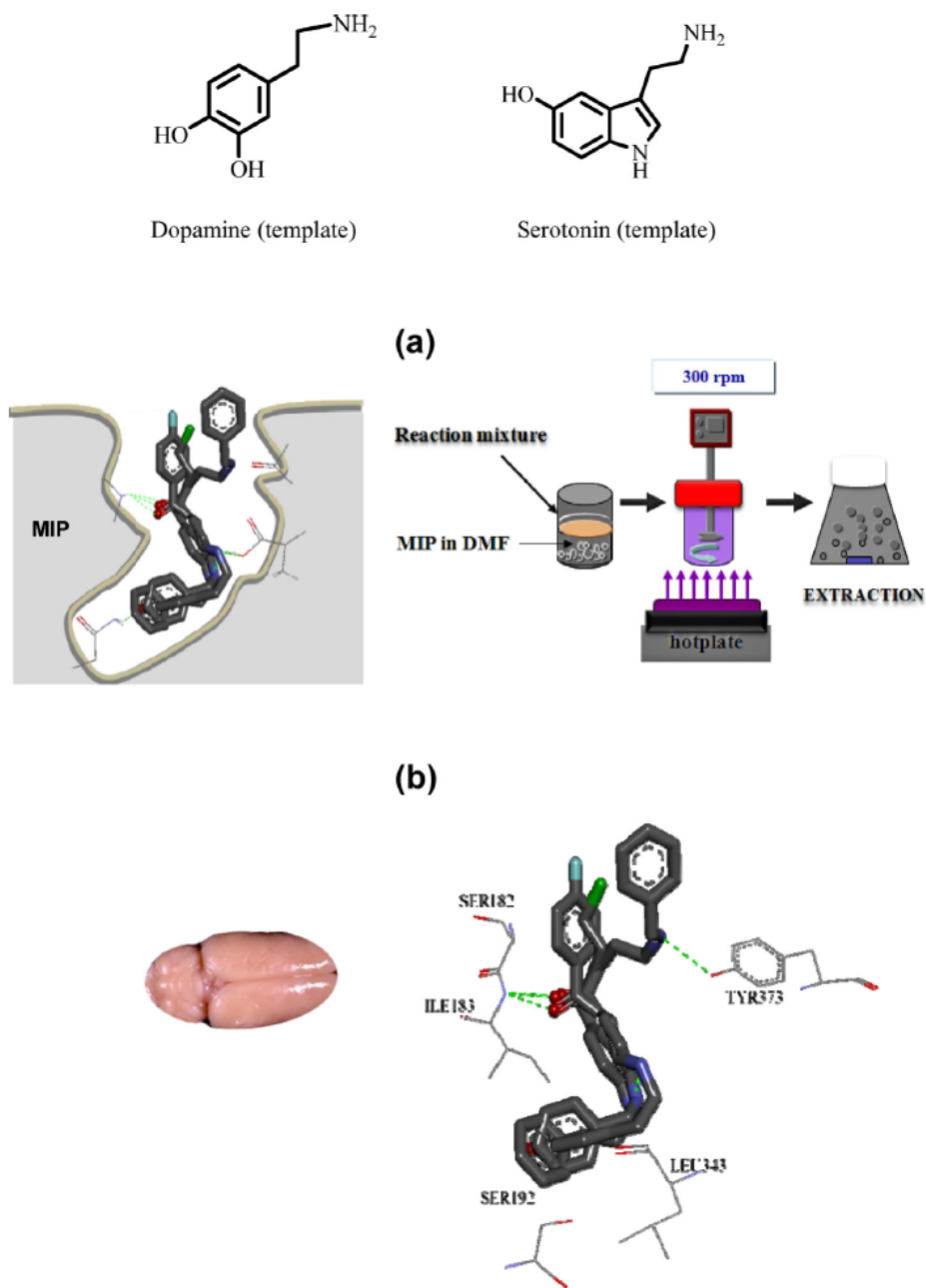
1. Introduction

The role of chemistry to provide good copies of neurobiological processes is still relatively unsophisticated yet is needed to help us to better understand the many integrated processes that occur in nature [1]. Self-assembly processes have begun to play an important role in pharmaceutical development. In most recent times it has become possible to generate synthetic self-assembly-based systems to copy and provide properties similar to those that occur in nature [2,3]. In addition such systems may allow for the development of unique applications that will enable an expansion in therapeutics to assist in ensuring clinical efficacy [4]. Research workers are now able to study biomimetics and

polymer–biopolymers, and this has led to a huge impact on biological sciences particularly those associated with many aspects of nanotechnology. This has encouraged support for research on various aspects of biomimetics. Self-recognition systems can use these self-assembly processes that are similar to those found in the selective recognition of chemicals by DNA, proteins or enzymes [5].

These specific binding interactions also occur during the assembly and formation of connections involved in brain functions that are affected by stress, illness and adaptation of reward cues in the neural network. It also allows the same brain cells to synchronize many different processes [6]. Molecular imprinting is an approach to target important components using molecular recognition. Molecular imprinting involves formation of a polymerizable preformed compound with a pre-defined recognition site within a highly crosslinked network in a polymer matrix for a template known to have biological activity [7]. Imprinted cavities that accommodate functional monomers can be fabricated when

* Corresponding author. Tel.: +66 74 288862; fax: +66 74 428239.
E-mail address: roongnapa.s@psu.ac.th (R. Suedee).



Scheme 1. (a) A schematic illustration for target identification, that was based on the synthesis of an imaged recognition surface of a hybrid molecule from the dopaminergic drug, and also included structures of the serotonergic motifs in the synthesized recognition material. (b) The view of the imprinted materials that engaged much more regioselective binding of the molecules and had direct implications for the selective D₃ receptor agonists. Inset: structures of dopamine and serotonin that were used as the templates in this study.

template molecules are mixed with a polymerizing mixture that forms a polymer matrix that is attractive for use in screening of a drug candidate and for applications in drug development [8]. The artificial receptor sites formed are capable of rebinding the target molecule with a highly complementary property comparable to those found for antibodies with antigens and other parts of the immune system; imprinted polymers can therefore be dubbed as synthetic “antibody mimics”.

The complex relationships between a drug and its specific molecular targets for treatment of schizophrenia are not fully

understood because of the complexity of the drug target networks. This impasse often leads to low drug effectiveness, a relapse and unwanted side effects following treatments by drugs of neuroleptic disorders. It is likely that some different psychoactive agents will provide significantly different side effects of the neurological therapeutics and physiological variables in the dopaminergic neurons or even result in a response tolerability. Dopamine (D) and serotonin (S) are important neurotransmitters (see the structure in Scheme 1) that regulate the autonomous neuronal activities and can regulate the functional responses of neural activity for

which they are clinically relevant compounds. Fluctuations in the D/S concentrations or the activities of their receptors affect mental depression and other psychotic disorders [9]. Dopamine levels can be reduced using a partial D₂ agonist or an auto receptor agonist together with an antagonist for the central 5-HT_{2A} receptors [10]. Antipsychotic agents differ in their relative potency because of their ability to bind to multiple complex receptors of dopamine subtype receptors [11]. The signaling of the regulation and connections between the multiple copies of its cell surface receptors or that involve activity-dependent refinements of receptor binding sites across the signaling networks [12]. Tremendous efforts are underway to develop functional materials that can rapidly assess the potential effectiveness and classification of new drug candidates or isolated compounds according to their mechanism of action, or serve as drug delivery aids for drug screening. Since there are huge numbers of dopaminergic drugs that differ in their relative potency due to their affinity and ability to bind to subtypes of the dopaminergic receptors and the cellular response that occurs when their receptor binds to its recognition target or acts as a neurotransmitter and receptor signaling into the functions of the cellular network. These responses are elicited in response to the molecules, hence it is important to understand the role of the receptor proximity to the regulation of signaling in these receptors. Recent studies on the binding of the therapeutic molecules to the D and S receptors have shown it is possible to have an increased efficacy against negative symptoms to make more efficacious and safer drugs [13].

Drug–protein complexations are likely to depend on defined structures, so a binding interaction should result in a number of different treatments of CNS mental disorders with different side effects to those of antipsychotics, including ones that interact with the D receptors [14]. Construction of a biosynthetic antibody-like material can be used through chiral selective synthesis with selected building blocks binding to target an enzyme inhibitor at the active site that also carries the important biological activities, and/or other preferentially exposed sites, as described previously [15]. A number of antipsychotic agents have been investigated for their binding range to proteins and enzymes including dopamine receptor subtypes, or Ca²⁺/calmodulin-dependent proteins [16], human serum albumin [17], and other synthetic models such as calixarene and cyclodextrin [18]. The knowledge of dopamine receptor genomics from advanced genomic technologies [19], proteomic analysis [20] as well as mechanistic studies [21] are highly useful to understand the structure and function of dopaminergic receptors and perhaps assist in drug discovery. Based on this information we have suggested using an artificial system fabricated by a self-assembly of molecules to produce selective recognition sites of the artificial system that could facilitate the design of bioactive molecules using the means of non-covalent molecular imprinting. This is reasonably well suited to other methods for modern drug discovery. Also, the functional material of the MIP system mimic a natural dopaminergic system that enabled them to recognize newly formed molecules that may provide effective therapeutic effects and also have neuroprotective properties. The imprinted cavity provided an opportunity to study the connectivity of adaptively responding to the reactants associated with the ability to recognize the molecules at the dopaminergic receptor with different binding affinities.

We sought to develop a novel strategic rationale, the so-called close to-and-avoid approach, for the molecular design using an artificial MIP recognition system that was similar to specific proteins that have grooves for the preferential entry of molecules that clustered in the binding pockets for which it had some preferential functional site that was distinguishable from the closed binding site. These bio-inspired, biomimetic materials allowed for

interactions of the desired reagents in close proximity to the multiple sites of interaction – had been generated for the recognition of dopamine or dopamine/serotonin as a single or a mixed template – that induced the groups within the MIP binding site but avoided the non-active center site in the D-binding site. This was attributed to the existence of a shadow mask on the binding group of the D mimics upon the polymerization process. This proof-of-principle close to-and-avoid approach was devised for the build-up of irreversible bond connections of the reactants in well-defined sites that were related to the self-assembly of molecules so that a pharmaceutical biologically important compound or neurotransmitter acting as a template would allow access for a biologically active entity surrounded by a nanosized space of polymer particles. We installed a small chemical to react preferentially and even for the utilization of a precisely defined specific binding, into a functional recognition cavity into the active site within the interior of the D imprinted receptor. This envisions that the whole binding interaction would be produced by nucleophilic substitution that should more specifically engage the binding mode of the organic molecules-associated with the dopaminergic receptors.

In this paper, we describe the synthesis and characterization of an imprinted dopamine receptor that was an effective binding site for identification of potential therapeutic agents. Two series of molecules derived from the D receptor agonists and antagonists were selectively synthesized to develop a set of hybrid molecules within the produced polymer matrix. We investigated the role of the active binding site in the MIPs on the many integrated processes of the dopaminergic receptor with self-assembled organic molecules. In the structural–activity relationship study, we introduced a known D receptor agonist and antagonist chlorobutrophenone and hydrazinoclozapine molecule fragments derived for biological recognition of D₁, D₂, D₃ and D₄ receptors as well as the D subtype of the serotonergic receptors, then selectively synthesized the complementary pairs to known fragment-associated receptors inside the imprinted cavities. In order to examine the effect of space and orientation in the dopamine-derived imprint cavity on that with the fragments that preferentially occupied the pocket close to functionally active site of natural receptor, compounds were characterized that were supported by the Surflex-Dock for molecular docking using the crystallographic structures of the D₃ receptors and the 5-HT_{1b} receptors. This task was aimed for the development of a highly potent and selective D₃ receptor agonist having a neuroprotective effect in Parkinson's disease. Also, the diversity of the pharmacological features in association with the specificity data of those compounds was compared to a set of known drugs then being testing for biological activity using a D₁ receptor from the hypothalamus of the Wistar rat.

2. Experimental

2.1. Reagents and chemicals

Dopamine hydrochloride, serotonin hydrochloride, alpha-ergocryptine, pergolide, ergonovine maleate, clozapine and (S)-(–)-terguride hydrogen maleate were from Sigma-Aldrich Chemical Company (Milwaukee, WI, USA). 1-Chloro-(4'-fluorobutylphenone), benzylamine, phenylethylamine, tyramine, phenylalanine methyl ester, 2-methoxybenzoyl chloride, 3-methoxybenzoyl chloride, phenylacetyl chloride, 4-methoxyphenylacetyl chloride, 3-chlorobenzoyl chloride, 4-chlorobenzoyl chloride, succinyl chloride, cyclopropanoyl chloride, 2-(3-(4-(3-chlorophenyl)-piperazin-1-yl)propyl)-[1,2,4]triazolo[4,3-a]pyridin-3(2H)-one, acrylamide (ACM), *N,N'*-methylene bisacrylamide (MBAA), methacrylic acid (MAA), (S)-(–)-raclopride tartrate salt, (R)-(+)-SCH-23390 HCl

and sodium 1-heptanesulfonate were from Sigma-Aldrich (Milwaukee, WI, USA). 2,2'-Azobis-(isobutyronitrile) (AIBN) was from Janssen Chimica (Geel, Belgium). MAA was purified by distillation under reduced pressure before use. 4-(3,4-Dichlorophenyl)-N-methyl-1,2,3,4-tetrahydronaphthalen-1-amine (DMTA) was derived from a commercially available sertraline hydrochloride-based pharmaceutical product [22]. Biorex-70 resin was from BioRad laboratories (CA, USA). All solvents used were of either analytical or HPLC grade. Working standards were always freshly prepared.

2.2. Synthesis of the molecular imprinted polymer

The dual D/S MIP (DS-MIP) was obtained by *in situ* polymerization of the template, MAA and ACM as the mixed functional monomers and a crosslinker MBAA. A molar ratio of template:MAA:ACM:crosslinker of 2:2:2:10 was used together with a 1:1 molar ratio of the D and S mixture as the template following a similar procedure to that for the single-recognition MIPs, for the D-MIP and S-MIP. These MIPs were synthesized by the procedures reported previously [23] with some modifications using different monomeric components consisting of a large volume of methanol/water (4:1, v/v; 30 mL) as the porogen. A control non-imprinted polymer (NIP) was prepared in the same way as the MIPs except that the template molecules were omitted. Each mixture was purged with nitrogen gas to remove oxygen. Copolymerization was performed at 60 °C for 18 h. The polymers were ground, and the template removed with acetic acid in methanol (10% v/v, 3 × 500 mL) and then methanol (8 × 100 mL). The polymer was separated by vacuum filtration. Complete extraction of the template was confirmed by fluorescence spectroscopy of the filtrate. The polymers were dried under vacuum and stored in air-tight containers at ambient temperature until required.

2.3. Measurements

The chemical functionalities of the polymers were examined by infrared spectroscopy using an FTIR spectrophotometer (Perkin Elmer 2000, Perkin-Elmer, Beaconsfield, UK). Surface morphology was observed by scanning electron microscopy (SEM; Quanta 400, FEI, Hillsboro, OR, USA). The mean sizes of the samples were analyzed by a laser particle size analyzer (Beckman Coulter, CA, USA) at a fixed scattering angle of 90°. Particle size distributions were expressed as $D(v, 0.5)$, that was the respective diameter for 50% of the cumulative volume. The surface area, pore volume and pore size were investigated by nitrogen adsorption/desorption using an automated gas sorption system (Autosorb, Quantachrome, FL, USA). Surface areas were determined from Brunauer–Emmet–Teller (BET) plots, while the average pore diameters and cumulative pore volumes were calculated using the Barrett–Joyner–Halenda (BJH) method. Diffusion coefficients (D_i) and hydrodynamic radii (R_h) were assessed by incubating the NIP and MIP in 50 μM D at 303 and 308 K in methanol/water (4:1) as a porogenic solvent. Control polymers were incubated in the absence of a template. The NIP and MIP with and without D were incubated in methanol and water as independent experiments. After overnight incubation, fluorescein isothiocyanate (FITC) (100 μM) was added and visualized after 60 min using a confocal laser scanning microscope (FV300, Olympus, Tokyo, Japan). Images were analyzed using Fluoview software (Olympus, Tokyo, Japan). R_h was calculated from:

$$R_h = \frac{KT}{6\pi\eta D_i} \quad (1)$$

where K is the Boltzmann constant and T is the absolute temperature in Kelvin. The viscosity factor η was assumed to be 1 cP, and D_i was calculated as

$$D_i = \frac{KT}{3\pi\eta d} \quad (2)$$

where d is the diameter of the diffusing molecule.

2.4. Displacement assay

The binding of the D analogs to the D-MIP complexes was elucidated in mixtures containing an excess of the starting D and other fluorescent compounds were eluted from the MIPs after incubation with an initiator. First, the contact time required for the D to bind was examined. MIPs (50 mg mL⁻¹) were incubated at room temperature by agitation with D (5 mL, 50 μM) in a binary solvent mixture – MeOH/water (4:1 v/v) – and AIBN (1% w/w). Unbound D was determined by fluorescence spectroscopy with an emission wavelength of 279 nm and an excitation wavelength of 320 nm. The presence of fluorescent compounds other than D was evaluated using HPLC (Shimadzu, Kyoto, Japan) with a C₁₈ ODS column (5 μm particle size), sample volume of 30 μL , a mobile phase of MeOH/acetate buffer (1:1) containing 2.5 mM sodium heptanesulfonate, and a flow rate of 0.5 mL min⁻¹.

In order to determine the binding-specificities, the D-MIP that consisted of MAA (0.5 mmol), 1-vinyl-2-pyrrolidinone (0.5 mmol) with dihydroxybisacrylamide (0.5 mmol) and dopamine HCl (0.2 mmol) as template in the polymer synthesis were used in a displacement assay using dopamine as a probe. Control experiments were carried out with the non-imprinted polymer (NIP). In a typical binding experiment, the particulate polymer (10 mg) was added to 2 mL of the solvent and the suspension was stirred, and then filtered into a 96-well multfilter plate. The analyte solution containing 5 $\mu\text{g/mL}$ of dopamine (or other related compounds), or 1 mL of the pure solvent (blank), were added and then washed out with 10% v/v acetic acid in methanol, and finally with methanol at room temperature (25 ± 1 °C). The rinses from the polymer were then analysed for their free drug content by LC–MS–MS analysis as described in Section 2.8 except that 5% acetic acid in distilled water was the mobile phase.

The ¹H NMR spectra were obtained at 25 ± 1 °C using a 500-MHz NMR spectrometer (DRX, Bruker, Billerica, MA, USA); chemical shifts were recorded in parts per million (δ) downfield from tetramethylsilane (TMS). The pre-polymerization mixture consisted of MAA or MAA and ACM with an MBAA cross-linker. The filtrate from the polymer after binding was reconstituted in a spectroscopic grade porogenic solvent (4:1 v/v d₄-methanol/D₂O) for the NMR studies. Different combinations of ACM and D were added separately, or a mixture of ACM-MAA (1:1, w/w), ACM-MAA-MBAA (1:1:5, w/w), or ACM-MAA-MBAA (1:1:5, w/w) with D (0.5 mg) in deuterated solvent (2 mL). The radical initiator (1% AIBN) was added in an amount that was suitable for the total amount of the monomer.

The recognition of the template by MIPs at 301, 308 and 313 ± 1 K was examined after rebinding using D-MIP, DS-MIP and the corresponding control NIPs (50 mg) with template solutions that ranged in concentration from 0.1 to 4 mg mL⁻¹ in MeOH/water (4:1 v/v). In a typical experiment, polymer (50 mg) was added to the D solution, that was stirred for 24 h. The mixture was filtered through a 0.45- μm filter, and the filtrate analyzed by fluorescence spectroscopy using the excitation and emission wavelengths of 279 and 320 nm, respectively. The amount of drug in solution was determined by reference to a calibration curve. The amount of the bound drug was calculated by subtracting the amount of the free drug from the total amount of the added drug. All experiments were performed in triplicate. D binding at

various concentrations was determined using fluorescence spectroscopy to quantify the unbound probe as described for the binding study.

2.5. Synthesis of the butyrophenone derivatives

The amount of amines formed should vary according to their affinity for the imprinted site on each MIP. The MIP (1 equiv.) and each of the amine reagents (10 equiv.), tyramine (1), phenylethylamine (2), benzylamine (3), phenylalanine methyl ester (4), DMTA (5) and 2-(3-(4-(3-chlorophenyl)-piperazin-1-yl)propyl)-[1,2,4]triazolo[4,3-a]pyridin-3(2H)-one (6), were dissolved in dimethylformamide (DMF) and incubated at room temperature for 2 h. 1-Chloro-(4'-fluorobutyrophenone) (10 equiv.) and Na₂CO₃ (10 equiv.) were added. The mixtures were stirred at 80 °C for 14 h, and then centrifuged at 6000 rpm for 10 min. The corresponding alkylation products were extracted from the MIPs with 0.2% acetic acid in MeOH and the solvent removed by filtering through a cellulose membrane. Binding sites of the MIPs were reused several times to produce new chemical species. Samples were filtered and then crude mixtures were analyzed by liquid chromatography/mass spectrometry (LC-MS) using selected ion mass spectrometry (SIMS), which allowed the products to be directly identified by their molecular weights. The final mixtures that contained alkylation products, excess of precursor amines and 1-chloro-(4'-fluorobutyrophenone) were analyzed by electrospray ionization mass spectrometry (ESI-MS). Each new compound was characterized by ¹H and ¹³C NMR spectroscopy (500 MHz, Bruker, MA, USA), FT-IR spectroscopy (Perkin-Elmer, Beaconsfield, UK) and high-resolution MS (MAT 95XL, Thermo Finnigan MAT GmbH, Germany).

2.6. Synthesis of the clozapine derivatives

We screened for reagents able to react within the MIPs by nucleophilic reactions between the hydrazine derivative clozapine and various acid halides. The initial step was a hydrazine reaction between clozapine and isoamyl nitrite to afford clozapine hydrazine derivatives. Clozapine was converted to hydrazine according to the following diazotization. Clozapine (1 equiv.) was dissolved in dichloromethane (DCM, 25 mL) and isoamyl nitrite (4 equiv.) at room temperature over a 3 h period. The solvent was removed and the crude solid was dissolved in glacial acetic acid. This solution was added dropwise to a suspension of Zn in acetic acid (6.67% w/v) over a 1 h period at 10–15 °C. After 3 h, the solution was filtered and extracted with DCM (3 × 100 mL). The conditions for modification of the clozapine derivatives in each polymeric recognition material were the same as reported previously [24]. A series of clozapine derivatives were synthesized using the MIPs as follows: hydrazine (10 equiv.) was dissolved in triethylamine containing the MIP (1 equiv.) in a round-bottomed flask and incubated at room temperature (27 ± 1 °C) with a single acid chloride (10 equiv.) from: 2-methoxybenzoyl chloride (7), 3-methoxybenzoyl chloride (8), 3-chlorobenzoyl chloride (9), 4-chlorobenzoyl chloride (10), phenylacetyl chloride (11), 4-methoxyphenylacetyl chloride (12), cyclopropanoyl chloride (13) and methacryloyl chloride (14), with stirring for 14 h. The resultant compounds were extracted from the MIPs using 10% acetic acid in MeOH, centrifuged and then filtered through a cellulose membrane. The crude product was purified by recrystallization from chloroform and hexane. Products were characterized as mentioned above. Other materials were prepared in the same manner using different reactant chlorides including succinyl chloride, cyclopropanoyl chloride and methacryloyl chloride.

2.7. Biological assays

The synthesized compounds were screened to assess their binding affinity for a soluble protein receptor from the rat hypothalamus. This study was approved by the Animal Research Ethical Committee at Prince of Songkla University (Ref. 30/2014). The hypothalami of dissected Wistar rats of both sexes with an age of approximately 3 months and weight of 200–210 g were immersed in ice-cold physiological buffer (pH 7.4). To prepare the pellets of the receptors, the hypothalamus was removed and homogenized in cold physiological buffer (50 mM Tris-HCl, 0.5 mM Na₂EDTA, 0.1% ascorbate and phosphate buffer). The homogenate was centrifuged at 2000 rpm for 10 min to remove gross debris and the obtained supernatant was re-centrifuged at 20,000 rpm for 10 min. This pellet was resuspended in buffer (10 mL) and centrifuged again at 43,000 rpm for 20 min. A typical screening affinity was performed with a slight modification of the original assay [25]. Bovine serum albumin (BSA) was diluted three to five times to prepare a standard of an equivalent concentration to the protein solution to be tested. The linear range of the assay for BSA was 0.2 to 0.9 mg mL⁻¹, whereas the linear range for the IgG was 0.2 to 1.5 mg mL⁻¹. Each standard and sample solution (100 μL) was added to a clean, dry test tube and incubated for 1 h at room temperature. Diluted dye reagent (5.0 mL) was added to each tube and mixed by vortex. Samples were then incubated at room temperature for 30 min and the absorbance at 595 nm was measured. Binding of the test compounds to the MIPs and biological receptor from the hypothalamus was compared. Control experiments in the presence of blank BSA instead of binding protein were also run as described above. In all cases each value was provided as the average of three replicates.

2.8. MIP sorbent assays and the biological test

The membranes used in this study were prepared from the rat hypothalamus. Brain tissue was ground in buffer A and included: 0.32 M sucrose, 50 mM Tris-HCl, 10 mM NaCl and 10 mM EDTA, with a protease inhibitor (10 μL mL⁻¹) for 1 h at 4 °C. The homogenate was centrifuged at 1000 × g for 10 min to obtain a pellet and supernatant. The D receptor was purified with a Biorex-70 resin that was washed several times with distilled water and buffer A until the pH was 7.2. The sample was loaded on the column and eluted with physiological buffer (100 mL), 0.5 M NaCl in buffer A (100 mL) and 1 M NaCl in buffer A (100 mL). The resulting solution was lyophilized to afford the D receptor and assayed for its content of protein. All fractions were examined by SDS-PAGE using 3% and 12% polyacrylamide gels under non-reducing conditions, and stained with Coomassie blue G250 in 95% ethanol (50 mL). Each solution was mixed with 85% phosphoric acid (100 mL) and made up to 1 L with distilled water. A sample (100 μL) was mixed with Bradford reagent (5 mL) by inversion [26]. After 20 min, the absorbances at 470 and 595 nm was measured against the blank. The affinity of the synthesized compounds for dopaminergic and serotonergic receptors was assessed using a competitive MS binding assay according to the described method [27]. The membrane suspension was incubated with 1.25 nM of SCH 23390 (in the saturation binding assay), and each of the synthesized compounds (2–12 μM) was added to the competitive binding assays with ammonium formate (50 mM) at pH 7.4 for 40 min at room temperature. Non-bound SCH 23390 was quantified by HPLC (Agilent 1100) with a triple quadrupole MS (API-3200, Agilent Technologies, CA, USA) to perform SIMS. Sample (1 mL) was injected into the LC-MS-MS with reference to a calibration curve. Data were collected by the MS detector from the precursor ion *m/z* = 288.1 to the product ion *m/z* = 91.2. The calibration curve of SCH 23390 in the incubated solution was linear over the range of 0.25–1.25 nM.

Control samples without test compounds were used to define the total binding. The ED₅₀ for each probing molecule was determined for various inhibitor concentrations.

2.9. Molecular docking studies

The semi-empirical Austin Model 1 (AM1) approach was used to optimize the geometry of the system. Geometrical optimization was performed using the Polak–Ribiere algorithm based on the conjugate gradient method. The semi-empirical convergence to the geometry was set to 0.001 kcal mol⁻¹ during the optimization stage. Calculations were performed using the HyperChem 8 package. The Discovery Studio 3.5 Visualizer was used to generate the van der Waals surface of the precursors and the MIP, in which the dispersion forces played an important role. The thermochemistry was then assessed to estimate the Gibbs free energies (ΔG) and entropy (S). A Surfex-Dock was used for molecular docking of a given ligand to the biological system. Protein structures were modified by removing the co-crystallized ligand and water molecules from the X-ray crystallographic structures of the D₃ receptor [PDB:3PBL chain A] and the serotonin 5HT_{1b} receptor and were deposited in the Protein Data Bank [PDB entry 4IAR Hydrogen atoms were added and side chains were fixed. The support vector machine (SVM) models were trained using the D₂ ligands with a binding affinity K_i and IC₅₀ < 1 μ M, and non-ligands, with no known active compound, were collected from an online ChEMBLdb database that provided information on the properties of the drugs [28]. Structural features were produced using the Tripos force field and partial atomic charges and calculated by the Gasteiger–Hückel method [29]. We also used the SVM approach to screen for active compounds. From the Surfex-Dock, a total score was obtained as $-\log(K_d)$ to represent the binding affinities including hydrophobic, polar, repulsive, entropic and solvation. The crash value was defined as the degree of inappropriate penetration by the ligand into the protein and the interpenetration between the ligand atoms (self-clash) that were separated by rotatable bonds. Crash scores close to zero were the most favorable. The polar value was the contribution from the hydrogen bonding and the salt bridge interactions to the total score. The polar score may be useful to exclude the docking results that made no hydrogen bonds. CHEM-SCORE estimated that the free energy of binding (kJ mol⁻¹) of a ligand to a protein was as follows: $\Delta G_{\text{binding}} = \Delta G_o + \Delta G_{\text{hbond}}S_{\text{hbond}} + \Delta G_{\text{metal}}S_{\text{metal}} + \Delta G_{\text{lipo}}S_{\text{lipo}} + \Delta G_{\text{rot}}H_{\text{rot}}$.

3. Results and discussion

3.1. Preparation of an imprinted dopamine receptor

An artificial receptor system for the D and S neurotransmitter and combination were based on an MIP affinity phase generated with each affinity site in the synthesized materials. The selective recognition sites of the artificial system for the chemical structures on its surface including the chemical and dynamic properties of the template was produced against dopamine (D) and serotonin (S) as a single and a mixed template. The key of this approach was to use only the binding cavities that were capable of assembling around complementary interactive reactants of functionalities as anchoring sites for the various reactants until the formation of pairs of irreversible bonds occurred at the same template cavity (Scheme 1). Since the molecules or therapeutics were assembled into functional units with multiple binding sites to close the space of the binding pocket of the proteins or the natural receptor. It was greatly influenced by the ability of the MIP to control and vary its features to form closely spaced binding sites. By using multiple recognition sites in a known bioactive compound, a

possible library of biologically active entities of dopamine analogues could be examined. Two series of molecules derived from the D receptor agonists and antagonists were selectively synthesized to develop a set of hybrid molecules within the produced polymer matrix. The building blocks for the production of the MIP had generated for the neurotransmitters dopamine and serotonin used either a single or double template approach. Removal of the template resulted in the imprinted cavities having specific spatially defined functional-binding groups for the rebinding of more than one type of functionally distinct, biologically important compound at a time. In addition to the above structural consideration, the imprinted species possessed remarkably different structures simply by the functionalization of serotonin with an extra NH group. Here, a mixture of methanol and water (4:1 v/v) was chosen as the porogen solvent for thermal polymerization because both the D and S were soluble in it. MeOH would directly affect the hydrogen bonding interactions of the template with the monomer through competition. However, studies on monomer–template complexes have shown that the MIPs can reform their covalent assembly to complement the structure of a target analyte [30]. Our strategy included the self-organization of a single template or binary templating species with several functional groups using a functional monomer, MAA, that can copolymerize with ACM to complement a template surrounded by crosslinked poly(MBAA)–polymer chains. By careful selection of the reagents we thought that it was possible to obtain an imprint of the surface features in the polymer once the coupling product that formed inside the MIP binding sites had been washed away, thereby yielding an imprint of the specific desired bioactive molecule. We have assessed the complex behavior of the imprinting effect of the binding sites achieved for the resultant recognition materials and found that the imprinted cavities facilitated the highly regioselective reaction because of the generation of an MIP at the surface on the structure of the particles. The imprinted cavities provided for a cloning of the drug where the pre-arranged functional monomer, MAA and ACM anchored the site to the ligands of the dopaminergic and serotonergic receptors and the reaction of the coupled products into the molded cavity. However, it was necessary to evaluate the multiple combinations of the structures that depended on the space and orientation of ligands inside the recognition cavity.

3.2. Characteristics of the MIPs

The surface morphology of the imprinted polymer particles was examined by SEM. As shown in Fig. 1, all the MIPs exhibited different surface topographies relative to their corresponding NIP as the imprinted polymers possessed more rough surfaces. Differences in the polymer pore sizes between the MIPs and the corresponding NIP could be distinguished. The MIPs were more porous than the control NIPs and both MIPs showed the presence of small particles with different pore structures in addition to the particle surface that had a larger surface area of the closed nanoparticles for the D-MIP than for the DS-MIP. There was the possibility of immobilizing the templates at or near to the surface of the MIP and this was anticipated to enhance the accessibility to the binding site. The difference in the surface morphology of the MIPs and NIP can be explained by the effect of the polarity of the environment on the formation of the imprinted polymer, that the diluted polymerizing mixtures affected the degree of crosslinking of the polymer matrix and the presence of the chemical surface properties that were different from the previous report [31]. This resulted in forming suitable sites from biological relevant molecules that provided the different functional group rearrangements required to produce synthetic polymer assemblies on the nanostructure and resulted in the array of different receptors.

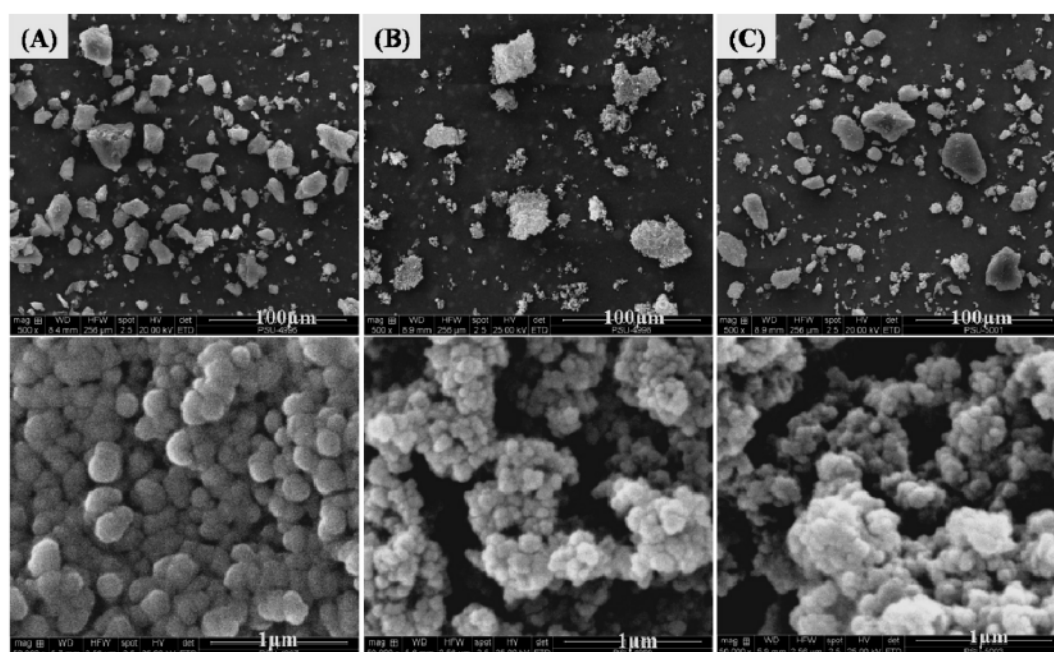


Fig. 1. SEM images of the D-MIP, DS-MIP and the corresponding NIPs, SEM image; (top) $\times 500$ (below) $\times 50,000$. (A) NIP, (B) D-MIP, (C) DS-MIP.

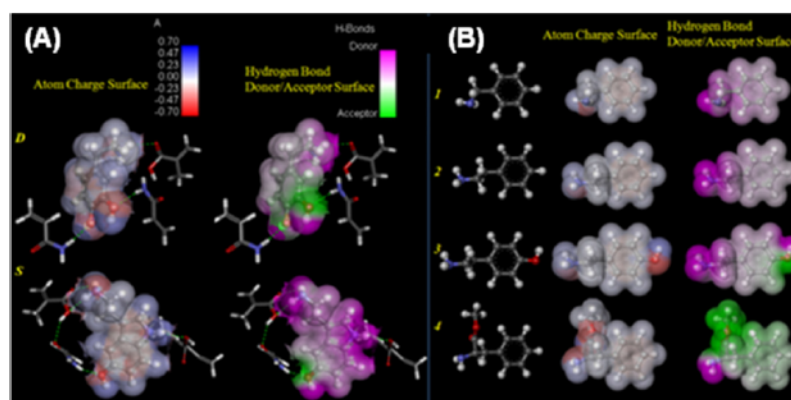


Fig. 2. (A) Theoretical model of the interactions between the functional monomer and the D and S templates. (B) Structures and the optimized conformations of the neurotransmitter and the reagents for the synthesis of a chlorobutyrophenone-type ligands, showing a polar surface area and the hydrogen bonding donor and the acceptor for the amine precursors from the computation studies.

All of the polymers exhibited FT-IR peaks at $3422\text{--}3418\text{ cm}^{-1}$ (OH or NH stretching vibration), $1660\text{--}1657\text{ cm}^{-1}$ (C=O stretching vibration), $1532\text{--}1528\text{ cm}^{-1}$ (--NH_2 bending), $1454\text{--}1452\text{ cm}^{-1}$ ($\text{--CH}_2\text{--CO}$ bending), 1388 cm^{-1} (--OH bending) and 1114 cm^{-1} (C–C–O stretching), and this indicated that the chemical composition of the MIPs after template removal was the same as that of the corresponding NIP. Fig. 2A shows a theoretical model of the interactions between the functional monomer and the D and S templates in the MIPs. Table 1 shows that all the polymers exhibited comparable nanosized pore diameters, while the D-MIP had a higher specific surface area of pores with larger pore diameters than the DS-MIP. The pores in the D-MIPs were comparable to those in the control polymer. The hydroxyl groups of D should increase the solvation of the MIP in aqueous methanol, so unlike S, it acted as an imprinting agent and a porogen. As a result, the D-MIP had a pore size that was twice that of the DS-MIP and the BET surface area. The

results of the surface morphology and pore analysis demonstrated that the MIP, particularly the D-MIP had a mesoporous structure with a uniform pore diameter and a high specific surface area that was suitable for the reaction of the synthesized compounds in the pore structures. The results obtained in this study indicated that the

Table 1
Pore size analysis of polymers in diameter, volume and BET surface area.

Polymer	Pore diameter (nm)	Average pore volume (ml g^{-1})	BET surface area ($\text{m}^2 \text{g}^{-1}$)
D-MIP	15.4	2.6 (0.035)	672.7 (94.2)
NIP 1	15.3	2.35 (0.011)	513 (31.39)
DS-MIP	12.6	1 (0.002)	316 (8.8)
NIP 2	13.2	2.33 (0.005)	702 (132)

Values of corresponding micropores are given in parenthesis.

Table 2
Diffusion coefficient (D_i) of the dopamine template in polymer matrices and molecular radius (R_h) of polymer particles at various porogenic solvents and temperatures.

Compound	MeOH–water				MeOH				Water			
	303 K		308 K		303 K		308 K		303 K		308 K	
	$D_i \times 10^{-3}$ ($\mu\text{m}^2 \text{s}^{-1}$)	R_h (μm)	$D_i \times 10^{-3}$ ($\mu\text{m}^2 \text{s}^{-1}$)	R_h (μm)	$D_i \times 10^{-3}$ ($\mu\text{m}^2 \text{s}^{-1}$)	R_h (μm)	$D_i \times 10^{-3}$ ($\mu\text{m}^2 \text{s}^{-1}$)	R_h (μm)	$D_i \times 10^{-3}$ ($\mu\text{m}^2 \text{s}^{-1}$)	R_h (μm)	$D_i \times 10^{-3}$ ($\mu\text{m}^2 \text{s}^{-1}$)	R_h (μm)
NIP	3.31	9.65	3.25	9.84	4.5	7.04	3.55	9.15	3.33	9.60	2.56	12.66
NIP + 50 μM dopamine	2.85	11.2	2.43	13.12	3.64	8.77	5.48	5.93	3.0	8.53	3.81	10.64
MIP	3.16	10.12	2.15	12.85	3.92	8.16	3.66	8.88	3.93	8.13	3.35	9.70
MIP + 50 μM dopamine	4.63	6.9	2.95	10.8	3.71	8.62	3.88	8.37	3.96	8.07	3.19	10.19

generation of the MIP by the two template approach distinguished the distribution of the D and the S binding sites from the D binding sites obtained by the single template approach.

We next examined the ability of the MIP to control the morphology of the porous nanostructures by determining the effect of an environmental stimulus such as temperature, solvent, and pH on the D_i and R_h (Table 2). The NIP and MIP were incubated with 50 μM of D at 303 and 308 K in methanol:water (4:1) and this was used as a porogenic solvent during the imprinting process. The changes in the D_i and R_h were greater for the MIPs and the control polymer incubated with D (50 μM) at a higher temperature and in all solvents except for methanol, that showed only a small change of R_h with an increase of temperature. The increase in the R_h for both the NIP and the MIP was attributed to their porous surface, pore plasticity and the accessible sites in the MIP because of their interconnected porous space. Thus the R_h of the MIPs manifested their recognition ability for the template, that was dependent on the environmental conditions. With the molecular imprinting polymer, specific analyte sites can be attributed to the structure and density of the accessible ligand for rebinding of the template to an imprinted dopamine receptor for both the synthesized materials.

Furthermore, the D-MIP polymerizations were investigated based on template–monomer prescreening by NMR spectroscopy in deuterated water and methanol that possessed intermolecular interactions with D compared to the dopamine alone (see Supplement 1). The vinyl peak of the monomers at 5.9 ppm was used to monitor the polymerization of the monomeric mixtures without the template. The D template had an L-configuration and showed peaks at 2.80 and 3.08–3.11 ppm that corresponded to its methylene protons. Accordingly, the complex was formed using the MAA-ACM-MIP provided that the anisotropic effect showed a slight down-field shift of 0.1 ppm for the aromatic template protons between 6.58 and 6.74 ppm after the polymerization process. This was a more significant shift than the shift of the vinyl peak. This can be explained by the crosslinked polymeric network of the imprinted polymer creating a binding site that controlled the conformation of the aromatic residue by a hydrogen donor–acceptor interaction. However, the imprinted image of the D structure and conformation in the original templated cavities occurred using the remaining dopamine HCl as the template. The ^1H NMR results showed that the functional monomers and crosslinking agent that were incorporated into the synthesized polymers possessed the carboxylate on the MAA and the amide of the ACM that became a functional monomer showing the most favorable interaction with the dopamine as template. There were also the underlying molecular recognition mechanisms of the MIP that was dependent on the spatial reorganization and the dynamic forces of the polymer that contributed to the template rebinding to engage the receptors at different binding sites.

3.3. Evaluation of the additional potential hits of the D-MIP

This approach was to use the multiple recognition sites in a known bioactive compound to identify a possible library of

biologically active entities of dopamine analogues. Dopamine is known to polymerize in aqueous solutions to form melanins and other similar biopolymers [32,33]. Obviously, the ability of the MIP for selective recognition could be expanded by the method to derive reactions that were more favorable interactions in the nanosized environment and may allow for assembling around a complementary interactive target within the spatial well-defined site of the designed MIP serves as a nanoreactor. In the preliminary study, we examined the molecular recognition of the MIP by studying the reaction of the D in the presence of AIBN that consisted of the adaptable crosslinked MBAA–polymer using fluorescence spectroscopy followed by HPLC analysis. When the dopamine solution with the polymer mixtures was injected into the HPLC column through cycling the reaction process, then the chromatogram obtained with the D solution in the presence of AIBN for 24 h differed from those for the standard D solutions with and without the initiator (see Supplement 2). This can be accounted for by recognition of the imprinted polymer since the reaction of the aromatic condensation of dopamine within an imprinted polymer matrix was most likely formed after the polymerization. This was in contrast to the chromatogram for the NIP that contained no extra peaks. This formation of aromatic condensation in the cavity surrounded by the poly(acrylamide)-based crosslinks was investigated by FT-IR spectroscopy in the presence and absence of free radicals (AIBN). FT-IR studies revealed peaks at 1650 and 1508 cm^{-1} for the dopamine in the presence of free radicals, to support the presence of the indole and indoleamine structures (Supplement 3). The carbonyl peaks of dopamine in the presence of the free radical initiator were also discernible at 1660–1750 cm^{-1} .

The distinct product signal with a molecular weight and retention time was determined by chromatographic analyses and fluorescence spectroscopy, and this increased the interactions with the dynamic MIP, that the irreversible bond-forming reaction should install inside the cavity. The chemical species present for the D template and the formed D-MIP were detected in the LC–MS spectra, peaks were observed at m/z 413, 551 and 687 for the respective products in the *in situ* reaction mixture of the D-MIP, and these peaks were absent from the corresponding NIP. Molecular mechanics and the free energy of the adsorbed D on the MIPs were calculated (Table 3). The energies of the D, dimers and trimers were calculated *in vacuo* and in the presence of water. It was of interest that the compounds had the newly formed D dimer and trimer products. The estimated binding energies for the dimers and trimers allowed for a π -stacking interaction between the D molecules, producing species with a different molecular mass [34]. This result indicated the possibility for the formation of the oxidation and cyclization via radical induced pathways within the MIP. These results revealed that the dispersive interactions between the aromatic groups spaced at a van der Waals distance played a crucial role in the shape of the chemical structure for the polymer due to the intrinsic relationship between the template concentration within the selective cavities upon templating and the polymerization processes. This interaction may involve the carboxylic oxygen atoms of the MAA and the amide groups of the ACM

Table 3
Energy minimization and geometry optimization of the structures of dopamine designed using Hyperchem software.

Molecules	Geometry optimization energy (kcal mol ⁻¹)		Molecular dynamics energy (kcal mol ⁻¹)		ΔG (kcal mol ⁻¹)	
	Vacuum	Water	Vacuum	Water	Vacuum	Water
Dopamine	6.606	23.017	35.65	-543.7	-	-
Dimer	34.35	65.35	71.52	-498.95	91.32	0.2
Trimer	63.95	109.44	38.85	-1673	40	-37

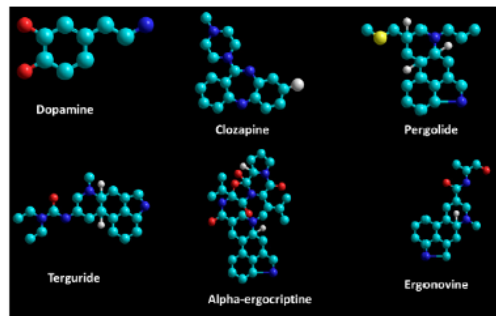
arranged at the active site of the MIP that was encapsulated to create a specific site within the imprinted cavities. Molecular dynamic calculations of the two D molecules showed that the energy transfer for the rotation of the larger interacting systems was better stabilized than for the monomers. Therefore, the conformational alteration and molecular dynamics of this site was formed around all the structural-processes of the intact MIP-drug assemblies achieved by the original template species present as a dopamine target.

3.4. Displacement assay

A method for extraction of the compounds that mimic the target D and S structures has been investigated by rebinding into the synthesized material of an imprinted dopamine receptor. Many drugs use biomimetic binding strategies to bind competitively to receptor proteins to repress the effects of regulatory molecules. A small molecule is able to attenuate or prevent the dissociation of D from a dopaminergic neuron that can bind to a specific location of the dopaminergic subtype receptors that produced a neuroprotective effect with leaching of the cytoplasmic dopamine or prevent the neurodegeneration in the CNS [35,36]. In this case, the use of an MIP composition of a more hydrophilic acrylamide-based polymer is that the selectively has a different array of the D-MIP that can exert control of their binding affinity in the dielectric environment, given a role as a well-studied synthetic model to elucidate the structural activity relationships of the specific absorption either as a single or an analyte mixture at room temperature ($25 \pm 1^\circ\text{C}$). Fig. 3 shows the displacement assay data of the D-MIP by using a large number of dopamine related compounds with structural differences when analysed by liquid mass spectrometry with D as a molecular probe. Ergots used in this study acted as a dopaminergic receptor agonist in the human brain, except for clozapine that was a potent antagonist of a dopaminergic receptor, by which the measurement of the free analyte in solution indicated the ability to replace their biological counterparts in the artificial polymer mimics. This was because one of the dopaminergic drugs represented a range of three-dimensional shapes from a favorable functional group on diverse aromatic rings that changed its structure in the environment and became reversible bound to be specifically oriented to the functional binding groups in the imprinted cavity. The MIP showed the highest affinity with a 100% binding of the dopamine so that the binding mimics selectively recognized the specific structural features for the template. The neuroactive drug of interest bound more favorably to MIP binding site, but was restricted in binding the motif of the analogues that were larger than the D template to the D-MIP. This can be interpreted in that if the specific analytical site of the D template saturated the MIP binding sites, hence they could not allow the other related molecule to the accessible sites. However the conformation change and rotation of the dopamine reduced the preorganization of the template-MIP complexation. For studying the recognition properties of the chirality in the synthesized material (-)-terguride was chosen to test for the specific selectivity of the MIP. There were slight differences in the ratio of the binding capacity (nmol/mL) of the separately loaded structural analogues and the ergots of interest, obtained with the MIP to the NIP, except that ergonovine produced

a three-fold difference of the free drug in solution between the MIP and the NIP with the bound drug (Fig. 3a). In comparison to the cross-reactivity, that was obtained from the adsorption value of the MIP for the related compound relative to D that was found to be in the order of: clozapine (for dopamine antagonist) > (-)-terguride > pergolide > alpha-ergocriptine > ergonovine from the elution of a single compound (see Fig. 3b). This result indicated that the polymer imprint bound to different binding motifs with some degree of size discrimination to the analogs but there was a restriction of the more spatially demanding-type analytes. The selectivity of (-)-terguride for the D-MIP resulted from the presence of the shaping of the secondary binding site around the template-MIP interaction to create an effective imprinted dopamine receptor mimic in the surrounded crosslinked architecture. Due to the ability to attain selectivity of the MIP binding site and it was reversible throughout the imprinting approach, and resulted in the structure-activity relationships with a wide range of psychoactive drugs that must be relevant to the biologically active entities. In order to establish the effect of the receptor mimic when the mixtures of dopamine and analogues were loaded onto MIP, in Fig. 3c, the extraction showed a D-MIP selective recognition, and a reversible rebinding to the template site. The highest selectivity of clozapine on the MIP among the other structurally closed compounds (see Fig. 3c), could be explained by the favorable analytes occupying the cavity, to form an intimate contact in the spatially well-defined environments, that minimized the steric effect of the remaining function on a selective analyte molecule. The different specificities for the analogues were found in the order of: clozapine > ergocriptine > pergolide > ergonovine > terguride. Although the binding of the substrates was lower, they still bound with a high selectivity to ergonovine compared to their binding to the NIP, and it was substantially greater than the highly potent dopamine agonist, (-)-terguride. Therefore, the partial selectivity was reflected with multiple conformations of the tested compounds that mimicked the bioactive template molecule on the adaptive binding sites. The D binding site mimics with a variety of psychoactive drugs as they contribute to the high selectivity that was present in an adjustable functional site "lock" for binding the molecules with a good fit to different "keys". The results indicated that it was possible to obtain a highly tailored cavity with a broad selectivity range for a larger, bulkier related dopamine as compared to the template, for which dopamine acts as a neurotransmitter, biomolecule, as well as a pharmaceutical agent in the dopaminergic nervous system.

Next, the relative intensity of the fluorescence of D present on the D-MIP was observed to be markedly influenced by the solvents, using rebound D (50 μM) as a fluorophore as shown in Supplement 4. The value of the imprinting factor, IF, was determined from the intensity of the fluorescence of D on the MIP compared with D on the NIP. The IF of the D-MIP and DS-MIP in methanol was 2.7 and 2.3 times, respectively, and this was greater than that in either an aqueous methanol mixture or water ($\text{IF} \sim 1.0$); this is because the fluorescence of D was extremely sensitive to the dielectric environment. This phenomenon of the enhancement of fluorescence reflected the strong imprinting efficacy of the MIP for the dopamine template in methanol and the specificity of the template for the imprinted cavity.



(a) Affinity of single compound

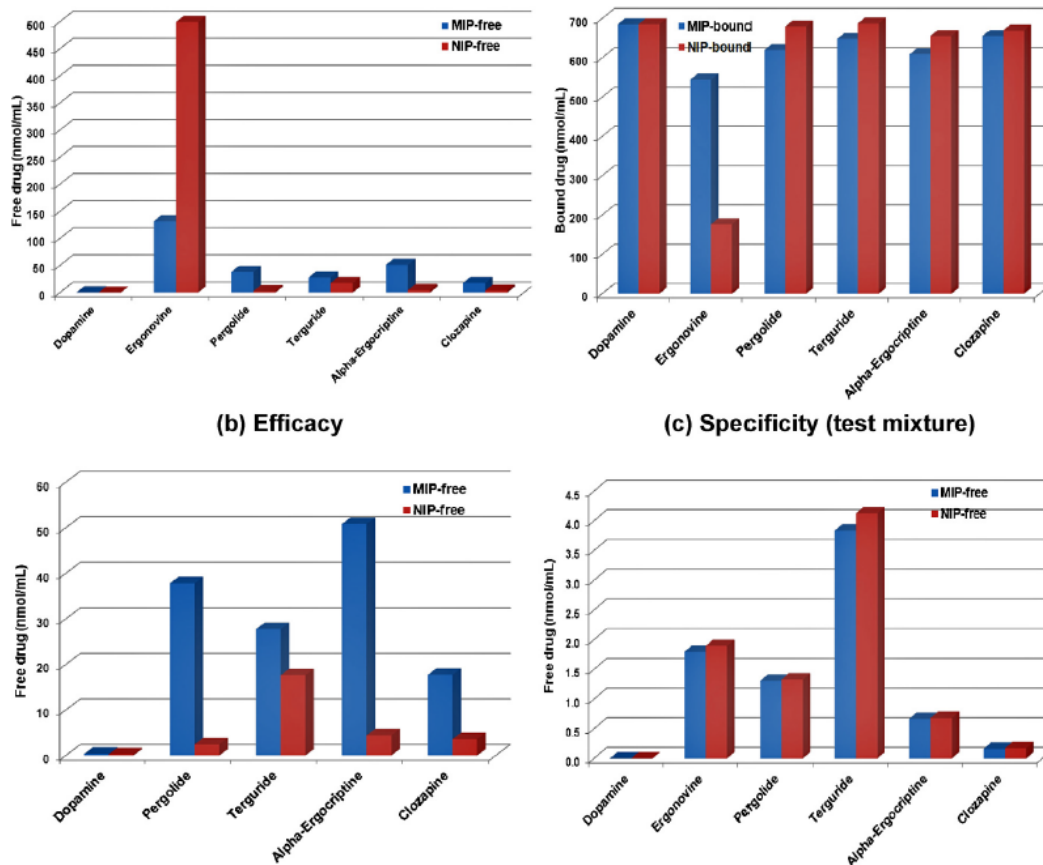


Fig. 3. Data for the LC-MS-based ligand-binding assay for the detection of a free or bound drug on a dopamine MIP and its corresponding NIP from the displacement of an unlabeled dopamine: (a) affinity; (b) efficacy and (c) specificity from either a single or a mixture of the analytes.

Further, the maximum binding capacity (B_{max}) of the polymers was investigated by measurements of the unbound D fluorescence at varying temperatures. The B_{max} of the D-MIP (1.2–1.6 M per g polymer) at 301 K was higher than that of the DS-MIP (0.8–1.0 M per g polymer). At 313 K, the B_{max} of the DS-MIP (1.0 M per g polymer) was about twice that for the D-MIP. The results indicated that applying the same dopaminergic drug to both MIPs might have different effects. In contrast, the B_{max} of the NIPs (1.4–1.6 M per g polymer) did not change with increasing temperature. Over the

temperature range of 301–313 K, the binding capacity of the DS-MIP exposed to the D did not change as a function of temperature, while that of the D-MIP increased in its affinity by about three fold with increasing temperature. This was indicated by a decrease of the measured fluorescence, and indicated that the D binding sites in both the MIPs had different conditioned responses. The binding affinity of D exhibited a marked dependence on temperature, but the increase in hydrophobic (non-specific) binding to the NIP was slightly greater than that to the MIP. The recognition properties and

selectivity as a function of temperature may have originated from a change in the affinity of the dynamic binding and a change of the binding capacity.

3.5. Analyzing the interactions in the chemically reactive dopamine imprinted receptor

The abovementioned features make the neurotransmitter-imprinted cavities for both MIPs promising for assembly of selected components in the cavities. The rational strategy for this synthesis employed various template analogues (1–6) that were occupied within the binding pocket through the reactants in the chlorobutyrophenone surrounded by the polymeric crosslinked networks. Reacting 1-chloro-(4'-fluorobutyrophenone) with a range of amine moieties from the neurotransmitter of interest (see structure of these compounds in Fig. 4a, panel A) under alkylation reaction conditions. The MIPs provided a convenient covalent bond formation in the MIP (see the spectroscopic data and MS for the synthesized products in Supplement 5). Nucleophilic substitution of tyramine (1) to give 1a by replacing a chlorine atom with an amine group was achieved using DS-MIP ($6.97 \pm 2.16 \mu\text{mol g}^{-1}$) and D-MIP ($3.98 \pm 0.51 \mu\text{mol g}^{-1}$), that was four times and twice as high, respectively, than that obtained for the NIP ($1.85 \pm 0.27 \mu\text{mol g}^{-1}$). These observations indicated that the chemically reactive dopamine imprinted receptor that was achieved by the dual imprinting approach had produced mainly 1a, and this allowed for identification of the conformations that was associated with this effect of enhancement of the reactivity over the MIP by a single template approach. Moreover, the longer phenyl side chains in phenylethylamine (2) formed 2a in comparison to 1 that formed 1a, which was displaced only at the chlorine atom ($\sim 4.5 \pm 1.2 \mu\text{mol g}^{-1}$), in the presence of all of the polymers. However, the amine group of the shorter side chain in benzylamine (3) formed a product by displacing both the halogen atoms in both the D-MIP and the DS-MIP, yielding 3.76 ± 1.37 and $4.65 \pm 0.93 \mu\text{mol g}^{-1}$ of 3a, respectively, while no product was formed using the NIP. The amino group of the amine reactant indeed resulted in a higher yield of the coupling product than the corresponding reaction in solution, and the DS-MIP was much better than the D-MIP, although the former imprinted cavity helped the regioselective formation in the synthesis of the newly formed chlorobutyrophenone-type ligand. In contrast 4 did not react because of the bulky methyl ester group that could associate within both the D-MIP and the DS-MIP. For the alkyl halides, there was generally a partial positive charge on the carbon atom and a partial negative charge on the halogen atom. Alkyl chlorides are also more reactive than the aryl fluorides toward nucleophilic substitution. Thus, a nucleophilic attack on the electron-deficient carbon and displaced the halide ion to form the products inside the cavity. However, steric hindrance affected the selectivity and the binding affinities of the reactants where the imprinted cavity combined with selected complementary reactants to synthesize the dopamine analogs. The amine nitrogen atom of 4 was the weakest nucleophilic agent of those investigated. It was of interest, that the absence of the product of the nucleophilic reaction of the ester analog of phenylethylamine (4) either in the mold or at a non-specific site, indicated the disturbance of a bulky group in the solvent to the chemical reaction within the binding sites. It appears likely that the close proximity of the residues to the functionalities in the MIP binding sites that were an *in situ* best fit and may stabilize the newly formed chlorobutyrophenone-type ligands in the complex and added to the reversible rebinding. This also evolved the counterparts held together into the pairs of the alkylation products. These observations indicated that the most basic reagent was the most reactive nucleophile, and the specific orientation of the

reactant molecules depended on the functionalities of the imprinted sites.

Despite the differences in the structure between D and S, they both possess a 1,2-diol structure on an aromatic ring. The amine compounds do not, but can enter the imprinted site and then react. This method enables the self-assembly of molecules that are complementary in shape and size to the chemical functionalities and the geometry of the imprinted cavities. Here, 1 was the most reactive nucleophile, and 2 was more nucleophilic than 3. However, the polar surface area and hydrogen-bonding donor and acceptor sites of the amine precursors in the alkylation reaction of 1 were similar to those of the other reactants except for 4. The position of the nitrogen structure in 5 may allow it to form a hydrogen bond within the cavity to promote formation of the coupled product. These in-cavity reactions indicated that 1 was a good precursor for the mold reaction. Nucleophilic substitution of 5 in DS-MIP ($11.75 \pm 3.31 \mu\text{mol g}^{-1}$) gave much more of the coupling product than the D-MIP ($8.15 \pm 1.43 \mu\text{mol g}^{-1}$), but produced a slightly higher yield than that in the NIP ($10.03 \pm 0.61 \mu\text{mol g}^{-1}$).

3.5.1. Molecular modeling

In this section, we examined the interaction of various amines with the functionalities of the binding sites in the MIPs. Molecular modeling showed the conformation of all the amine reagents that were readily bound to the binding sites in the MIPs (see Fig. 2B). The space factor occupied by the volume and the binding of the template analogue structures was defined to examine the location selected for each binding site. This information can be used to determine the optimum level of each variable in the immobilized chlorobutyrophenone derivatives in the MIPs. The amount of the chlorobutyrophenone product was closely related to the volume of the amine and the Gibbs free energy of binding in the MIP. Fig. 4a (panel B) depicts an area of the response surface that was generated by the binding score (K_i) for the molecular volume of each amine and the free energy of binding to the MIP. The flat profile indicated that there was little or no interaction between these two parameters. The steric reagent appeared to form less than the small molecules for all the four amines because of the possibility of adsorption, so it could be confined in the cavity more easily; 3 can enter the cavity and react, 1, 2 and 5 can react on a non-specific surface and within the MIP cavity, except that compound 5 afforded a very low yield. However, the steric amine 4 as the target analyte cannot enter the cavity to afford the coupling product. K_i is lowest with a larger volume, particularly for the larger and bulkier compound 5 as compared to the phenyl ethyl ester compound 4. Our results indicated that the active center of the receptor mimics and substantially changes the aromatic connectivity, and plays an important role in the substitution of the aromatic compounds. Consequently, barriers to rotation of the probe of the aryl ring in the reaction depended on the spatial orientation and geometry of the surrounding MIP, which lead to their complementary of the reactant retained at the region of the nucleophilic reaction.

Fig. 4a (panel C) shows the K_i response model for pK_a , which indicated that the structure similarities of the dopamine analogues, and confirmed that small changes in the pK_a would have little effect on the reaction. For any one particular experimental condition, the geometrical center of the utilized space factor depended on the response of the K_i of the nitrogen amines. It was a surprise that, all the hit compounds had the newly formed amine moieties separated by the aromatic ring. Other compounds having the same spatial and a similar volume between the tyramine and phenylethylamine molecule fragments, but a different location of a different steric requirement because of the introducing of the *N*-methyl ester of phenylethylamine, when there was an absence of covalent interaction, but was easy to produce similar template assemblies. For the most reactive nucleophile, the highest yield of product 5 was

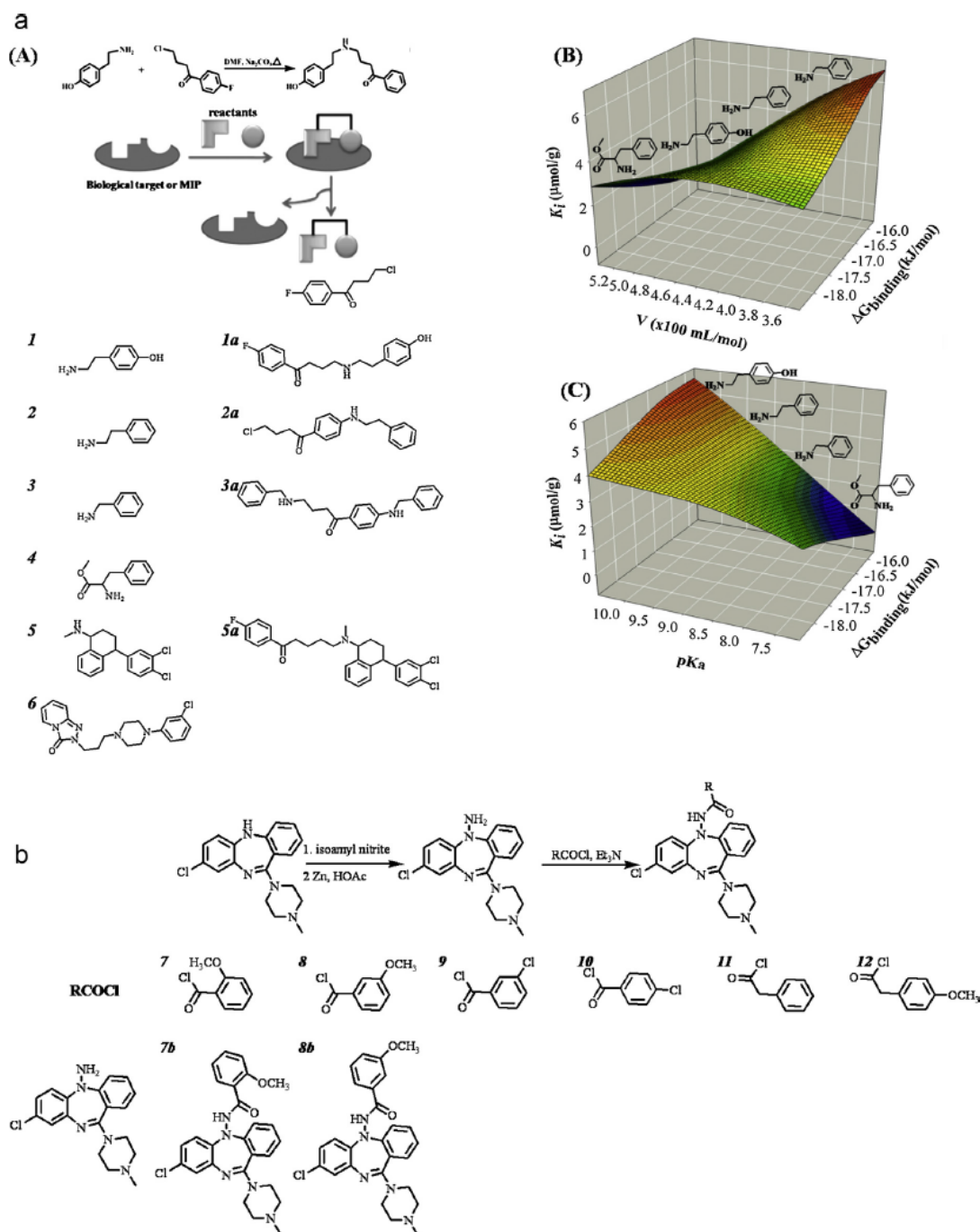


Fig. 4. (aA) Structure of the chlorobutyrophenone and the amine-associated receptors used in this study. (aB) Response surface data for the K_i of the neurotransmitters at different volumes, and (aC) The pK_a value and free energy after modifications for the chlorobutyrophenone-type ligand. (b) Illustrations of the preparation of hydrazinoclozapine derivatives by nucleophilic substitution in the imprinted cavities, and the structure of the clozapine derivatives used in this study.

formed in the imprinted cavities. They were capable of constructing hydrogen bonds, that provided for an electrostatic interaction of molecules but with a different steric requirement. Our results indicated that the newly formed chemicals improved the production. This was attributed to the nanosized pore geometries that possessed the steric requirements of the reagent that occupied the cavity. Hence, the rate of any particular reactions was increased,

and the MIP acted as a protective agent for the selective modification with only minor side products.

3.5.2. Evaluation of the selectivity pattern of the dopamine receptor mimics

The reactions here must be reversible and the nucleophilic reaction of haloalkanes to install the α -carbonyl group in or close to the

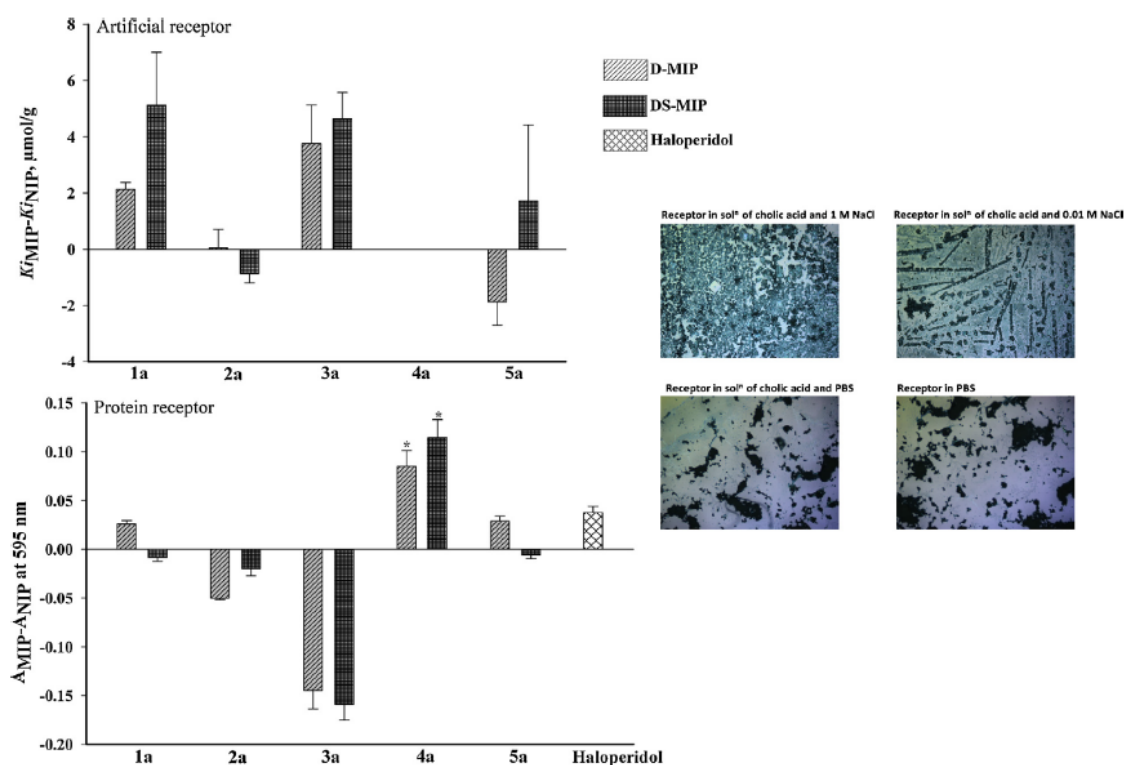


Fig. 5. Comparison of the absorbance between the MIP and the NIP control polymer toward the detection of the neurotransmitters after the modification for the chlorobutyrophenone-type ligands, left panel, Top: MIP; Bottom: the receptor in the membrane from the rat hypothalamus. * Mixture of free substrates. Inset (right panel): Light microscope micrographs of the pellets of receptors from the rat hypothalamus in various media upon their isolation.

binding group that has the selectivity of the optical isomer of the template. Addition of the DS-MIP to the reactions between clozapine hydrazide and *ortho*- and *meta*-monomethoxybenzoyl chloride reagents in the DMF produced a higher yield of the coupling products compared with those obtained by adding it to the NIP (see Fig. 4b). For the clozapine derivatives, the *ortho*- and *meta*-methoxy substituted aromatics of the shorter acid chlorides reacted with hydrazine in the cavity of the MIP to afford the coupling products 7 formed 7b and 8 gave 8b. Their presence in the MIP particles could be detected by using ^1H NMR. However there was no reaction of the *meta*- or *para*-chloro or *para*-methoxy substituted aromatics or unsubstituted aromatic with the hydrazine to obtain the free acid chlorides in both of the MIPs. Our approach involved the specific spatial sites for interactions within the matrix because of the steric constraints within the structure toward the target/analyte within the template pattern. The chloro and methoxy groups of 10 and 12 were too far from the amine moiety of the clozapine hydrazine to fit into the nearest hydrophobic binding site, that did not favor nucleophilic substitution with the hydrazine derivatives. It was of interest, that the reaction occurred within the imprinted cavities and then the product was adsorbed onto the cavity binding sites, because free hydrazine was not observed in the MIP particles when we used other substrates. This striking result indicated that the specificity of the receptor was associated with the S binding site, which mimicked the switchable residues, and provided a lower dopamine affinity but substantially improved the affinity to the natural serotonin receptor. In comparison, the NIP prepared in the absence of the template did not allow for the control of the orientations of the precursors. Therefore, the MIP showed a high specificity for the synthesis of D-related compounds because of the geometry of its cavity.

However, the MIP could not immobilize some chloro- (or *p*-methoxy) substituted benzoyl chloride reagents and clozapine hydrazide in a specific orientation. The acid halides reacted with the carbonyl groups of the *meta*- and *ortho*-substituted analogs of clozapine. In this case, the amide moieties of the clozapine derivatives may be located too deeply within the D imprint, so that alkylation was hindered but the reaction with the acid chloride was still possible. Sasikumara and coworkers [37] produced acylated hydrazinoclozapine, but it was very sensitive and not stable, using acid chlorides with yields of 60–80%. In this manner, the aromatic rings of hydrazinoclozapine reacted in the DCM modifying chemical environment of the reagents in a way that we can detect reaction products. The methyl ether derivatives of clozapine were oriented in two different ways; one inside and the second outside the MIP cavity. The *meta*-methyl ether substituent could bind at different positions inside the cavity. The complex with an *ortho*-methyl ether substituent on the aromatic ring has a restrained structure with an *exo* arrangement of the aryl substituent.

3.6. The screening of proteins in the hypothalamus

We investigated the specificity of the D analogs to the brain receptors for the neurotransmitter dopamine and for comparison to structurally related compounds that had been incubated with the MIPs to those receptors from the isolated rat hypothalamus, which may yield a potential hit by significant differences between the absorbance of MIPs and biological receptor. However, the mixture of free substrates [(1-chloro-(4'-fluorobutyrophenone) and amine] interfered with the immunoassay reagent, thus we performed measurements of the absorbance at 595 nm for all the test compounds, due to protection of the receptor binding sites. Fig. 5(left), bottom

panel, shows 1 and 5 products using both MIPs that exhibited the similar absorbance when incubated with the protein. Because the products of tyramine (1) and sertraline (5) had different chemical structures, this resulted in almost complete selectivity for the *syn*-isomer by both the imprinted polymers. Evidently, the products using the D-MIP for amine 1 and amine 2 using DS-MIP had a similar effect on the protein receptor. These results demonstrated that the imprinted cavities facilitated the induced function as an effective nanoreactor and led to the regioselective formation that was more similar to the D template due to having closely spaced binding sites in the polymer matrix. The chlorobutyrophenone derivative of clinical significance was the highly potent haloperidol. When the haloperidol (control) was incubated with the receptor protein it turned out to have a positive absorbance. Likewise, a validation assay using the control experiments was carried out using the chlorobutyrophenone reagent, that reacted with amine 4a under the same procedure of synthesis and made it possible for a comparison of the absorbance between the MIP and the natural receptor isolated under the conditions described in the Experimental section, despite the differences of binding receptor features of the hypothalamus isolated in various media, as shown in Fig. 5 (insert, right hand side) can affect to the binding affinity of the test compound. The receptor that was exposed into the transmembrane of the lipid bilayer with various buffer and salts, possessed the structural features with an orientation that was essentially important for the specific functions of the receptor to a biological candidate. It was intriguing that the product of the amine 3 and 5 had a different effect, from either of the two MIPs. Also a higher absorbance and phenomena was demonstrated in an opposite way to the natural receptor, to indicate that they had the possibility of an interaction for the protein. Especially, it was clearly observed that the products of 2 and 3 that had a negative absorbance for their binding on the polymer with respect to the corresponding NIP (Fig. 5, top panel) was stronger than on the protein surface of the brain receptor (Fig. 5, bottom panel) compared to the relative absorbance on the natural receptor that was opposite to that for either of the MIPs. The receptor–ligand interactions were examined and the difference in the absorbance was the largest for the benzylamine fragment compared with those for the receptors in the rat hypothalamus. This indicated that an additional potent hit was obvious and most effective.

3.7. Molecular docking of the dopamine and serotonin receptors

In this study, we produced a model crystal structure of the dopaminergic and serotonergic receptors that showed substantial differences in the extracellular electrostatic surfaces and that could affect the binding of ligands. Fig. 6 shows the lowest energy conformations of the newly formed compound from the mold reaction in the MIP materials for both the 3PBL of D3R structures and the 4IAR of 5HT_{1b} described in the experiment. Compound 3a with two benzyl amine groups exhibited a folded short chain for the butyrophenone moiety with two hydrogen bonds for the binding site of the natural dopaminergic receptor. The NH group of 3a formed another hydrogen bond with an oxygen atom on the benzene ring of TYR373 (2.05 Å) and there was a unique interaction of NH(ILE183)–O=C (2.03 Å) in the lowest-energy structure. The aryl substituent on the butyrophenone at the dopaminergic binding site enhanced the binding energy between the benzylamine entities, and resulted in interactions with a large surface area contact. This could be interpreted as a consequence of the two benzylamine groups, and revealed the importance of the butyrophenone derivatives. The contact interaction of 4IAR with 3a contained a hydrogen bond with ASP352 (1.78 Å) that should be of much importance to the receptor specific activities. However the biological activity was determined by the higher K_c and the more favorable free energy at

the binding site in the MIP. The accessible surface area was crucial for the rebinding of the initial template, especially for the extent of the energetic dominance for the MIPs. The spatial defined distances between the groups play important roles in the binding of the D receptors to proteins.

Fig. 7a illustrates the overlay of the synthesized compounds and contact interactions of the two types of D-related compounds with the 3PBL chain A of the D₃ receptor [PDB:3PBL chain A] and the 4IAR of the 5HT_{1b} receptor [PDB:4IAR], respectively. In most cases, the minimum energy conformations can be used to explain the structure of the receptor assemblies, that influence the distances and even the orientation of a complex inside the cavity. For the D₃ complexes, the higher affinity of the *syn* regioisomer of the aromatic residue induced a change in the conformation of 5a that enhanced the interaction of the aromatic π – π association at the peripheral site. In the case of 1a, a change in conformation occurred but with a lower affinity. The chlorobutyrophenone derivatives had Surflex-Dock scores or a $pK_d > 5.94$ for both the D₃ and serotonin 5HT_{1b} receptors. Also, the oxygen atom of the carbonyl group of 1a and 2a markedly formed an interaction *via* hydrogen bonds with the amide group of ILE183 (2.03 and 1.85 Å, respectively). However, 5a and 7b did not form hydrogen bonds with ILE183. In addition, the *o*-methyl ether derivatives of clozapine (7b and 8b) were bound to the D₃ receptor. Compound 1a and 2a bound more tightly to the 3PBL than to 4IAR. Conversely, the 5a, 7b and 8b bound most strongly to the 4IAR with the side chains in the binding pocket. 3a formed a hydrogen bond with the ASP352 of 4IAR (1.78 Å). The NH group of 1a contained a fluoro-aromatic group in the same way as that in the 5a that exhibited hydrogen-bonding interactions with CYS199 (2.07 Å) and the phenol group formed two bonds, one with ASP352 (2.75 Å) and the other with the NH₂ of the amide group of GLN41 (2.05 Å). A hydrogen bond formed between the hydrogen atom of the amine group of 2a and the oxygen atom of the hydroxyl group of THR134 (2.19 Å). Concerning the ChemScore values, the free energy of binding of 3PBL and 4IAR with 2a was less than the free energy of binding with 3a for both the 3PBL and 4IAR. The interaction of the 3PBL chain A of the D₃ receptor to the most active compound 3a as well as the binding to 4IAR of the 5HT_{1b} receptor [PDB:4IAR] is shown in Fig. 7b.

This approach has highlighted the intermolecular hydrogen bond interactions of the template and complexation in the MIP, to the significant role leading to reversible assemblies of template and adsorption of the favourable reagent. Collectively, the preparation of the dopamine imprinted polymers and the possible binding site of the D-MIP after the polymerization process in this study was summarized in Fig. 8. As can be seen, the monomers were aligned around the templates in the polymerized mixture prior to the polymerization that was obtained from the spectroscopic data and a computational method. Also, the fine-tuning affinity can be accounted for by the hydrophobic effect with the indole and indoleamine moieties, forming accessory binding sites for the D mimics that should precisely assess the action of the artificial receptors. The selectivity patterns of the binary template approach for a dopamine imprinted receptor that, succeed in conversion of the covalent bonds with effective immobilization suggesting the presence of both of the two ring systems (D and S) that most likely provide a complex combination of building blocks because typically four rings or more can be located inside the imprinted cavities. We anticipated that the difference of selectivity achieved from both the D mimics was caused by the condition of synthesis during the synthetic procedures, and was attributed to the optimization of the geometrical fit with a favorable molecule on the prepared D and S molecularly imprinted receptor. However, when each of the remaining compounds were bound to the D or S receptors, from the complementary reagents that were related to the surface chemistry and positions of the functionalities in the MIP

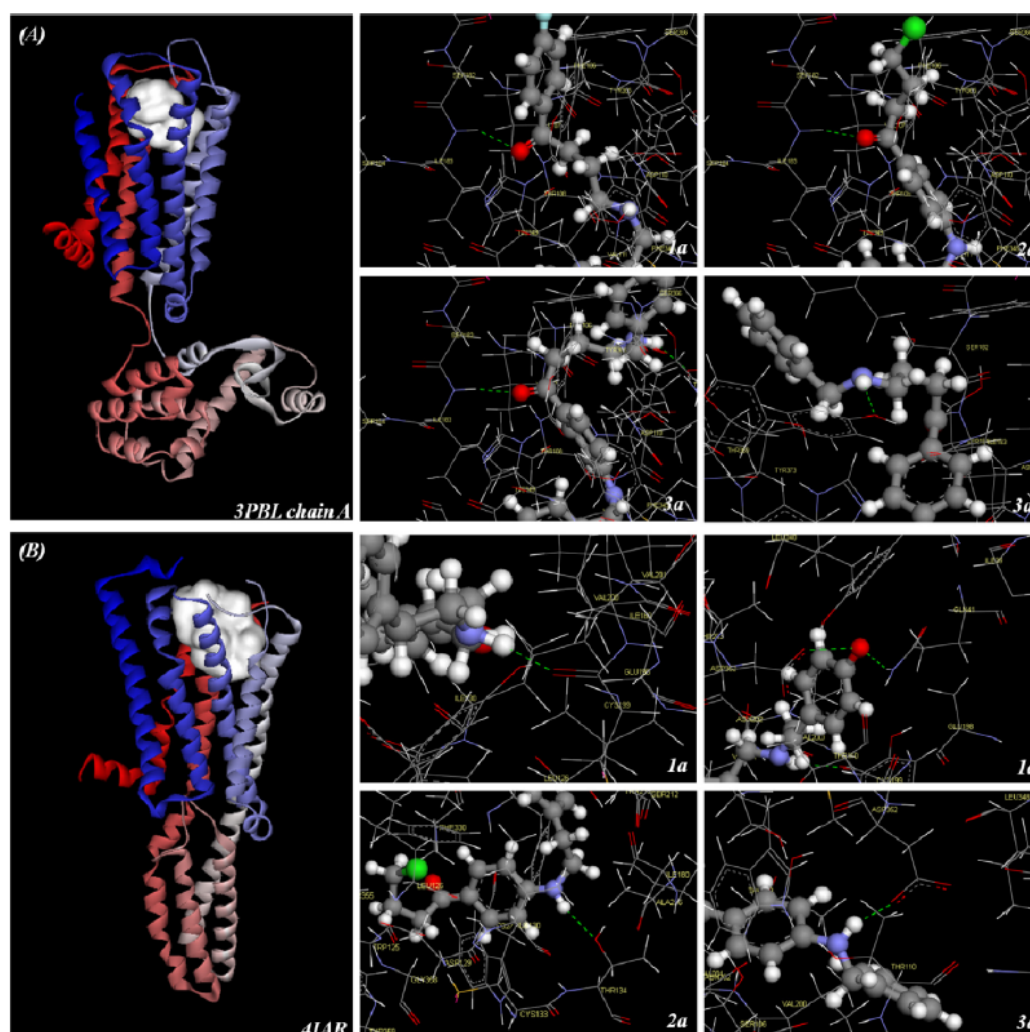


Fig. 6. The differential contact interaction of the neurotransmitters toward the chlorobutyrophenone derivatives *1a*, *2a*, *3a* and *5a* with, (A) the subunit interface of the D_3 receptor binding protein with a common binding surface and (B) the 5-HT_{1b} binding protein with a common binding surface. Hydrogen bonds are displayed as green dashed lines between the donor and acceptor atoms.

binding site that was in close proximity to the multiple active sites but avoided the non-active center of the D imprint cavity by forming an irreversible connection bond. Consequently, the co-templating species can optimize the binding site for the synthesized organic compounds as the ability of the MIPs provided for the optimization of the spatial specific organization.

Docking studies yielded ChemScore values for the D_3 receptor complexes based on the set of known selective antagonists including aripiprazole, clozapine, fluphenazine, haloperidol, olanzapine, risperidone, spiperone, (*S*)-(–)-raclopride tartrate salt and also the agonists of 5HT_{1b} (*R*)-(+)-SCH-23390 HCl and bromocriptine. Fig. 7c shows the free energy of binding determined from the ChemScore values. A clear energetic preference was calculated for the affinity of the biologically relevant compounds and known drugs, which exhibited energies from -21.82 to -45.89 kJ mol^{-1} . *1a* and *2a* bound more tightly to 3PBL than to 4IAR. However, the aryl substituents on the aromatic compounds *5a*, *7b* and *8b* had different structures, i.e., a long chain hydrocarbon and a planar structure

that were not observed in the hydrogen-bonding interactions at the D or S binding sites of the receptor with the strongest binding in the 4IAR. Furthermore, the two separated benzylamine groups on the structure of *3a* resulted in specific intermolecular interactions in addition to van der Waals interactions. This resulted in an aligned structure for a greater area than that found for the comparable interactions with a single molecule of neurotransmitter of interest. Pharmacophore models were constructed and the docking of the six compounds obtained in this study and the eight marketed D antagonists and the serotonin agonists that showed high docking scores were determined. The results demonstrated a good binding capacity with the dopaminergic receptors for *1a*, *2a*, *3a* and *5a*, with a good correlation to the D antagonists clozapine, risperidone, fluphenazine and spiperone ($R^2 = 0.7728$). For *1a*, *5a*, *8b* and clozapine they showed a good correlation with clozapine, fluphenazine, haloperidol, and (*R*)-(+)-SCH-23390 ($R^2 = 0.9971$) in reproducing the experimentally observed binding for a serotonergic receptor. Assessing these observations, the dopaminergic receptor readily

binds to *1a* and *5a*, and supported the notion that there was an enhanced potency to the serotonin receptors. Consequently, the docking results can explain the pharmacological effects of the synthesized organic compounds produced at the recognition sites in the MIPs.

3.8. The proposed model of the ligand-binding selective D₃ receptor

The structure of the D analogs was crucial for the efficacy of the response of the D receptors. The carbonyl group is not just involved to the most tightly bound of these stabilized product interactions in that location inserted between the PHE-345 and the SER-192 near to the gorge rim, as shown in Fig. 9a. The MIP cavities controlled the

shape and size of the products, that yielded active regions because of the template that was used to form the MIPs. All the chlorobutyrophenone derivatives docked into the active site of a D receptor. The pharmacophore model and the mapping of the butyrophenone derivatives *1a* and *2a* are presented in Fig. 9b. The results indicated the presence of multiple sites of interaction within the MIP binding sites that included the newly formed chlorobutyrophenone-ligand types due to optimization of the geometry fit between the binding group and the target analyte. A common pharmacophore model was proposed: the distance between a hydrogen bond acceptor and the *N*-location was 6.09 Å, and the distance between a hydrogen bond acceptor and the aromatic region to the *N*-location was 3.7–6.6 Å. This new pharmacophore model will be used to design compounds of this class in the future.

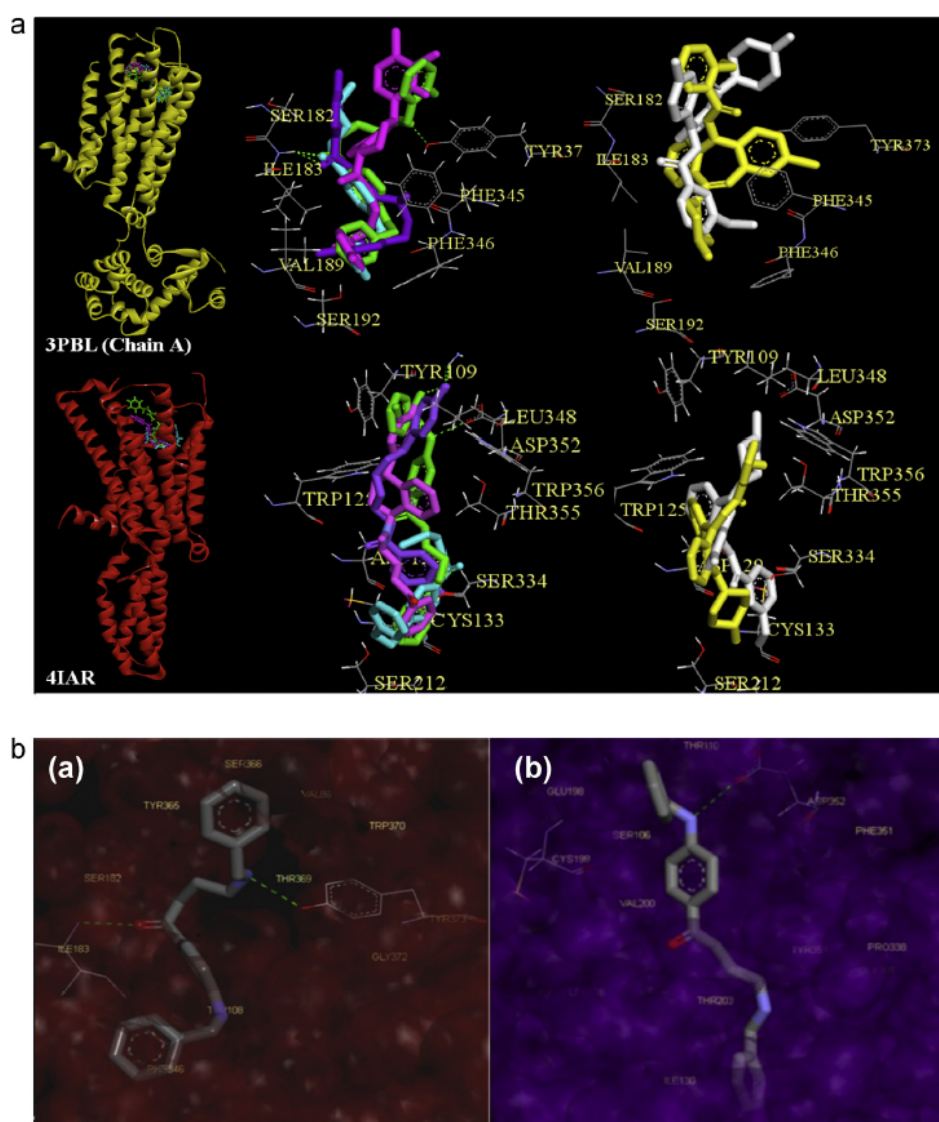


Fig. 7. (a) Schematic diagram of the interactions of Tyr373, Phe345, Ser182 and Ile183 of the complementary subunit in addition to those noted in the principal subunit for, Top: the D₃ receptor; Below: CYS199, ASP352 and GLN41 of the 5HT_{1b} serotonin receptor for the chlorobutyrophenone-type ligands (left) and clozapine derivatives (right). (b) Illustration of the specific binding interactions of *3a* in the D₃ receptor and the 5-HT_{1b} serotonin receptor. Hydrogen bonds are displayed as green dashed lines between the donor and the acceptor atoms. (c) The data for the molecular docking of the chlorobutyrophenone and clozapine derivatives, selected antagonists of D₃ and the agonists of 5HT_{1b} by Surfex-DOCK and SVM. (For interpretation of the references to color in this figure legend, the reader is referred to the web version of this article.)

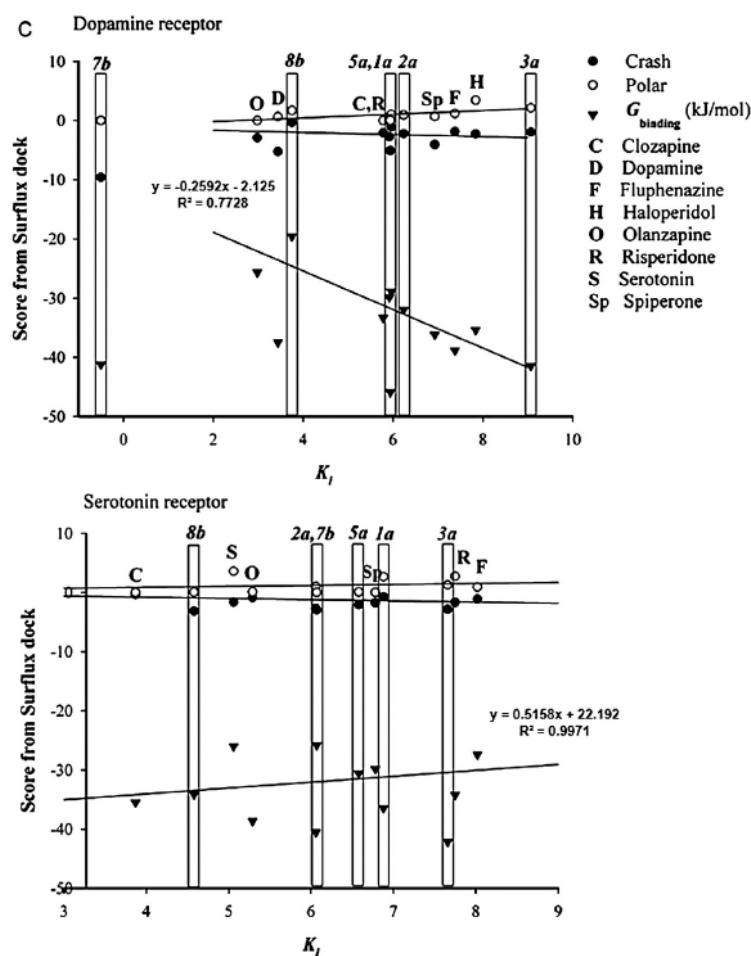


Fig. 7. (Continued).

3.9. Activation profiles of the dopaminergic libraries

The affinity of the synthesized compounds obtained from the modification of the neurotransmitter in the chlorobutyrophenone-type ligands was examined for the isolated D₁ receptor using competition affinity assays with specific probes. The competitive binding assays revealed that the chlorobutyrophenone-type ligands could bind the D₁ receptor isolated from the rat hypothalamus (Fig. 10). The concentration dependence of the drug-receptor binding implied that all the sites were accessible and active. An essential feature of maximizing the pharmacological properties between the biological candidates and the natural receptor, D₁ is supported by biological assays, which should maintain their function and biochemical entities during templating synthesis, and hence resulted in the preservation of biologically active molecules. Table 4 shows the biological activity of the synthesized compounds for the natural D₁ receptor. 3a showed the highest binding affinity, while 5a shows the highest log ED₅₀ of the compounds. With the optimized binding buffer, the complex structure found for these products was consistent with the binding assay that turned up the rapid discovery of an active ligand binding to the D₁ attractive drug. Thus, this approach could lead to improved medications, which is highly desirable for the treatment of neurological diseases with fewer side effects.

Drug screening on the cloned receptor of the D₃ receptor has been recently reported, however the testing and identification of the cloned receptors are difficult yet are needed for accuracy and specificity. Despite the usefulness of the dopamine receptor biomimics based on these molecular imprinting techniques are likely to address the problem of the availability of the dopaminergic receptor, although the orientation of the neurotransmitters in the MIPs may differ from its biological counterparts. Our approach even precisely defined a specific binding site for the action of the drug that affected dopamine transmission as the above-mentioned allowed for the identification of the subtype selective D₃ receptor drugs which indicated that the good docking scores provided a

Table 4
Activation profiles of various chlorobutyrophenone derivatives to D₁ receptor.

Compound	B_{max}^* (μ M)	K_d^{**} (nM)	Log ED ₅₀
1a	0.423	141	6.26
2a	0.435	227	3.20
3a	0.437	207	5.02
5a	0.467	558	6.79

Data extracted from best fit to $[analyte]_{bound} = B_{max} [analyte]_{free} / (K_d + [analyte]_{free})$; ($R^2 > 0.990$).

* Maximal binding capacity.

** Dissociation constant (30 μ g of the receptor was used).

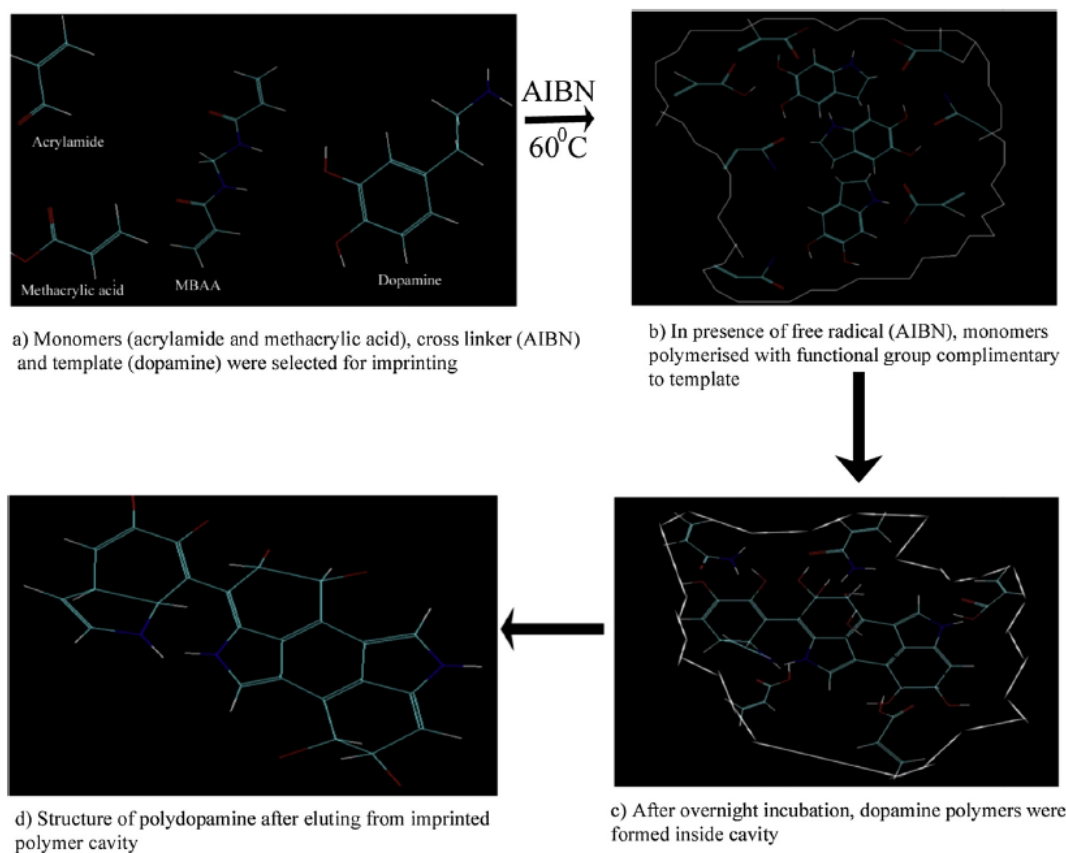


Fig. 8. Possible binding sites in the dopamine imprinted receptor and the proposed procedure for preparation of an imprinted dopamine receptor with collection of sample data and the interpretation of the phenomenon observed in this study.

correlation with a number of known pharmaceutical compounds for both the D_3 and 5-HT_{1A} . As a consequence we can generate selective D_3 compounds with neuroprotective effects. The pharmacophore model achieved for interaction of the D_3 receptor with the synthesized compounds obtained from the imprinted nanovesel will also allow us to understand the role of this receptor subtype in producing anti-parkinson effects in the brain.

Different dopamine agonists have been shown to provide a critical response to medication since practical guidelines for the useful management of Parkinson's diseases that have been previously reported and the incidence of the dopamine modulation with neurobehavioral-related side effects was able to induce the development of impulse control disorders (ICD) that have occurred most frequently [38]. The occurrence of neuropsychological behaviors during the treatment of Parkinson's patients can be linked to other neurological disorders such as restless leg syndrome and amyotrophic lateral sclerosis. The use of dopamine agonists for Parkinson medication has induced the hypersensitivity of neuropsychiatric behaviors and in particular ICD has focused the connections of neural activity through the pathway of subtype receptors [39,40]. Any strategies for the discovery of anti-psychotic drugs related to the selectivity of action that is relatively specific to the subtype receptor that will impact to respond to Parkinson's disease may increase the risk of ICD incidence in the patients, so that our approach may remarkably provide the opportunities for introducing a strategy that is promising to help in this context. Our present approach has demonstrated that the development of the synthesis of dopamine binding ligands that generated

potent molecules that were chiefly selective for the D_3 receptor compounds resulted in a reduced concentration of the dose and were tunable into receptor subtypes and other related dopaminergic receptor which afforded D_3 selective compounds and would provide for more efficient therapeutics. In the current study, using a nanosized mold having the functional counterparts they were complementary to the pharmaceutically active compound as the template that can be used for engineering of bioorganic molecules with an identically biological entity on a natural dopamine receptor could be a promising way to solve clinical problems and manufacturing issues. Combined with pharmacophore model studies, the alternative approach should improve a better interplay of distinct structures, by providing a powerful tool to predict clinical issues and gain an understanding of the pharmacotherapeutic dopaminergic receptor agonists in the treatment of Parkinson's disease. Previous studies have reported the role of dopamine modulation in relation to the possible emergence of impulse control disorders that led to hyperkinetic/hyperdopaminergic neuropsychiatric conditions [41]. However precise screening of a dopamine receptor agonist on a receptor or with participation of an autoregulation of the CNS or having a self-reinforcing property that genetically regulates a significant deal to a CNS function in disease and the relevant issues of neurochemicals, homeostatic and circadian regulation are carried out when examining for biological and physiological activities [42]. Housing from single molecules in minimal model systems to complex proteins that were based on molecular imprinting techniques with multiple templates similar to this study will lead to receptors with a significantly better affinity and adjustments to

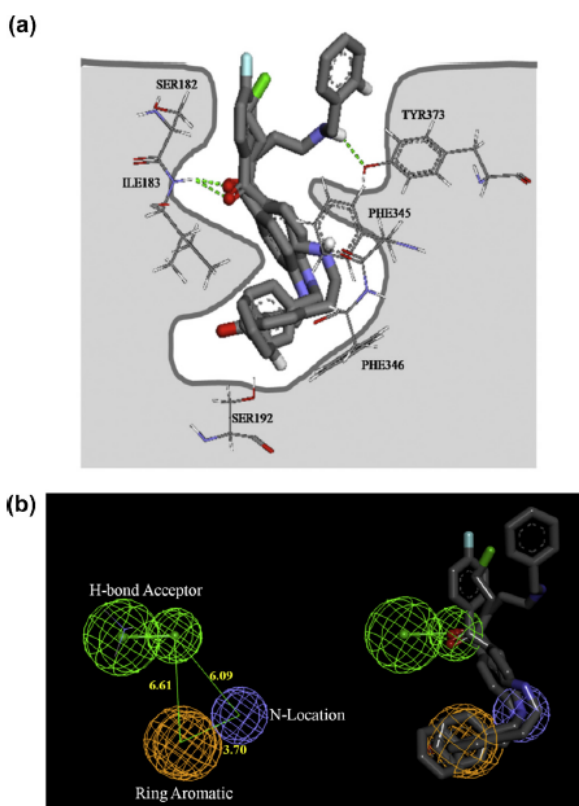


Fig. 9. (a) The proposed model of the interactions between products *1a*, *2a* and *3a* that were close to the subunit binding site of the D_3 biological receptor. (b) The best pharmacophore model and the molecular alignment of the compounds used to establish the model showing a possible role from the molecule fragments that were inserted into a specific binding pocket of the protein near to the gorge rim as being the significant pharmacophore of this class.

their suitability with respect to *in vivo* concerns. This may provide great promise to assist in the discovery of psychoactive drugs with features that reduce the burden of disease. This biomimetic recognition material would create novel processes applicable to the field of medicine and pharmaceutical industries.

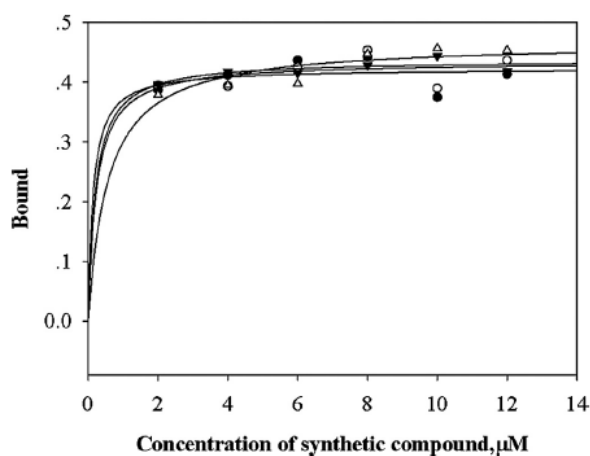


Fig. 10. The competitive binding assays of the D_1 receptor isolated from the rat hypothalamus for various compounds.

4. Conclusions

In this report, we have prepared an imprinted dopamine receptor that exploits multiple recognition sites for known bioactive compounds to identify a possible library of biologically active entities of dopamine analogues. Based on the FT-IR studies and observations from chromatographic analyses, the chemical functionalization of the acrylamide-imprinted cavities ensured the dynamic control of the polymer, while providing for the interaction of functional group anchor sites and the reactant into the molded cavities. The results obtained for the ligand binding and from competitive assays with the dopamine imprinted receptor for both the MIPs revealed the possibility for reversible binding and assembly of the activities of a drug, biomolecule. The result has illustrated the possibility of a visiting molecule that will certainly be close to the multiple active sites of the MIP binding site that was generated by the newly formed compounds and resulted in additional potential hits for determining the binding affinity of a natural dopaminergic receptor. On the other hand the imprinted site appeared to be distinguishable by a favorably adsorbed reagent because of the existence of a shadow mask in the MIP binding site, which did not yield any alkylation product. The increased obscurity of the assay systems can be used to test ability to detect differences in the pharmacological effect and the vitally important facets of the global target activity is of considerable importance. The imprinted cavities could be exploited for the study of the structure and selectivity of the ligand binding sites of the dopamine receptor by their conditioned responses that were difficult to be detected by the conventional imprinting method. The versatility of this approach has been directed to produce the specifically site-binding affinity for the treatment of various neuroleptic disorders in the CNS and for the application of a search for a dopaminergic library. The important finding is the possibility for creating the image of the original template species allowing close proximity of the binding site of the protein to be offered a maximized specificity of a dopamine imprinted cavity for producing a highly potent agonist and selective molecules for the D_3 agonist. Reactions that possess hydrogen-bonding interactions can be inferred from the D_1 interaction activation profiles of the biological test for the potent compounds that could maximize the clinical effects or mitigate drug toxicity.

Acknowledgments

This work was supported in part by the Thailand Research Fund (grant no. DBG5480006), Strategic Scholarships Fellowships Frontier Research Networks (Specific for the Southern region, grant no. 01/2554) and Graduate Study, Senior Project Funding and a post-doctoral fellowship from the Prince of Songkla University, Higher Education Research Promotion and the National Research University Project of Thailand, Office of the Higher Education Commission, Drug Delivery System Excellence Center, Nanotechnology Center (NANOTEC), Ministry of Science and Technology, Thailand, through its program of the Center of Excellence Network and Department of Pharmaceutical Chemistry, Faculty of Pharmaceutical Sciences, Prince of Songkla University. The authors thank Mr. Sarunyoo Moonlaong and Miss Ratchadaporn Pratum for the initial preparation of the polymers and Mr. Mitree Naunplub for assistance with animals and Dr. Brian Hodgson for assistance with English.

Appendix A. Supplementary data

Supplementary data associated with this article can be found, in the online version, at [doi:10.1016/j.procbio.2015.06.018](https://doi.org/10.1016/j.procbio.2015.06.018)

References

- [1] T.R. Kosten, T.P. George, The neurobiology of opioid dependence: implications for treatment, *Sci. Prat. Perspect.* 1 (2002) 13–20.
- [2] S.A. Rotenberg, T. Calogeroopoulou, J.S. Jaworski, I.B. Weinstein, D. Rideout, A self-assembling protein kinase C inhibitor, *Proc. Natl. Acad. Sci. U.S.A.* 88 (1991) 2490–2494.
- [3] P.F. Damasceno, M. Engel, S. Glotzer, Predictive self-assembly of polyhedral into complex structures, *Science* 337 (2012) 453–457.
- [4] A.M. Whitney, S. Ladame, S. Balasubramanian, Templated ligand assembly by using G-quadruplex DNA and dynamic covalent chemistry, *Angew. Chem. Int. Ed. Engl.* 43 (2004) 1143–1146.
- [5] O. Ramström, J.-M. Lehn, Drug discovery by dynamic combinatorial libraries, *Nat. Rev. Drug. Discovery* 1 (2002) 26–36.
- [6] S. Lesné, M.T. Koh, L. Kotilinek, R. Kaye, C.G. Glabe, A. Yang, et al., A specific amyloid-beta protein assembly in the brain impairs memory, *Nature* 440 (2006) 352–357.
- [7] L. Ye, P.A. Cormack, K. Mosbach, Molecular imprinting on microgel spheres, *Anal. Chim. Acta* 435 (2001) 187–196.
- [8] K. Mosbach, Towards the next generation of molecular imprinting with emphasis on the formation, by direct molding of the compounds with biological activity (biomimetics), *Anal. Chim. Acta* 435 (2001) 3–8.
- [9] A. Nakazato, S. Okuyama, Recent advances in novel atypical antipsychotic agents: potential therapeutic agents for the treatment of schizophrenia, *Expert Opin. Ther. Pat.* 10 (2000) 75–98.
- [10] M.D. Wood, C. Scott, K. Clarke, K.J. Cato, N. Patel, J. Heath, et al., D.N. Jones, Pharmacological profile of antipsychotics at monoamine receptors: atypicality beyond 5-HT_{2A} receptor blockade, *CNS Neurol. Disord. Drug Targets* 5 (2006) 445–452.
- [11] G.J. Rodriguez, R. Yao, O. Lichtarge, T.G. Wense, Evolution-guided discovery and recoding of allosteric pathway specificity determinants in psychoactive bioamine receptors, *Proc. Natl. Acad. Sci. U.S.A.* 107 (2010) 7787–7792.
- [12] P.A. Garay, A.K. McAllister, Novel roles for immune molecules in neural development: implications for neurodevelopmental disorders, *Front. Synaptic Neurosci.* 2 (2010) 1–16.
- [13] C. Enzensperger, T. Görmemann, H.H. Pertz, J. Lehmann, Dopamine/serotonin receptor ligands. Part 17: A cross-target SAR approach: affinities of azecine-styled ligands for 5-HT_{2A} versus D1 and D2 receptors, *Bioorg. Med. Chem. Lett.* 18 (2008) 3809–3813.
- [14] P. Seeman, T. Lee, M. Chau-Wong, K. Wong, Antipsychotic drug doses and neuroleptic/dopamine receptor, *Nature* 261 (1976) 717–719.
- [15] H. Zhang, T. Picham, M. Drew, M. Patek, K. Mosbach, L. Ye, Molecularly imprinted nanoreactors for regioselective Huisgen 1,3-dipolar cycloaddition reaction, *J. Am. Chem. Soc.* 128 (2006) 4178–4179.
- [16] Z. SuFang, X. ChengLong, W. Qiang, L. ZhenGuo, Interactions of CaMKII with dopamine D2 receptors: roles in levodopa-induced dyskinesia in 6-hydroxydopamine lesioned Parkinson's rats, *Sci. Rep.* 29 (2014) 6811.
- [17] F. Gabriella, R. Viviana, M. Alessandra, B. Alessandro, L. Leonardo, A. Paolo, et al., Binding of anti-Parkinson's disease drugs to human serum albumin is allosterically modulated, *IJBMB Life* 62 (2010) 371–376.
- [18] S. Andreas, K. Burkhard, Molecular recognition of organic ammonium ions in solution using synthetic receptors, *Beilstein J. Org. Chem.* 6 (2010) 1–111.
- [19] A.D. Macrae, S. Brenner, Analysis of the dopamine receptor family in the compact genome of the puffer fish *Fugu rubripe*, *Genomemix* 25 (1995) 436–446.
- [20] X. Hu, H.C. Rea, J.E. Wiktorowicz, J.R. Perez-Polo, Proteomic analysis of hypoxia/ischemia-induced alteration of cortical development and dopamine neurotransmission in neonatal rat, *J. Proteome Res.* 5 (2006) 2396–2404.
- [21] C. Missale, S.R. Nash, S. Robinson, M. Jaber, M.G. Caron, Dopamine receptors: from structure to function, *Physiol. Rev.* 78 (1998) 189–225.
- [22] C. Mark, P.J. Thomas, Treatment of CNS disorders with *trans*-4-(3,4-dichlorophenyl)-1,2,3,4-tetrahydro-*n*-methyl-1-naphthalenamine. USA Patent EP 2005; 1545485:A2, 2005.
- [23] R. Suedee, V. Seechamnaturakit, A. Suksuwan, B. Banyuk, Recognition properties and competitive assays of a dual dopamine/serotonin selective molecularly imprinted polymer, *Int. J. Mol. Sci.* 9 (2008) 2333–2356.
- [24] J. Su, H. Tang, B.A. McKittrick, D.A. Burnett, H. Zhang, A. Smith-Torhan, et al., Modification of the clozapine structure by parallel synthesis, *Bioorg. Med. Chem. Lett.* 16 (2006) 4548–4553.
- [25] S.E. Senogles, N. Amlaiky, P. Falardeau, M.G. Caron, Purification and characterization of the D₂-dopamine receptor from bovine anterior pituitary, *J. Biol. Chem.* 263 (1988) 18996–19002.
- [26] M.M. Bradford, A rapid and sensitive method for the quantitation of microgram quantities of protein utilizing the principle of protein-dye binding, *Anal. Biochem.* 72 (1976) 248–254.
- [27] G. Höfner, K.T. Wanner, Competitive binding assays made easy with a native marker and mass spectrometric quantification, *Angew. Chem. Int. Ed.* 42 (2003) 5235–5237.
- [28] L.Y. Han, X.H. Ma, H.H. Lin, J. Jia, F. Zhu, Y. Xue, et al., A support vector machines approach for virtual screening of active compounds of single and multiple mechanisms from large libraries at an improved hit-rate and enrichment factor, *J. Mol. Graphics Modell.* 26 (2008) 1276–1286.
- [29] V.K. Vyas, M. Ghate, A. Goel, Pharmacophore modeling, virtual screening, docking and in silico ADMET analysis of protein kinase B (PKB β) inhibitors, *J. Mol. Graphics Modell.* 42 (2013) 1276–1286.
- [30] N.W. Turner, C.W. Jeans, K.R. Brain, C.J. Allender, V. Hlady, D.W. Britt, From 3D to 2D: a review of the molecular imprinting of proteins, *Biotechnol. Prog.* 22 (2006) 1474–1489.
- [31] P. Luliński, M. Dorota, B.-K. Magdalena, S. Miroslaw, Dopamine-imprinted polymers: template-monomer interactions, analysis of template removal and application to solid phase extraction, *Molecules* 12 (2007) 2434–2449.
- [32] B.L.L. Seagle, K.A. Rezaei, E.M. Gasyna, Y. Kobori, K.A. Rezaei, J.R. Norris, Time-resolved detection of melanin free radicals quenching reactive oxygen species, *J. Am. Chem. Soc.* 127 (2005) 11220–11221.
- [33] D.D. Dreyer, D.J. Miller, B.D. Freeman, D.R. Paul, C.W. Beilawski, Elucidating the structure of poly(dopamine), *Langmuir* 28 (2012) 6428–6435.
- [34] Y. Fut Kuo, Z. Boxin, Adhesion properties of self-polymerized dopamine thin film, *Open Surf. Sci. J.* 3 (2011) 115–122.
- [35] J.N. Joyce, S. Presgraves, L. Renish, S. Borwege, T. Osredkar, D. Hagner, et al., Neuroprotective effects of the novel D₃/D₂ receptor agonist and antiparkinson agent, S32504, in vitro against 1-methyl-4-phenylpyridinium (MPP⁺) and in vivo against 1-methyl-4-phenyl-1,2,3,6-tetrahydropyridine (MPTP): a comparison to ropinirole, *Exp. Neurol.* 184 (2003) 393–407.
- [36] T.L. Volz, Neuropharmacological mechanisms underlying the neuroprotective effects of methylphenidate, *Curr. Neuropharmacol.* 6 (2008) 379–385.
- [37] T.K. Sasikumar, D.A. Burnett, H. Zhang, A. Smith-Torhan, A. Fawzi, J.E. Lachowicz, Hydrazides of clozapine: a new class of D₁ dopamine receptor subtype selective antagonists, *Bioorg. Med. Chem. Lett.* 16 (2006) 4543–4547.
- [38] G.J. Macphee, K.R. Chaudhuri, A.S. David, P. Worth, B. Wood, Managing impulse control behaviours in Parkinson's disease: practical guidelines, *Br. J. Hosp. Med.* 74 (2013) 160–166.
- [39] S. Balarajah, A.E. Cavanna, The pathophysiology of impulse control disorders in Parkinson disease, *Behav. Neurosci.* 26 (2013) 237–244.
- [40] V. Le Foll, S.R. Goldberg, P. Sokoloff, The dopamine D₃ receptor and drug dependence: effects on reward or beyond? *Neuropharmacology* 49 (2005) 525–541.
- [41] A. Wright, H. Rickards, A.E. Cavanna, Impulse-control disorders in Gilles de la Tourette syndrome, *J. Neuropsychiatry Clin. Neurosci.* 24 (2012) 16–27.
- [42] J.R.L. Schwartz, T. Roth, Neurophysiology of sleep and wakefulness: basic science and clinical implications, *Curr. Neuropharmacol.* 6 (2008) 367–378.

PAPER 2

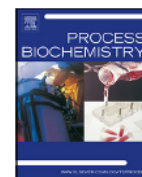
Molecularly Imprinted Polymer Microprobes for Manipulating Neurological Function
by Regulating Temperature-Dependent Molecular Interactions.

(Published in *Process Biochemistry*)



Contents lists available at ScienceDirect

Process Biochemistry

journal homepage: www.elsevier.com/locate/procbio

Molecularly imprinted polymer microprobes for manipulating neurological function by regulating temperature-dependent molecular interactions[☆]



Wanpen Naklua^a, Krishna Mahesh^a, Yu Zong Chen^b, Shangying Chen^b,
Suede Roongnapa^{a,*}

^a Molecular Recognition Materials Research Unit, Drug Delivery System Excellence Center, and NANOTEC Center of Excellence, Department of Pharmaceutical Chemistry, Faculty of Pharmaceutical Sciences, Prince of Songkla University, Hatyai, Songkhla 90112, Thailand

^b Bioinformatics and Drug Design Group, Department of Pharmacy, National University of Singapore, Blk S16, Singapore

ARTICLE INFO

Article history:

Received 2 August 2015
Received in revised form 10 October 2015
Accepted 2 November 2015
Available online 11 November 2015

Keywords:

Molecularly imprinted polymer
Close proximity
Dynamic binding
Molecular identity
Neuronal circuit
Neurobiology

ABSTRACT

We describe molecularly imprinted polymer (MIP) microprobes for manipulating neurological function by the thermoregulatory process. Some target and disease areas show raised temperature than normal temperature which are involved in neuronal diseases, such as Alzheimer's, Parkinson's and Huntington's diseases. As well thermodynamic parameters can be obtained in the environments *in vitro*, which that the assay involves a temperature variable, at or beyond body temperature. We applied for studying molecular aspects of hypothalamus regulated physiology and behaviors. Steady-state binding was detected by fluorescence and Boltzmann energies-based fluorescence emission showed interactions of clozapine with altered energy levels. Dynamic spectra revealed dramatic effects on the fluorescence of the drug in dopamine imprint of MIPs exposed rat hypothalamic membranes at different temperatures. The MIPs that cooperatively occupied and provided the response to the neural proteins were not likely to be involved in the binding of clozapine within the cavity. The results indicated that the dynamics on the surface of proteins exposed to the drug–MIP with assembly, mediated specific function through temperature-dependent molecular interaction in the hypothalamus. Thus, this approach is applicable to processes of key importance of controlling the energy homeostasis and, plausibly, to selective signaling can affect in plasticity of the neural response.

© 2015 Elsevier Ltd. All rights reserved.

1. Introduction

Drug or substrate interactions at the binding pocket of a specifically functional protein in the human brain is one of the essential processes that can be manipulated to selectively separate the therapeutic effects of drugs or drug candidates from their unwanted side effects. Their molecular and cellular interactions are central to studying how biologically active compounds exert their efficacy related to their distributions and structural dynamics in their molecular environments. Such approaches have potential importance for medicine and pharmaceuticals [1,2]. By taking the feature of a unique interface produced by assembly that occurs normally in

the function of a biological system that gives rise a desirable interaction of the delivered molecule [3]. The interacting of specific protein receptor can sense to the extracellular environments producing the developmental signals and improved responses [4]. The tremendous complexity of a molecular interaction in a living system has led to the evolution of physiological signaling molecules that evolve the receptor-mediated neuron in brain. Technology of a single molecule signal passing through a periodic mesoporous material where the specific structural feature influenced on the mobility of the desired molecule [5], this will be able to provide studying for particular cellular functions and even transducing for downstream signals in body. Of even more importance of the specialized responses of the receptors influence from the substrate-binding of anti-psychotic drugs for the psychotic responses and the behaviors and that were dependent on the active functional protein are associated with the physical environments that can affect the actual organization of protein binding sites and assemblies [6].

[☆] This article is dedicated to Prof. Dr. Vimon Tantishaiyakul for the occasion of her 60th birthday.

* Corresponding author. Fax: +66 74 428239.

E-mail address: roongnapa.s@psu.ac.th (S. Roongnapa).

The self-organization involved in the cellular processes of the neural system, though at a relative minor level, can alter the conformational segregation through the ability of the network's that relies on the selective recognition of biomolecules. Signaling molecules within synapse give temporarily or emerging responses in the brain to minimize damage of the cells [7]. The homeostasis control, to circuits, centrally, primarily controlled by the biological activity of the hypothalamus which attenuating the dopamine and serotonin neurotransmitters release by regulating the social behaviors and influenced the balance of emotion and the post-traumatic disorder. The differences of therapeutics traverse the dopaminergic system that can be important to the drug sensitization in the behavioral phenomena, is not discovered, although the possibility it precisely identifiable different intrinsic activities of highly specialized neural proteins in the hypothalamus [8]. This neural system regulates basic function triggered other neurons and that evolve a cluster of populous receptors [9], or the coordination of the functional domains or counterparts [10], that affected to the function. They also regulated the body by respond to minor external stimuli such as motion, pH, carbon dioxide, light and temperature. There have been reported with the reinforced physiological effects and behaviors by the drug and the addiction related to dopamine D₁ receptor reward signaling in the nervous system. The successful development of a drug candidate that required the optimization of selective compound affected to the neural system regulating body to external stimuli. Some previously methods provided for further understanding of the specific aspects of the neurotransmitter receptors. Advance knowledge of the refined binding site is crucial for probing functionally modify selective therapeutics and manipulate biased signaling pathways [11,12]. Previously reported work focused on the role of the human immune systems interacting with specific receptors ultimately regulating responses in the neural system that how they are involved to the neural function have been not widely known [13]. Methodologies enable the study of different functional processes involving on the feedback methods within the neural systems and have been applied in the field of neurosciences in either cells or animals [14]. The recently reported involvement of stimuli on the dopaminergic receptor induced the local protein synthesis implicate the neurotransmitter receptors in the process of the neural circuit and neural plasticity in the hippocampus about which is very little was known [15].

Prescription costs for antipsychotic drugs in the United States totaled about \$18.2 billion USD in 2011 and has since increased by 13%. Clozapine was chosen for this study because it is an atypical antipsychotic agent that acts as an antagonist for dopamine D₁, D₂, and D₄ receptors and serotonin HT_{2A} and 5-HT_{2B} receptors, and as a potent agonist at serotonin 5-HT_{1A}. It also affects epinephrine, acetylcholine and histamine receptors [16]. Clozapine has been used to treat clinical disorders including schizophrenia, Parkinson's disease, other neuroleptic disorders, attention deficit hyperactivity disorder and different spectrums of autism [17]. This drug had evolved to the extrapyramidal side effects, yet the risk of the mortality for long term use has not yet known [18]. If we can understand fundamental ability of receptor response regulating the function it might be interested in developing precisely manipulate specific molecular interactions that mediate nervous system function.

Molecular imprinting technology have aroused extensive attention and been widely applied in many fields and have drawn much attention in recent years [19,20]. The molecular imprinting technique is a well-known emerging approach allowing targeting of crucial components by its ability to recognize naturally occurring templates [21]. Upon polymerization, a three-dimensional network can be generated with selective recognition sites for a template. These biological analogous systems provided the opportunities to customize a preferred selectivity of the recognition element [22].

A microprobe is a molecule that has the ability to measure the properties of other structures or even to activate them to trigger signaling that causes interactions in many fields. They can be used to study the functional selectivity of targets or diseased cells for use in medical diagnostic and biosensor applications [23]. The monolithic polymer obtained by bulk polymerization has to be debrided, ground and sieved to an appropriate size, a process that is time consuming and would reduce the functional properties of the polymer product. In addition, the grinding operation results in producing irregular particles in shape and size, and some high affinity binding sites are destroyed and changed into low affinity sites. Suspension polymerization, emulsion polymerization, seed polymerization and precipitation polymerization has been developed to overcome these drawbacks and surface imprinted polymers are now widely used. In this work microprobes have been prepared based on molecular imprinting technology that allows the synthesis of MIPs by bulk polymerization [24]. We think that the bulk polymerization method offers a high yield of product and that whole template imprinted within the surrounding polymer matrix.

Nonetheless, the reactive substrate binding domain of a neural protein receptor in the hypothalamus is even more complex. While this question has been approached, the present approach offers a better potential as the molecularly imprinted polymers offer a great potential for probing manipulation by the pharmacological effects of antipsychotic drugs. Clozapine can be used as a fluorescent tag exquisite specificity and affinity for selective receptor. Investigating a drug-related structure where the effects in modulating the neural activity of the specific functional protein responses to stimuli, it is possible that this could allow for the improved survival or a reduced serious side effect of anti-psychotic drugs, this has been carried out by present method using MIPs. Use of a MIP is of interest because of the polymers' enhanced chemical stability, superior to that of their natural counterparts and which possibly enabling use for longer periods of time. Indeed we have recently applied this approach to discover potent dopaminergic receptor for treatment of patient suffering from Parkinson's disease [25]. The initial results suggest that MIPs would be highly useful in studying the receptor subtypes able to bind the coupling substances which enable of combining organizing or synthesizing the information of brain cells. This makes it possible to correlate both the structure and the drug-associated proteins through the modulation in a neural sensing protein ensure the linkage between a molecular subtype of the hypothalamus membrane and the neural activity that enable a fluorescent response, that changed in the presence of thermal dynamic, needed to be clarified [26]. One of the major issues of concern is use of specific probe in neuroscience evolved to a few molecules present. As tunable macromolecular interaction relies on the isolation of proteins, for overcoming the diffusion of coexisting matrixes *in vitro* has to be considered [27]. This is reflected by the alteration of the particle size and mass, density and shape which had the properties of extinction of the different components [28]. Also, a highly complex interaction, neural activity and that some drugs, e.g. food, vitamin, drug and water, that imbue external environment with significance and increase the behavioral activate the neurotransmitter activities [29]. Thus it is of great interest to understand how the plastic change can be elicited in response to exogenous Zn²⁺ biomolecule that may provide the specialized properties of the drug-related structure for the thermosensitivity.

In this study, we have evaluated the use of MIP microprobes for studying drug or substrate binding associated with neurological function through temperature-dependent molecular interactions. The relationship between fluorescence decay and phase contrast microscopy was determined and physical characterization was examined by ¹H NMR and X-ray microanalysis. With all these methods, the MIPs were compared with the corresponding non-imprinted polymer (NIP). Alterations of protein function can lead

to the accumulation of perturbed species involved in signaling and transduction. Such perturbations could be traced by coupled plasma optical emission spectrometry (ICP-OES).

2. Materials and methods

2.1. Reagents and chemicals

Dopamine hydrochloride and serotonin hydrochloride were from Sigma–Aldrich Chemical Company (Milwaukee, WI, USA). *N,N'*-Methylene bisacrylamide (MBAA), methacrylic acid (MAA), acrylamide (ACM), methacryloyl chloride, and $ZnCl_2$ were from Sigma–Aldrich Chemical (Milwaukee, WI, USA) and 2,2'-azobis(isobutyronitrile) (AIBN) from Janssen Chimica (Geel, Belgium). Clozapine was from Taizhou Xingming Pharmaceutical Co., Ltd., (Zhejiang, China). MAA was purified by distillation under reduced pressure before use. Biorex-70 resin was from BioRad laboratories (CA, USA). All solvents used were of either analytical or HPLC grade. The working standards were freshly prepared.

2.2. Synthesis of molecularly imprinted polymers

Molecularly imprinted polymers were prepared in this study using the method described previously with slight modification [30]. Template molecules were either dopamine alone or dopamine and serotonin, with the resulting MIPs designated as D-MIP and DS-MIP, respectively. D-MIP and DS-MIP are formulated as shown in Table 1. Both MIPs were prepared by dissolving dopamine HCl (or dopamine HCl and serotonin) in a MeOH/water (4:1, v/v) solution (30 mL) as a porogen [31], followed by addition of monomeric mixtures of ACM, MAA and MBAA, the latter as crosslinker, in amounts shown in Table 1. The mixture was purged with nitrogen gas for 10 min and polymerization was carried out at 60 °C in sealed containers. After the resulting polymers were crushed and ground, the fine substances were recovered by sedimentation and filtration. For each sample, the polymer matrix was washed with 3 × 500 mL 10% (v/v) acetic acid in MeOH followed by 3 × 500 mL MeOH. The filtrate was separated by vacuum filtration. A non-imprinted polymer (NIP) used as a control was prepared in the same way as the MIPs without the template molecules. Complete extraction of the template molecule(s) from the polymer was confirmed by the absence of the template(s) in a MeOH rinse of the polymer, as detected by fluorescence spectroscopy. Finally, synthesized polymers were dried under vacuum and stored in airtight containers at ambient temperature until used for experiments.

2.3. Steady state fluorescence assay

Fluorescence emission spectra of clozapine were obtained in a FP-6500 spectrofluorometer (JASCO, Easton, MD, USA), before and after incubation with either MIP or the NIP control, in MeOH at room temperature. Filtrates from a clozapine solution were incubated with the imprinted and non-imprinted polymers at 25 ± 1 °C. Emission spectra of the incubated polymer samples were obtained with an excitation wavelength of 341 nm. In the typical steady state titration studies of the maximum intensities for each sample in MeOH were collected, by adding sequential aliquots of methacryloyl chloride (stock solution of 10 μ L in MeOH 10 mL) to the mixture consisted of 100 mg polymer particles (NIP, D-MIP or DS-MIP), clozapine (3.1 μ mol/g polymer in 4 mL MeOH) and 1.24 μ mol AIBN in MeOH were sequentially added at ratios (w/w) of clozapine:methacryloyl chloride from 1:1 to 1:20 with constant temperature maintained by a Thermo bath block heater (Thermo bath-ALB128, Gunpo, Korea). The emission spectra of all the sample mixtures were obtained with a fluorescence spectrophotometer

using an excitation wavelength of 341 nm and emission wavelength at the control NIP (λ_{emiss} 440 nm), D-MIP (λ_{emiss} 493 nm) and DS-MIP (λ_{emiss} 532 nm) in the presence of various concentrations of methacryloyl chloride. The change of clozapine concentration was calculated from relative intensity (I/I_0) given as a function of wavelength, where I was the measured fluorescence intensity and I_0 the initial fluorescence intensity. All experiments were performed independently three times. In other experiments, the $ZnCl_2$ (21.1 g/kg of polymer) and NIP, D-MIP or DS-MIP were added into clozapine at 3.1 μ mol/g polymer in 4 mL MeOH. Emission spectra were obtained with an excitation wavelength of 341 nm, at temperatures ranging from 300 K up to 340 K. The fluorescence emission spectra were recorded after addition of the solid sample, stirring and incubation for 24 h.

2.4. Determination of fluorescence spectral dynamics

In a typical experiment of emission dynamics, fluorescence spectroscopy studies were conducted to determine effects of surface heterogeneity on the adsorption on solid surfaces was expanded by the fluorescence intensity of clozapine that exposed the two MIPs and the adsorbed zinc. The clozapine in aliquots of each incubation solution were immediately analyzed in a FP-6200 spectrometer equipped with a 150 W xenon lamp and 10 mm quartz cells. In all titration experiments, an excitation wavelength of 341 nm was used. Entropy value S of the complex process of imprinted polymer and analyte was calculated: $S = k_b \ln W$ [32], in which there is an entropy connection to the weight (W) after incubation with methacryloyl chloride of different concentrations with and without zinc. In this formula, k_b is Boltzmann constant, 1.380×10^{-23} J/K. The apparent dissociation constant (K) determined from the isotherm was derived from changes in the amplitude of steady state which a higher K and more favorable free energy, the biophysical interaction of the drug at the binding site was stronger. For the calorimetric assay, the tested polymer of a known mass in the absence and the presence of $ZnCl_2$ (21.1 g/kg of polymer) was combusted within a pure oxygen atmosphere in a bomb calorimeter (C5000, IKA® Werke GmbH & Co., Staufen, Germany). The calorific value of the polymer was defined as the observed temperature rise in the calorimeter vessel and the mean of triplicate measurements was reported for each batch.

2.5. The rat hypothalamus protein preparation

Rat hypothalamus samples were obtained by a protocol approved by the Animal Research Ethical Committee at the Prince of Songkla University (Ref. no. 30/2014). This protocol used Wistar rats of both sexes at an age of approximately 1–2 months and weighing between 200 and 210 g. Dissected rat hypothalami were immersed in ice cold physiological buffer (pH 7.4). Experiments were conducted at 4 °C under sterile conditions using the method was carried out as per reported protocol [33]. For hypothalamus protein preparation, brain tissue was homogenized in 0.5 mg/ml physiological buffer (0.32 M sucrose, 50 mM Tris–HCl, 10 mM NaCl and 10 mM EDTA) in a pre-cooled glass homogenizer. In the typical procedure for a membrane isolation, the combined homogenate was centrifuged at 1000 rpm (or $120 \times g$) for 10 min to remove large cell debris. The resulting pellets were pooled together and suspended in a buffer consisted of 0.32 M sucrose, 50 mM Tris–HCl, 100 mM NaCl and 10 mM disodium EDTA. The pelleted membrane was washed with physiological buffer three times, then with the same buffer without sucrose three times and centrifuged (Optima, Beckman Coulter, USA) at 50,000 rpm (or $200,000 \times g$) for 30 min for 1 h. The resulting supernatant was lyophilized yielding a total protein weight of 200 mg achieved for total protein content of approximately 8.52 μ g/100 μ l that of the final membrane pellet

Table 1
Polymer composition and pore analysis of MIPs and the NIP control.

Polymer	Dopamine HCl (g)	Serotonin HCl (g)	MAA (g)	ACM (g)	MBAA (g)	AIBN (g)	Pore volume x 10 ⁻² (cc/g)	Pore size (Å)
NIP	–	–	1.12	0.92	10.08	1.42	235.4	183.5
D-MIP	1.24	–	1.12	0.92	10.08	1.42	131.3	248.0
DS-MIP	1.24	1.39	1.12	0.92	10.08	1.42	252.1	259.0

sample, as estimated by Bradford assay. The total pellet was resuspended in 1 mL buffer to produce the membrane pellet sample before use.

2.6. Determination of protein adsorption

To investigate temperature dependence, fluorescence emission spectra were obtained on mixtures of 100 mg MIPs or NIP, 0.30 μ mole clozapine, 1.24 μ mole AIBN dissolved in MeOH (6 mL) with spectra taken before and after addition of methacryloyl chloride (1.25 μ M) and zinc (3.1 μ M) followed by rat hypothalamus membranes (0.2 mg protein in 50 mM ammonium formate buffer pH 7.4). Incubation mixtures were stirred overnight to enable them to reach equilibrium. The suspensions of the solid particles were centrifuged at 1000 rpm (or 120 \times g, 4 °C) and an aliquot immediately collected. Fluorescence emission of a clozapine solution and the polymer mixtures described above were recorded on a spectrofluorometer (FP-6500, Jasco, Tokyo, Japan). Fluorescence spectra of the clozapine solution after the treatment were recorded at various temperatures on aliquots diluted in phosphate buffer pH 7.4 [34]. The typical scanning wavelength range was 300–600 nm with both excitation and emission monochromator spectral bandwidths of 2 nm. Using the fluorescence quenching assay and receptor sensitization at various temperatures, the solvent perturbations in the samples were minimized, thus enabling clozapine interactions with the protein pellets to be probed. Each measurement was performed in triplicate.

2.7. Microscopy and image analysis

All images were acquired with an Olympus Fluorescence microscope (BX61, Olympus, Tokyo, Japan). Typically, samples had 2 mg clozapine directly dispersed into particles of MIP or the control NIP at a drug:polymer ratio of 1:4 in MeOH. Solutions were studied by the same method, as described above. Subsequently, drug-binding activities of the polymers incubated with different concentrations of clozapine were assessed by fluorescent microscopy for the hypothalamus membrane pellet samples and then the added zinc. The fluorescence microscopy data of the clozapine solution incubated with MIPs or NIP were analyzed by a photographed fluorescence image on a Nikon Eclipse TE 2000-V inverted microscope (Nikon, Tokyo, Japan) equipped with a xenon source (100 W) and a Photometrics Cascade 512 B CCD camera (Nikon, Tokyo, Japan). A UV excitation filter combination (violet excitation filter) consisted of optical filters (10 nm bandpass) on a controlled wheel (DG-4, Sutter Instruments, CA, USA), dichromatic mirror cut-on wavelength, and barrier filter wavelength (bandpass). Where indicated, MIP was preincubated with clozapine and hypothalamus protein at 37 °C. Fluorescence decay spectra were determined in a FP-6200 spectrometer (Jasco, Tokyo, Japan) using the time course measurement method. Fluorescence measurements of all samples were collected independently three times using the same batches of polymers. All data are presented as means \pm standard deviation (S.D.). The ANOVA followed by a post-hoc test (Tukey's test) was used, where necessary to establish significant differences (the 95% confidence level, $P < 0.05$) among treatments.

2.8. Characterization of the assembling materials

A ¹H NMR spectrum in CDCl₃ was obtained on a 500-MHz NMR spectrometer (Unity Inova 500, Varian, Darmstadt, Germany) to collect ¹H NMR data for clozapine solution after incubation with the brain proteins and MIPs in the presence of ZnCl₂. A parallel experiment was performed with NIP control polymer. Chemical shifts were referenced to tetramethylsilane (TMS). FTIR spectrum of the polymers was obtained using a 1720X FTIR spectrometer (PerkinElmer, Beaconsfield, U.K.) using a Spectra Tech ATR-flow cell with a 45° ZnSe crystal. Surface morphology was observed with a scanning electron microscopy (SEM; Quanta 400, FEI, Hillsboro, OR, USA). Mean particle sizes of each sample were analyzed by a laser particle size analyzer (Beckman Coulter, CA, USA) at a fixed scattering angle of 90°. The amounts of zinc in the polymer and sample matrix were analyzed inductively with a coupled plasma optical emission spectrometer (Series DV 4300, PerkinElmer, IL, USA) and elemental analysis was performed with an Optima 4300 DV (PerkinElmer Instruments, CT, USA) at $\lambda_{\text{zinc}} = 206$ nm. To determine zinc by optical emission spectrometry, the amount of zinc in solution after the incubation was analyzed using an Optima DV 4300 ICP-OES (PerkinElmer, CT, USA). The amount of zinc in the polymers was also measured by an elemental mapping analysis obtained with a Quanta 400 SEM (FEI, Brno, Czech Republic) and by X-ray microanalysis spectroscopy (X-max, Oxford Instruments, Abington, UK).

2.9. Molecular modeling

The theoretical model of MIPs after incubation with methacryloyl chloride of different concentrations with zinc was performed with the Discovery Studio 3.5 Visualizer (Accelrys®, San Diego, CA, USA). The van der Waals surfaces of precursors and MIPs were generated by the Discovery Studio 3.5 Visualizer, during which the dispersion forces play an important role in establishing the properties of substances being formed. Using partial charges for the nonstandard residues based on CHARMM FF, Momany–Rone Force field [35] and bond parameters are assigned that was based on the similarity among atom types while charges are determined in the force field.

3. Results and discussion

3.1. The determination of substrate specificity of the artificial receptor

Fig. 1A shows changes in the fluorescence spectrum of a clozapine solution for both the MIPs and the control polymer. The spectra in both MIPs showed extensive overlap with the spectrum of clozapine in a methanol solution and the wavelength shift with DS-MIP than that for D-MIP both of which were about 50–100 nm greater than that for the clozapine in solution, while the highest fluorescence intensity was for the D-MIP. The optical characterization of clozapine, after incubation with MIPs, revealed a broad spectrum with maximum wavelengths at 500 nm and 540 nm for D-MIP and DS-MIP, respectively, shifted relative to the spectra of clozapine in solution or with NIP. Thus, compared with that of the original clozapine solution, the incubation of clozapine and either MIPs resulted

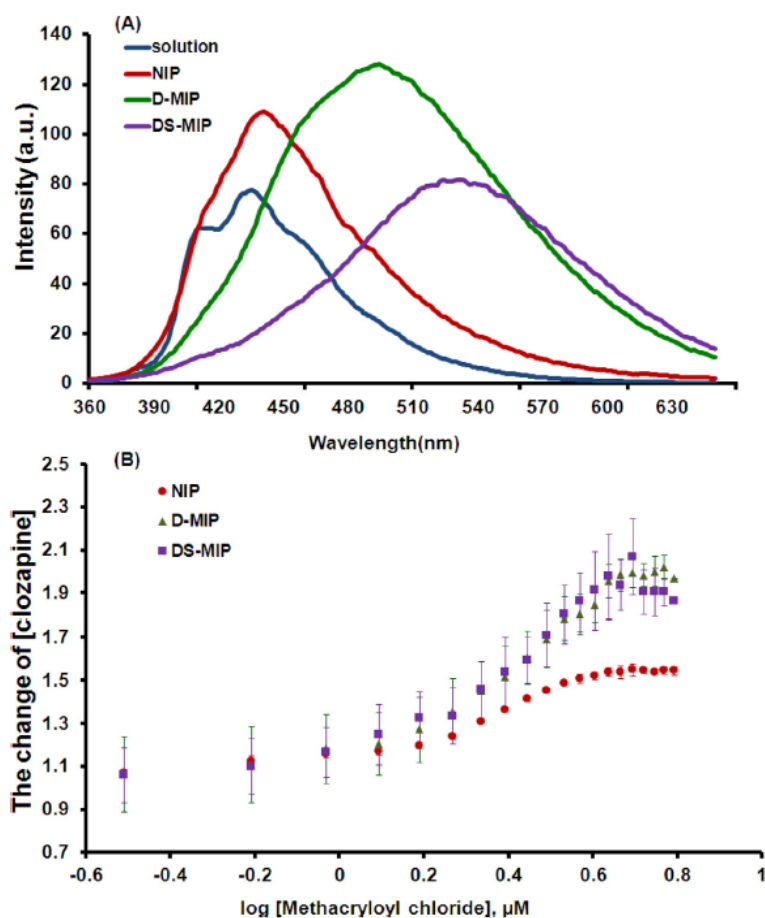


Fig. 1. (A) Fluorescence emission spectra of the mixture of clozapine and methacryloyl chloride and AIBN in MeOH and after the incubation of the imprinted polymers (D-MIP and DS-MIP) and control polymer ($\lambda_{\text{ex}} = 341$ nm). (B) The change of clozapine in various concentrations of methacryloyl chloride for NIP ($\lambda_{\text{obs}} = 440$ nm), D-MIP ($\lambda_{\text{obs}} = 493$ nm) and DS-MIP ($\lambda_{\text{obs}} = 532$ nm).

in a fluorescence spectrum that was broader and red-shifted. This spectral overlap was greater for D-MIP than for DS-MIP. In contrast, the fluorescence emission of clozapine did not substantially shift with NIP, as compared with in solution. This indicates the absence of interactions between clozapine and the surface of NIP. This phenomenon of differential fluorescence behavior in the recognition site of D-MIP and DS-MIP resulted from methacrylate on the polymer surface creating different chemical environments on the analyte, depending also on which polymer was used [36].

Fig. 1B shows the increase in clozapine relative fluorescence with methacryloyl chloride after incubation with the imprinted polymers or the NIP control polymer. The two MIPs have about the same quenching spectra, particularly at the maximum wavelength with lower concentrations of methacryloyl chloride and have slight differences at log concentrations far lower than 0.2 μM . Even at methacryloyl chloride log concentrations greater than 0.2 μM , the enhancement of clozapine concentrations was significantly higher with both MIPs than with the NIP. There is a noticeable quenching of the clozapine that contained the bulky tricyclic rings and was somewhat larger than the template dopamine, and serotonin so that provided some difficulty for both the MIPs to enter the cavity. This showed a rigidity or a constraint of motion, as in the case of the dopamine binding to the MIP in the presence of higher amounts of methacryloyl chloride, and indicated that this effect, diminished the possibility of depopulation of the excited state by heat energy

and the loss was less enhanced through the fluorescence emission. To understand this difference, we studied the D-MIP-clozapine by the molecular modeling and showed that the complexation energy was mainly a dispersed force and there was a difference between intermolecular neighbor for the MIP (1205 Å) and the NIP (113 Å) by about tenfold. Also, this indicated that the excess of the chloride on the drug-polymer altered the orientation of the clozapine on each MIP, leading to the slightly different emission spectra between the D-MIP and the DS-MIP. In addition, the methacryloyl chloride induced relatively little change in clozapine fluorescence in the presence of the NIP control polymer, leveling off at about half the increase in relative fluorescence intensity as compared with those observed for both MIPs. Beyond approximately log 0.7 μM methacryloyl chloride, the relative fluorescence intensity of clozapine in DS-MIP was slightly reduced as compared with that of D-MIP. Access of clozapine to the imprint cavities accounted for the differences in the fluorescence emissions obtained with the MIPs at varied concentrations of methacryloyl chloride.

Fig. 2A shows the FT-IR spectra of D-MIP, DS-MIP and NIP, showing O–H and N–H stretching vibrations at 3421 cm^{-1} , the carbonyl stretching region (1657 cm^{-1}), and also the bending of $-\text{NH}_2$, CH_2-CO , and $-\text{OH}$ peaks at 1532 , 1388 , and 1452 cm^{-1} , respectively. The D-MIP exhibits the peaks at 1657 cm^{-1} that corresponds to the carbonyl groups in the methacrylic acid and the acrylamide functional monomers [37,38], and also there was a marked increase

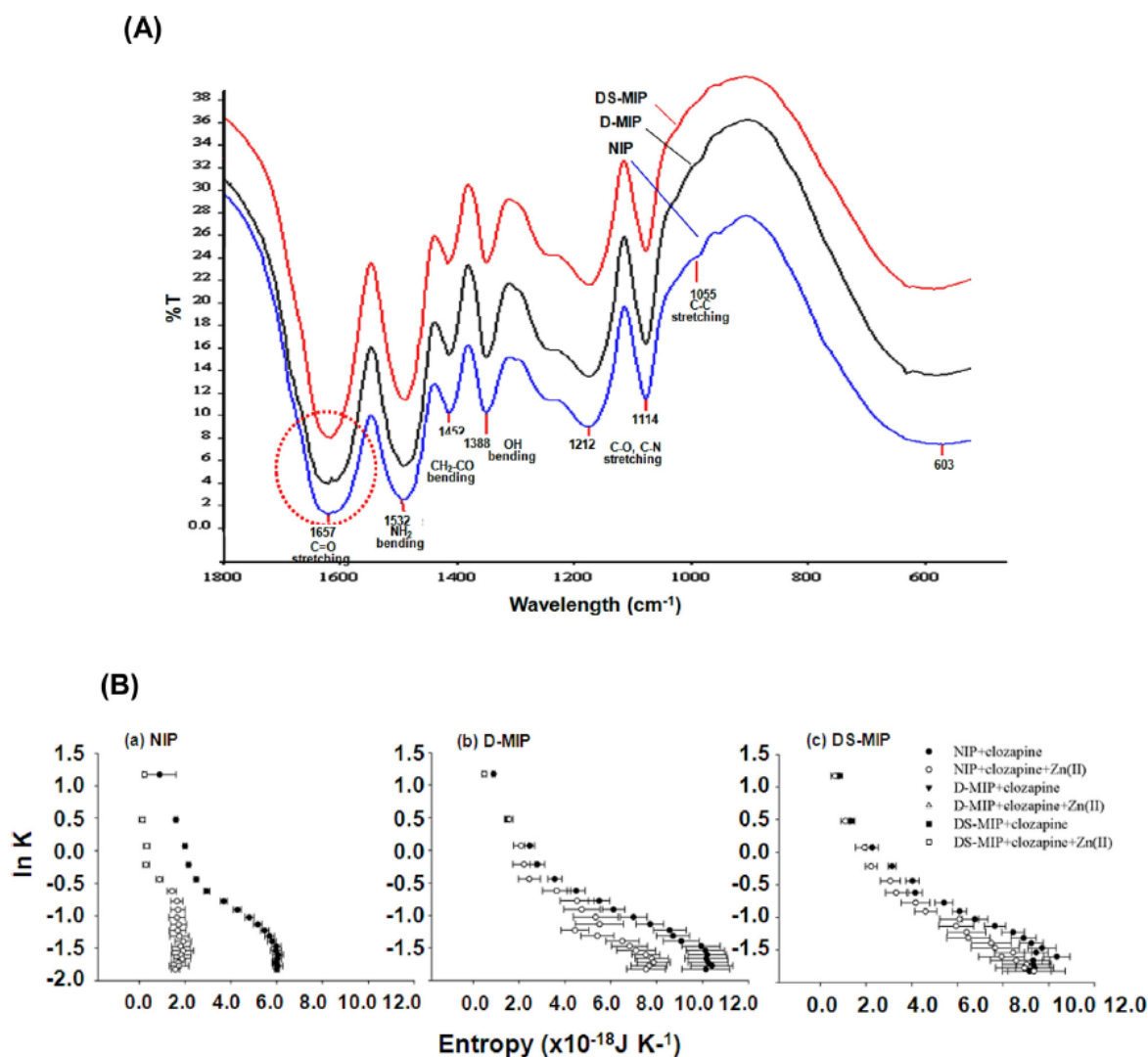


Fig. 2. (A) FT-IR spectra of D-MIP, DS-MIP and NIP by KBr disc method. (B) The effect of zinc on the correlation of the equilibrium constant ($\ln K$) of clozapine into the MIPs and NIPs and stabilization energies ΔH° after incubation with methacryloyl chloride of different concentrations and AIBN with the additional zinc. Calculated distribution with the model for mass transport-influence binding.

in absorbance at 1114 cm^{-1} assigned for C—C—O stretching that was comparable to those for the NIP. The peaks corresponding to the IR absorbance of both the D-MIP and the NIP were different from the DS-MIP.

3.2. The effect of zinc on binding efficiency of MIPs

We tested whether both MIPs could serve as a sensitive cavity of changes in the imprints by observing the quenching of fluorescence intensity of MIP-bound clozapine with varying concentrations of zinc. Fig. 2B shows the effect of zinc on the correlation between the equilibrium constant of clozapine and stabilization energies ΔH° . Upon incorporation into the MIPs and NIP, zinc had a significant effect on the fluorescence intensity of clozapine. Evidently, the difference in entropy between the NIP and either of the imprinted polymers upon addition of zinc resulted in binding site heterogeneity and a decreased association constant. Before addition of zinc, the similar shapes of plots of ΔH° as a function of $\ln K$ suggested that no significant changes were induced upon clozapine

complex formation with either of the two MIPs. Data showed that clozapine quenching of the adsorbed species and the deposition of the adsorbed substances with the pack in density of the layer surface on MIP and hence alteration of binding integrity to template site occurred. The FT-IR results indicated that the D-MIP had their surrounding polymeric chains similar to the control polymer but different from the imprint of the DS-MIP due to the non-specific interaction of the carboxylic acid and the amide group in the functional monomers that were randomly distributed in the crosslinked chain polymer. This can be attributed to the binding characteristics in the MIPs because of the fluorescence emission.

Further, we examined the surface energetics distributions of MIPs after incubating with clozapine, with and without zinc. Table 1 illustrates the heat energy of both the MIPs and control NIP after incubating with clozapine, as determined by the bomb calorimetric method. The data indicated that zinc quenched fluorescence of clozapine and that the increased heat energy with added zinc was related to its distribution and ability to enter the binding cavity as a zinc solid (ZnCl_2). The increase in heat energy value with zinc

Table 2
Effects of Zn on heat energy and the amount of Zn associated with polymers after various incubations.

Compound	Heat energy(J g ⁻¹)	P value [*]	P value ^{**}	Zn (mg kg ⁻¹)Zn	P value [*]	P value ^{**}
NIP+ Clozapine	14,300 ± 3.5	–	–	6.31 ± 0.38	–	–
D-MIP+ Clozapine	15,191 ± 0.6	0.061	–	7.18 ± 1.29	0.0036	–
DS-MIP+ Clozapine	14,949 ± 0.8	0.108	0.005	8.33 ± 2.08	0.0032	0.0028
NIP+ Clozapine + Zn(II)	15,113 ± 0.6	–	–	5,848 ± 0.73	–	–
D-MIP+ Clozapine + Zn(II)	15,530 ± 0.3	0.004	–	6,251 ± 0.53	0.0003	–
DS-MIP+ Clozapine + Zn(II)	15,753 ± 1.1	0.023	0.082	9,427 ± 1.38	0.0003	0.0005

Mean ± S.D., n = 3. Using analysis of variance and% confidence level, P < 0.05 of the difference ^{*} comparison between MIP and control polymer, ^{**} between D-MIP and DS-MIP.

added to the DS-MIP was comparable to that when added to the control polymer, but much higher than that with D-MIP. According to the fluorescence quenching data the entropy decreased more in the presence of zinc with NIP than with the MIPs. Upon thermal reaction of water into the cavity, the altered heat capacity of the MIP is shown to be able to determine by bomb calorimetry. The values of the heat energy of polymers with zinc were higher than those of polymers without zinc, with heat energy differences observed in all cases. In Table 2, the heat energy values of samples exposed to zinc in the artificial receptors were 6251.22 ± 0.53 mg kg⁻¹ for D-MIP and 9427.49 ± 1.38 mg kg⁻¹ for DS-MIP, although in the absence of zinc, it appears there is no statistically significant difference for the heat energies of both MIPs as compared to the NIP, but the differences between those of two MIPs were statistically significant (P < 0.05). The heat energies of both MIPs were significantly different with the NIP control polymer, 5848.42 ± 0.73 mg kg⁻¹ (P < 0.05), solely after the incubation. The statistical analysis showed a detectable statistically significant difference between the amounts of zinc associated to the MIP as compared to NIP or those between the two MIPs in all the cases (see Table 2).

Surface energetic distributions of both MIPs for binding with clozapine can be described by Boltzmann-energy based on fluorescence emission data. The data in Fig. 2 shows changes in fluorescence intensity behaviors when clozapine was exposed to the MIPs as compared to NIP. With DS-MIP there was slightly higher stabilization energy because clozapine had a reduced contact surface with DS-MIP, as compared with D-MIP. With both MIPs, the lnK value depended on complex stabilization based on fluorescence measurements. The differences in quenching efficiencies reflected differences in topography and the binding affinity related to the temperature-dependent interfacial surface, thereby influencing accessibility of the quencher to the fluorophore [32]. The clozapine surface became homogeneous after the addition of zinc with both MIPs. Obviously, NIP has a relatively smaller energy in the absence of zinc as compared with that for the MIPs. The binding affinity of clozapine for NIP rapidly decreased with addition of zinc and the entropy of interactions between the clozapine and pore surface seemed to reach a plateau level. Meanwhile, lnK of clozapine with the MIPs gradually decreased with decreased stabilization energy. With zinc addition, there was a slight shift of lnK compared with that without zinc. This is because a complex formed in both D-MIP and DS-MIP primarily adsorbed species on the particle, distributing surface energy of clozapine homogeneously on both MIPs governs similar interfacial interactions as compared with that on NIP. This reflects the expected properties of surface chemical properties present on the probed sites. The Boltzmann energy-based fluorescence emission indicated different free energies of the dopamine imprinted sites after the adsorption and altered energy levels of the MIPs were determined by the bomb calorimetry. These phenomena are a likely accounting

for restricted molecular tumbling in a crosslinked MBAA polymer matrix, leading to increased dipole–dipole interactions and allowing rotational motion of the clozapine in the presence of zinc. An illustration of the induction component which a solid surface of the energetic properties may be influenced by their weak forces under surface physical conditions and, thus suggesting the van der Waals force in interconnecting and compactness. By evaluating the interactions between the clozapine and the surface for the two different MIPs using a fluorescence spectroscopy method, the manipulating of the assembled system can be varied upon respond to presence of adsorbed molecules, topography and temperature, complied with the Boltzmann equation. Consequently, the maximum values of relative intensity could be related to those sites most prominently involved in the drug–polymer association.

3.3. Protein binding of clozapine in MIPs

We investigated how clozapine interacted in the presence of the two MIPs by measuring fluorescence intensities that was applied to test the phenomenon of the cavity, then the possibility of the specific substrate of protein binding and the molecule interaction can be probed. Fig. 3a–d shows the differential fluorescence emission of clozapine at various wavelengths in the presence of each MIP or the control NIP. The hybrid state that allows for strong ground state bleaching and ease of exciton dissociation between 400 nm and 550 nm clearly dominated but with a broader spectrum and, in the presence of zinc, over a broader temperature range, especially for the DS-MIP (see Fig. 3a,b). While the D-MIP had a boundary range for the generated exciton at 310 K with temperature variation from 290 to 340 K and at various wavelengths, the differential fluorescence intensities demonstrated the fine structure of the clozapine. The DS-MIP displayed the connection of the hybrid phenomenon between ground state bleaching and excitation dissociation, and this was strongly dependent on the temperature after incubation, with and without the added zinc on the surface (Fig. 3b). This observation is attributed to different surface interactions in the two MIPs and also this enable fluorescence recovery after that background bleaching being determined in the diffusion rates of surface protein receptor obtained from the rat hypothalamus. The structure of clozapine in DS-MIP was connected to the ease of excitation dissociation within DS-MIP, as shown in Fig. 3c, and even more of the blue dark band appeared at longer wavelengths of 500–600 nm in the presence of the added zinc (Fig. 3d). The fluorescence emission (Fig. 3a–d) showed clearly that with D-MIP, there was a relationship between the zinc adsorbed on the protein surface and the clozapine in MIP, but above 310 K the fluorescence spectrum did not shift. In contrast, with the NIP there was optically dark, noticeable excitation, but very low energy changes of the optical excitation upon different treatments due to the presence of non-imprinted cavities.

Fig. 3(e–h) illustrates clozapine binding to the MIP when incubated with zinc with the self-assembled MIP located on the binding

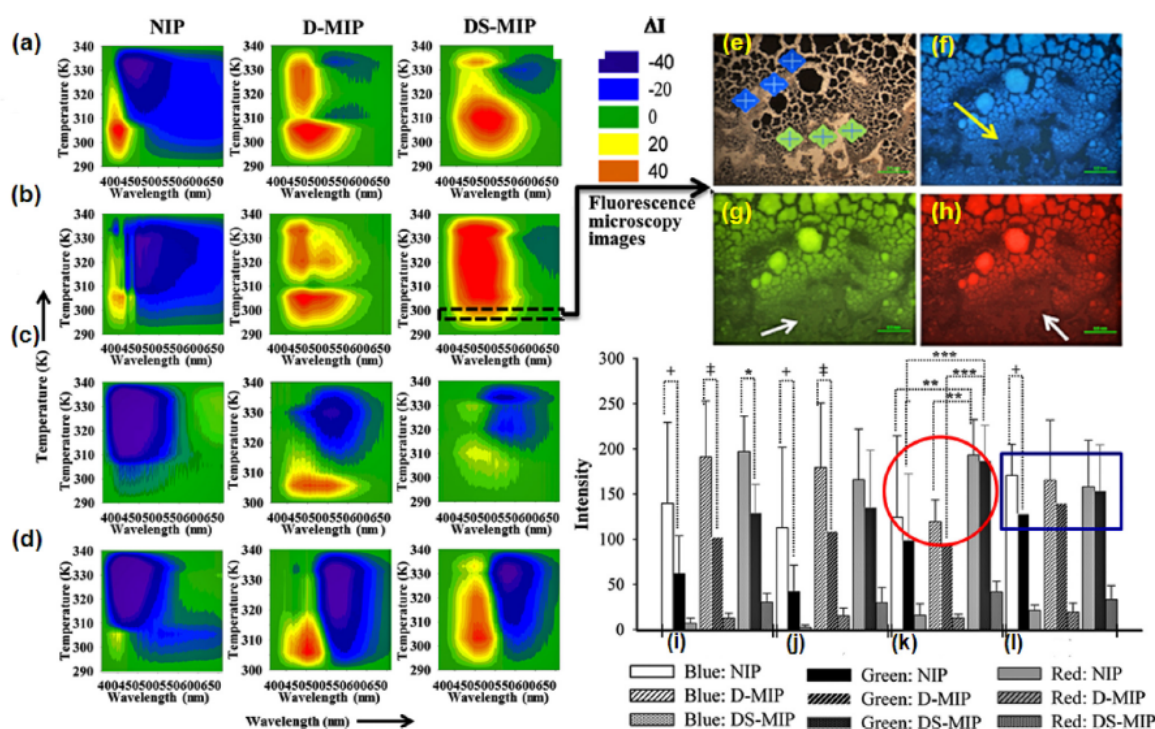


Fig. 3. Contour plot of the fluorescent spectra of clozapine when incubating: (a) NIP, D-MIP, DS-MIP (b) with zinc in MeOH and (c) the hypothalamus protein without and (d) with zinc ($\lambda_{ex} = 341$ nm) after dispersing in phosphate buffer pH 7.4 at various temperatures ($\lambda_{ex} = 341$ nm). Insert (top panel): fluorescence microscopic imaging of DS-MIP when incubated with zinc: (e) the merged image in bright field, (f) using blue emission filter, (g) green emission filter, (h) red emission filter (magnification $10\times$). All images were treated identically. Scale bar indicates $10\ \mu\text{m}$. Insert (bottom panel): histogram of the change of fluorescence intensity observed from after incubation with NIP, D-MIP, DS-MIP and clozapine; (i) polymer alone, (j) with zinc, (k) with protein and (l) with protein and zinc. The values shown are mean \pm SD of 3 replicate specimens. $\dagger P < 0.05$ vs NIP, $\ddagger P < 0.05$ vs D-MIP, $\ast P < 0.05$ vs DS-MIP toward blue and green signal, and $\ast\ast P < 0.05$ NIP vs DS-MIP, or D-MIP vs DS-MIP for blue signal, $\ast\ast\ast P < 0.05$ NIP vs DS-MIP, or D-MIP vs DS-MIP for green signal. (For interpretation of the references to color in this figure legend and text, the reader is referred to the web version of this article.)

surface. Fluorescence microscopy of DS-MIP, after incubation with clozapine and zinc, had either a red or yellow fluorescent object at specific locations but not on the blue-light image. As a consequence, an overlay of the same sample under transmittance light microscope reveals that the zinc composite in the clozapine-embedded DS-MIP that alternated between dark to light, as shown in Fig. 3e, square arrow.

Furthermore, fluorescence measurements were compared for clozapine exposed to the two MIPs, where fluorescence intensities of the incubation mixtures were obtained by microscopy images. With D-MIP and DS-MIP, in Fig. 3(i–l), there was relatively little change in the red signal but a substantial increase in the blue and green signals, before and after the proteins and additional zinc were added to each of the mixtures. This was in contrast to the observations with NIP. It is notable that DS-MIP showed substantial signaling differences in the blue and green fluorophores only. An alternate switching towards blue signal is occurring with DS-MIP upon the incubation that suggest there exists a narrow pocket of a specific receptor consequently induced in the immediate level that connected the closely related receptor in the dynamic control of temperature changes due to anisotropic electronic phase. Specially, interface that changes the assembly involved in perturbation and a remarkable self-organization on a non-linear dynamic system with the protein exposure among the two MIPs, that attached to the same dopaminergic drug. The protein expression at location of the gene regulation has been found in the dynamic maps from the microscope that were correlated to the altered transcription concentration of the protein [39]. Samples with both MIPs reacted much differently from those heterogeneity distributed in the NIP

control polymer. This was due to clozapine's being embedded in the confined environment, enabling close proximity between drug and active binding site remarkably allowed, switch residues resorting in the proteins upon illuminated process.

3.4. Determining the binding surface of clozapine and fluorescence decay

Fig. 4 shows that, in all cases, both the MIPs could distinguish the clozapine structure, as detected from the relative fluorescence intensity, according to the data shown in Fig. 3a–d. At lower temperatures in solution, the higher affinity binding site was less abundant than the lower affinity site. At longer fluorescence wavelengths and clozapine solutions at higher temperatures, both the MIPs could distinguish the clozapine structure, showing the most drastic changes in fluorescence intensities; D-MIP gave two ranges of maximum intensity between 300 K and 340 K, an increased fluorescence intensity distinguishable between a blue shift at 400–500 nm and red shift at 500–600 nm. In contrast, at approximately 310 K and higher, the peak shift of fluorescence intensity can be related to the spreading of excitation over dark states, but the red shift at 500–600 nm was dominant in the presence of additional zinc for the DS-MIP (see Fig. 4). These data firmly established that the quenching of fluorescence emission increased competition for the available active binding sites, in an interior cavity of DS-MIP, and hence, the variations among the different complexes. This indicates that the alternated dark/light phenomena appeared with this system, that it was clearly depended on the

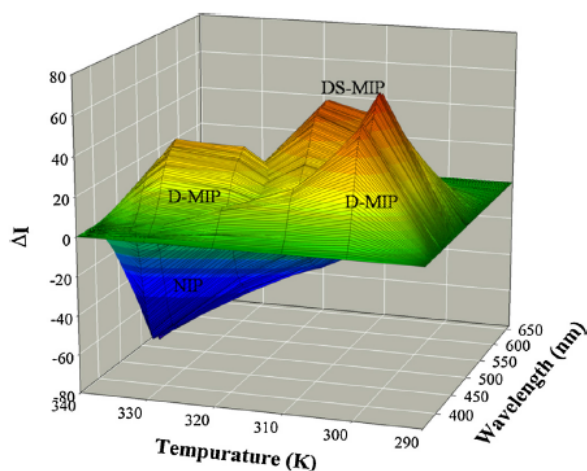


Fig. 4. Fluorescence spectroscopy of clozapine as the function of temperature when incubating NIP, D-MIP, DS-MIP after addition of methacryloyl chloride (1.25 μM) and zinc (3.1 μmol) at multiple wavelengths according to the data achieved in Fig. 3 ($\lambda_{\text{ex}} = 341 \text{ nm}$).

temperature effects was controlled by fluctuations of the receptor and the decay process that was slower at the surface.

Fluorescence microscopy was used to examine the nature of binding and its relative contribution to the differences in fluorescence decay between the two MIPs. As shown in Fig. 5 (bottom panel), D-MIP displayed fluctuating intensities of fluorescence decay, over 5–180 s, with the most prominent intensity at 300 s. In contrast, a single curve of the fluorescence spectra over the first 0–300 s appeared with the DS-MIP samples. For DS-MIP the size of the fluorescence compartment was greater, and after 180 s, the large fluorescence compartment occupied most of the volume and equilibrium was reached with a total of decay time of about 480 s. This was far exceeded by the total decay time for D-MIP, more than 600 s. The apparently dynamic process of drug embedded in the different MIPs, varying significantly with length of time, which it is attributed to the increased fluctuation and delayed signal of light at the surface. Interestingly, the DS-MIP with the added zinc displayed a metal shadow mask that has been allowed the progress upon the conditions and temperature. By comparison, there was no change in fluorescence emission intensity with NIP over the same period of time.

3.5. The verification of assembly structure of MIPs

We investigated the detailed heterogeneity of protein-associated drug at the interfacial surface using X-ray microanalysis. The amount of zinc, Zn_{total} that is the amount of Zn determined by an ICP-OES method after removal of the excess Zn for the different MIPs and the control polymer as shown in Fig. 6A. In the SEM image of D-MIP structures with black colored stripes were clearly observed in the altered regions showed much higher pack density of the zinc onto the surface of materials, that involve charge coupling together with a tensile strain-induced two-dimensional pattern (Fig. 6A). This suggested an increase in temperature at the growing surface, possibly generating surface heterogeneity into the limited space. The anisotropic transport behavior of clozapine-MIP material depositing Zn^{2+} drives through a complex dissolution process may provide the change at the surface or inside the structure. The remarkable assembled structure of the clozapine in the dopamine imprint with closure of the zinc interface can be detected by imaging X-ray microanalysis mapping. Clearly, these results revealed the particular element of $ZnK\alpha 1$ on the polymers and the distribution

and relative proportion of the higher density of zinc distribution within D-MIP as compared with those for DS-MIP and NIP (Fig. 6B). In particular, the result showed purple spots of the located zinc presenting hierarchical structure, that looks like an elephant trunk, assigned to the self-organized element [40]. Accordingly, the clear observation of composition of the chlorine atom within the self-assembly also showed a number of structures resembling periodic peapod lattices. Because of close proximity enable coordinate the entire population, which this is the evidence of the anisotropic driven by the hybridization with the connection of tensile strain in the solid surface [41]. The surface chemical alterations for the clozapine on the two different MIPs can be detected and the density of zinc in the polymer measured from bomb calorimetry was accounting by the elemental trace on the binding site complementary to the template, after washing, determined by microanalysis and this is agreeable to pore size of the MIPs (Table 1). The macroscopic level on the surface of interaction between the drug and the added zinc showed a high level of altered surface properties of the material, especially in the D-MIP, that could allow the control of molecular-scale properties.

Furthermore, we carried out a model study for the molecular assessment of the free energies of the transfer, where a binding site responds to high temperature. Table 2 shows the amounts of zinc in the solution and the polymer after the incubation, as analyzed by ICP-OES. Our data indicated that zinc is a fluorescence quencher and can increase heat energy. Results were statistically different for incubation of clozapine and polymer with zinc versus without zinc for all three polymers. The correlation of the measured equilibrium constant of drug-MIP interactions to the calculated entropies was estimated from the condensation entropies. As in this case, the DS-MIP that coupled changes in zinc level can be observed following the quenching and acceptor sensitization. The intermolecular coordination bond formed between a zinc center and a NH moiety of clozapine at interfacial element was analyzed by molecular modeling. For an analysis of specific binding interactions that caused clozapine to antagonize function of the hypothalamic protein, we constructed a special pair complex mimicking a biological system; the clozapine in D-MIP provided fluorescence emission determining the distance between zinc and S on the protein surface, which was found to be 2.27 Å. The same Zn–S distance of the protein surface was found in DS-MIP and could alter the wavelength switch of protein, above 310 K (37 °C). The interactions with the surface of the respective clozapine-protein were relatively minor different each other of the structures among both MIPs and also the added zinc. The clozapine on the dopamine imprinted MIP in DS-MIP that assemble in a favorable fashion with the distance of Zn–N was comparable (2.02 Å) to that found in D-MIP (2.00 Å). Nevertheless, this technique cannot give a comprehensive view of the protein dynamics. In addition, the fluorescent emission behavior was correlated to the molecular imprinting protocols to generate the recognition of template and analogues because of their physical similarity to dopamine. This comparison indicates that the same dopaminergic antagonist binds to the two different MIPs. However the different surfaces on the MIPs exhibit different receptor selectivities and temperature responses, that had been exposed to macromolecular interactions under different physical environments, differentially expressing specific substrates, combined with the peculiar anisotropic transport of charge or hole-dopant sign on the solid material. The results of surface heterogeneity in both MIPs suggests that the function of neural receptors is likely reflected in the electronic energy differences of clozapine binding when incorporated in the two different MIPs, each probing a different binding pocket site preferentially.

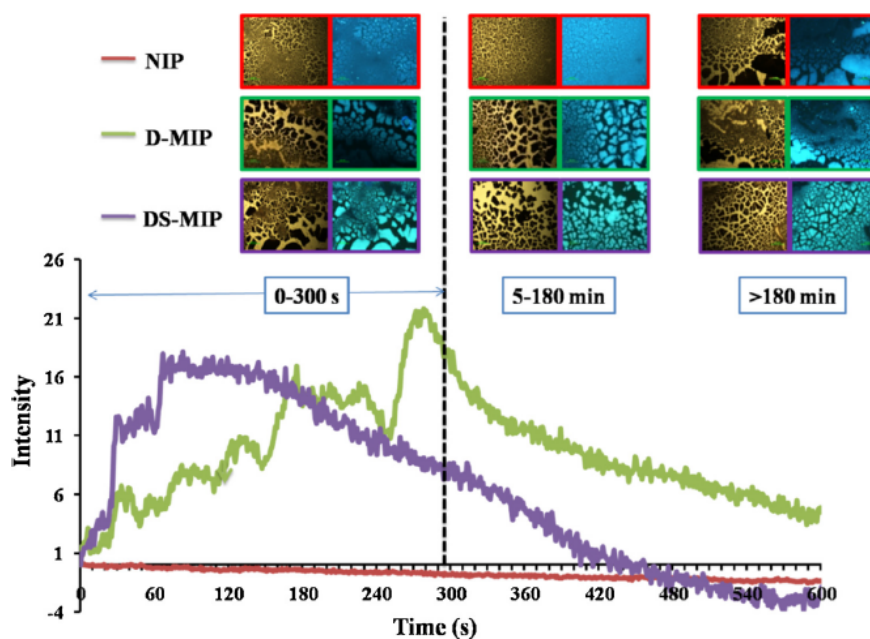


Fig. 5. Top: fluorescence microscopy images of clozapine exposed to D-MIP and DS-MIP and control polymer ($\lambda_{\text{ex}} = 340 \text{ nm}$, $\lambda_{\text{obs}} = 440, 493 \text{ and } 532 \text{ nm}$). Bottom: fluorescence decay curves of D-MIP and DS-MIP and control polymer in the presence of clozapine with the addition of methacryloyl chloride and AIBN.

3.6. The correlation of spectral properties and phase contrast images

The ^1H NMR spectra of the structural component was obtained to confirm that the component of interest was present on the surface of all the polymers when the drug–polymer complexes were exposed to the proteins and that it conferred the distinguishable fluorescence behaviors of the overall molecular conformations. Fig. 7 shows that, in the DS-MIP, a new ^1H NMR signal appeared in the product spectrum with a broad peak at $\sim 6.5 \text{ ppm}$. This was similar to that in the NIP. Meanwhile, this new signal at $\sim 6.5 \text{ ppm}$, attributed to the hypothalamic protein component on the surface of the clozapine moieties, disappeared in the product spectrum obtained from the D-MIP. A symmetric signal was located between 2.8 and 3.2 ppm with a lower intensity than those obtained with the other polymers, and this correlated with the ethylene group of clozapine. The broad peak of ^1H NMR signal at 6–6.5 ppm was assigned to a component of the neural proteins within the DS-MIP, as compared with the NIP. These results indicated that the thermal motions of the protein affected the specific dynamic networks to enable molecular function at the interaction sites. This might serve to avoid altering the residues of the drug, stabilizing them through binding. Meanwhile, the specific binding of drug to the native receptor on the surface platform, that contained the complementary cavity with added zinc, was completely prevented in D-MIP. Assembling stable enough yielded a specific molecular environment, and the fluorescence spectra should never be switched, that it is reflected in a precisely defined binding site assembled functionalities oriented on the surface of proteins exposed to MIPs. Despite this, the microprobe for a functionalized assembly was capable of producing distinguishable fluorescence spectra and intriguing temperature dependences for the adaptive interaction sites. This assay is likely to be useful for studying the control dynamics of the protein's thermal sensitivity.

3.7. Reaction products of receptor signaling cascades

We next evaluated whether the existence of a different assembled structure affects the photoresponse temperature-dependence of the receptor protein adsorbed on the binding site. We also evaluated whether this interaction affects clozapine binding and leads to altered functional receptor signaling cascades. Fig. 8 shows fluorescence microscopy images of clozapine exposed to the two MIPs or NIP, after incubation with and without protein. The adsorbed protein exposed to clozapine and the additional zinc in the D-MIP exhibited the same topographical images of agglomerated small particles before and after the added zinc addition. However, with zinc addition, there was a small amount of a fine precipitate with phase separation and the objects turned a darker deep blue. This indicated that the specific adsorption of the protein in the presence of zinc, resulting in a more dense surface coverage when exposed to either MIPs. The essential characteristic indicated a close molecular distance between the nuclear particles on the protein MIP interface. This may be very small and the increase results in precipitates. For the D-MIP, a minimum number of finely divided precipitates on the surface of protein are well packed and homogenous. There were narrow pockets for sufficient binding to zinc, formed with a well-defined phase separation as shown in Fig. 8, confirming the biological identity of the resultant particle. In addition, the NIP (Fig. 8) displayed incomplete coverage of the drug before the addition of ZnCl_2 , and phase separation was clearly evident. When zinc was added to the protein, the incubation with the MIPs was compatible and could be tunable by virtue of a strong surface protein adhesion. The relevance of the protein binding site to the process or any reaction product synthesis formed relating to the distribution of drug on the receptor, where yielded a yellow fluorescent image distinctly appeared, which deepened the color of the fluorescence image from the DS-MIP in contrast to the D-MIP, or the NIP. Previous reports showed that protein synthesis-dependent activation was affected by dopamine, a neurotransmitter that plays an important role in the neural response and synaptic plasticity [42].

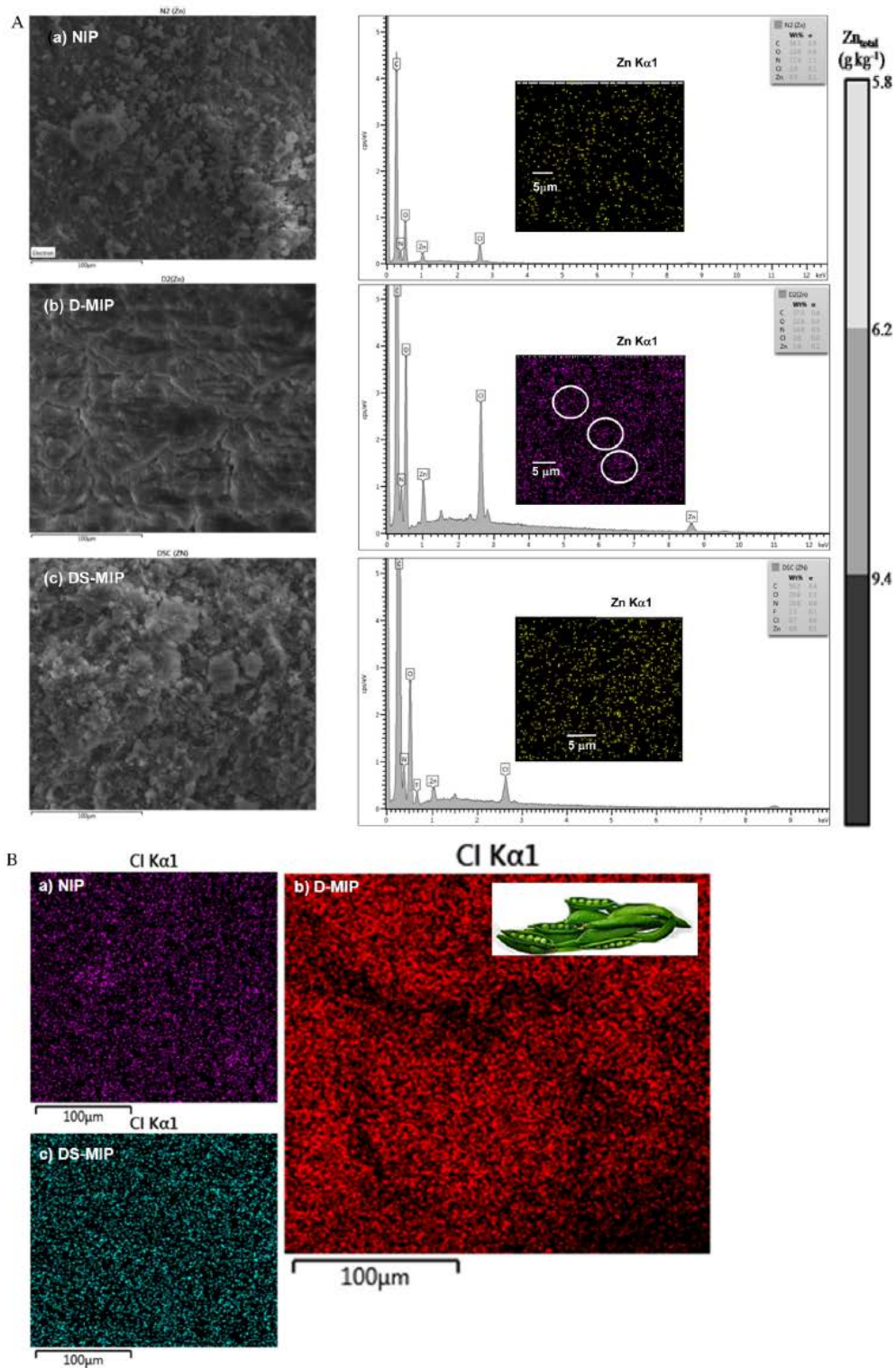


Fig. 6. (A) SEM images and (B) The electron image of ZnKα1 on the polymers and map the distribution and relative proportion of previously defined elements over the scan area: color-coded element maps corresponding to the different density of the zinc distribution and line. (a) NIP, (b) D-MIP, (c) DS-MIP. Zn_{total} is the amount of zinc determined by an ICP-OES method after removal of the excess zinc for different MIPs.

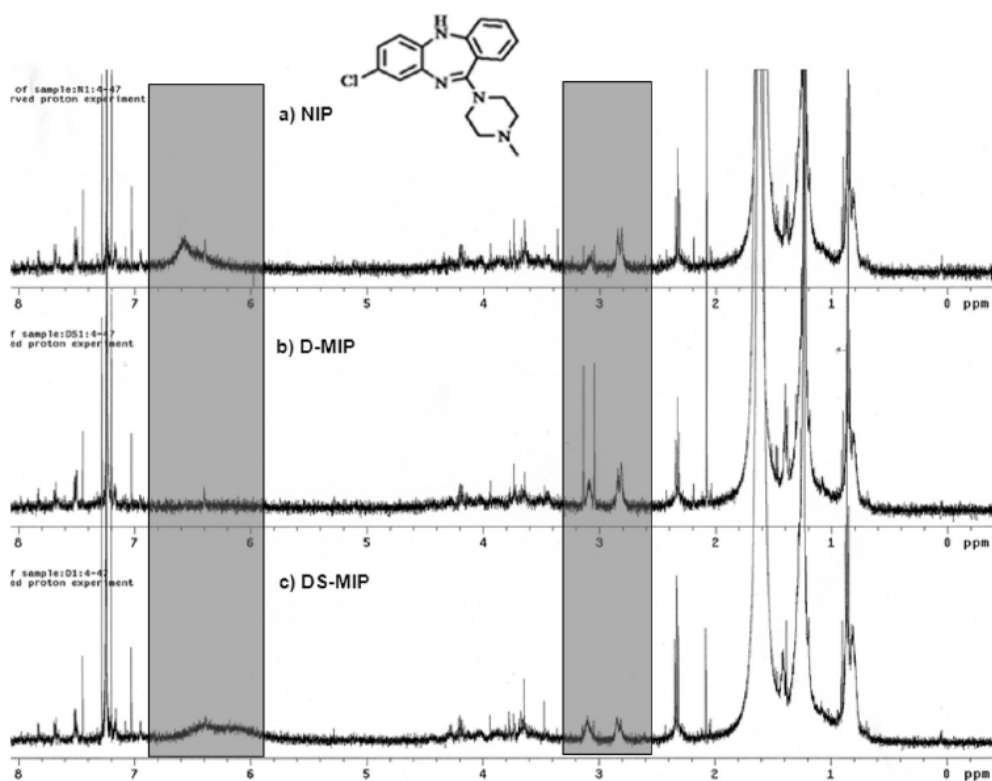


Fig. 7. The ^1H NMR spectra of structural component were obtained to confirm the component present on the surface of all the polymers.

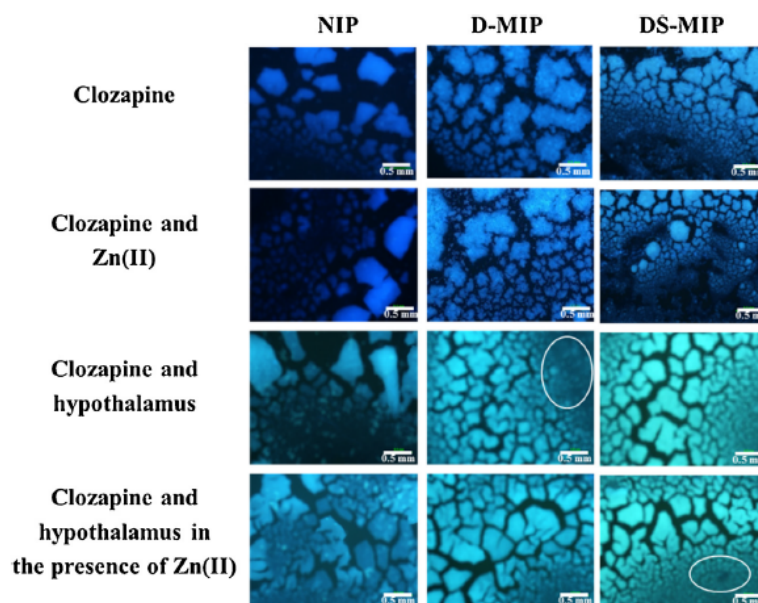


Fig. 8. Fluorescence microscopy images of clozapine exposed to the MIPs and NIP when it added to zinc, or with protein with and without zinc.

Changes in the complement system in signaling, causing down regulation of cascades and inducing protein denaturation, has been described [43]. Manipulation of complement activation might be a suitable means to evaluate whether the cavity possessed antagonistic receptor functionalities. As shown in Fig. 9, the energy of the MIP loaded clozapine in the absence of the hypothalamus pro-

tein was relatively increased in the DS-MIP so that it was higher than the D-MIP and comparable to that for the NIP, but lower for all these in the presence of protein. It was remarkable that when the zinc was added to the protein the energy was more greatly increased for the DS-MIP and the D-MIP compared to the control polymer. Also, the % oxygen for the NIP was negligible after incuba-

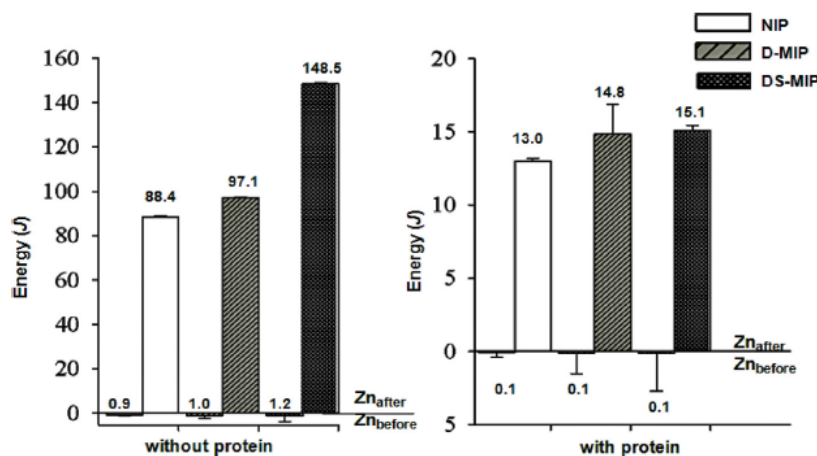


Fig. 9. The effect of the clozapine before and after adding zinc on the altered energy in the absence (left) and presence of the hypothalamus protein (right) in the imprinted polymers and control polymer.

tion with the protein, while both the D-MIP and DS-MIP exhibited an increased% oxygen by approximately 5%. The addition of zinc to the clozapine in the MIP exhibited a marked increase in the % nitrogen but only for the D-MIP (2.5%). By comparison, NIP had a similar effect whereas D-MIP was less effective. This result suggested that induced the exposed protein with an increase of the adsorbed oxygen species higher than that of the nitrogen species, which those for D-MIP being higher, and this was accordance to the pore volume of D-MIP was the lowest among the other polymers. Also, this result indicated the thermal energy conversion use heat in the presence of oxygen and the substances associated to the N species because of exogenous zinc can coordinate to oxygen [44]. The decay process in the active site of DS-MIP was prolonged more than in that of D-MIP, resulting in a relatively higher free Zn^{2+} at the surface. In contrast, D-MIP produced free Zn^{2+} at levels similar to NIP much lower than when clozapine was associated with DS-MIP. These results are consistent with a negligible or weak charge transfer when clozapine is associated, either with or without the additional protein receptors, with the NIP control polymer. These results suggests that hypothalamus receptor–clozapine complexes induced generated O and N species in the neural proteins that expressed the pharmaceutical effect of this atypical anti-psychotic drug on the basis of the pattern of the neural proteins that became adsorbed on the surface of MIPs.

3.8. The model of differential binding of MIP–drug assembly suggests the structural variation within the protein

A suitable model to address the specific interactions of these biological macromolecular systems is needed to help interpret the relevant interactions between the protein and clozapine in the imprinted cavity. Structural molecular modeling for the two MIPs when exposed to the biological receptor. Fig. 10 shows the temperature-dependence of the neural response, indicating closing or opening of the receptor-activated channel, the activation of the hypothalamus membrane protein–clozapine complexes is likely related to the differed adjustable surface of the engaged functional motifs among the MIPs. The gating effect on the membrane protein and dopamine receptors plays a major role in either the connection of neural functions or reward-mediated behavior. The affinity distribution spectra, obtained from fluorescence emission data, illustrated the relationship between the substrate binding properties and molecule environment that induced the interactions of binding site and the drug within the cavities. As a

consequence, the dopamine receptor antagonist, clozapine in MIP assembly, constructed in the presence of zinc, engages a binding pocket as that in this case, the minor structural differences indicating a clear difference in the fluorescence responses can be induced by temperature-dependent molecular interaction. However, MIPs have a small impact in the selectivity of the neural signaling protein. Much faster decay process at greater than 310 K, because of additional thermal energy effects, altered the interaction of the surface adsorbed species of the protein with exposure of the clozapine in DS-MIP. The coupling interface through the molecular orientation and protein corona is highly sensitive, promoting faster transport kinetics and change of the physical features. The 1H NMR, imaging and SEM results indicated that the change in the microscopic environment surrounding the protein contributed to photoresponse behaviors strongly dependent on temperature, an observation likely related to the surface recombination process [45]. These observations revealed the relevant interactions between the protein and the substrate in the active protein binding pockets. The spatial separation of the conformation identified by functional materials on the DS-MIP highlighted the crucial motif of the neural protein, that is, like a lock that favors drug binding. Hence the materials on the DS-MIP had the ability to influence nervous system function. However, these circumstances were made to study the neural system and bias of the signaling pathways eliciting by the dopaminergic antagonist clozapine having the activities of partial subtypes exert efficacy by interacting with the refined binding site that was much more complex. The important finding was that the remarkably assembled structure of the clozapine-MIP, at temperatures greater than 310 K, did not show a shift in fluorescence spectrum. This spectrum, dominated by the clozapine structure, showed a slower decay process and recombination dynamics that also altered the accessibility to the proteins. Consequently, the dynamic process of the recombination process was increased by temperature, potentially promoting more excitons and increased trapping of free carriers in the D-MIP.

The therapeutic potential of a receptor can be increased by the ability to tune the neural sensing protein for responses in the presence of external temperature that drive the drug access into the protein. In this manner, MIPs can be used for manipulation of the neural function, just being in active or inactive states, the receptors in the hypothalamus modulating the connection between the related counterparts of receptor and the regulation by them. The observed effects due to the substrate-binding of anti-psychotic can potential effective role of the protein modality in the neural func-

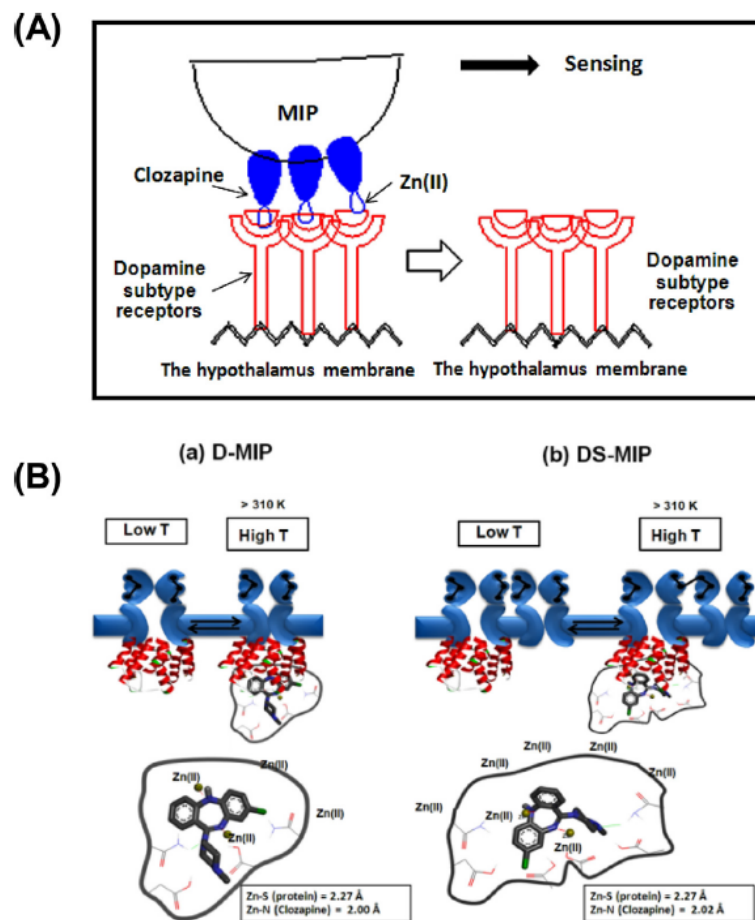


Fig. 10. (A) Schematic of clozapine in a dopamine-MIP with $ZnCl_2$ can bind to coordinate the adjacent functional counterparts of other subtypes of receptor including serotonergic receptor, reorganization conformation of membrane protein and also provided for opposing excitation and de-excitation of the receptor by signaling through the gated channel. (B) MIP-clozapine-protein complexes. A model of MIP for dopamine mimic cell surface in the hypothalamus membrane manipulating neurological function and the regulation through temperature-dependent molecular interactions. There is a direct relationship between the pharmaceutically active entities for D and S receptor and the desired interaction. The backbone of the D_1 dopaminergic receptor is shown as red ribbons, focusing on the particular conformation of the clozapine at the surface of protein solid interaction in the presence of the additional zinc.

tion that played a crucial role in the specialized functions of the neural signaling protein. This influence from the receptors of the hypothalamus is responsible to homeostasis controls through the effect of light and temperature regulation, and also the alteration of perturbed species in the nervous system. A better understand of the role in temperature homeostasis that has profound implications on energy homeostasis due to relationships between the energy metabolism and energy regulation [46]. This approach will allow for therapeutic strategy by that application of a tool to shed light on the specific functional modality in the nervous system that are affected by functional motifs from substructure of molecular environment in the neural signaling protein. Overall these results should be of interest to the pharmaceutical industry or to others interested in developing improved drugs for the nervous system.

4. Conclusions

In this study, we have compared substrate-binding properties and clozapine release from rat hypothalamus-derived receptor-drug complexes using two MIPs *in vitro*. We have shown that the approach can be applied for a reproducible assembly targeted on the action of an ensemble of anti-psychotic drug cloza-

pine at receptor sites and their increased well-defined domain and connections to closely related counterparts of the receptor. Also, the markedly higher free Zn^{2+} and increase the exposed protein with the adsorbed oxygen on the Zn^{2+} , induced by clozapine that allowed the additional benefit in pharmacological effects of this drug. Because this can precisely manipulate specific molecular interactions that mediate nervous system function. An alternative advantage of this approach is for the identification of the high affinity complexes, perhaps existing in the drug-substrate binding, particularly in the hypothalamus. By using molecular imprinting and applying it as a structure-capture tool provide to process of key importance relevant to temperature homeostasis. Therefore, MIPs can be novel tools to probe for small molecules that interact with a neural sensing protein in hypothalamus. Their use can illuminate subtle processes of therapeutic relevance, by controlling the temperature that provides for monitoring the neuronal activity and its neuro plasticity. The interactions with hypothalamic proteins, mediated more complex function, particularly in a well-defined site of protein domains that have emerged the central activities to the differentiation of distinct neural responses. This approach can accelerate discovery of the neuroleptic potential of drugs or new

drug candidates, enabling functional selectivity and, thus, reducing the risk of potentially dangerous side effects.

Acknowledgments

This work was supported partly by the Office of the Higher Education Commission Strategic Scholarships Fellowships Frontier Research Networks (Specific for Southern region) and Graduate study, Thailand Research Fund (Grant No. DBG5480006), a post-doctoral fellowship from the Prince of Songkla University, Higher Education Research Promotion and the National Research University Project of Thailand. The authors are also grateful for the financial support from the Drug Delivery System Excellence Centre and the NANOTEC Center of Excellence on Drug Delivery Systems at the Prince of Songkla University, Thailand. The authors would like to thank Mr. Mitree Naunplub for the assistance with the animals and Dr. Brian Hodgson for the help on the English language component.

References

- [1] P. Schuck, H. Zhao, The role of mass transport limitation and surface heterogeneity in biophysical characterization of macromolecular binding process by SPR biosensing, *Methods Mol. Biol.* 627 (2010) 15–54.
- [2] K. Engelhardt, U. Weichsel, E. Kraft, D. Segets, W. Peukert, B. Braunschweig, Mixed layers of β -lactoglobulin and SDS at air–water interfaces with tunable intermolecular interactions, *J. Phys. Chem. B* 118 (2014) 4098–4105.
- [3] A. MaHam, Z. Tang, H. Wu, J. Wang, Y. Lin, Protein-based nanomedicine platforms for drug delivery, *Small* 15 (2009) 1706–1721.
- [4] S.-K. Shin, S. Huang, N. Fukata, K. Ishibashi, Top-gated germanium nanowire quantum dots in a few electron regime, *Appl. Phys. Lett.* 100 (2012) 073103–073107.
- [5] C. Argyo, V. Weiss, C. Brauchle, T. Bein, Multifunctional mesoporous silica nanoparticles as a universal platform for drug delivery, *Chem. Mater.* 26 (2014) 435–451.
- [6] S.-K. Choi, M. Mammen, G.M. Whitesides, Generation and in situ evaluation of libraries of poly(acrylic acid) presenting sialosides as side chains as polyvalent inhibitors of influenza-mediated hemagglutination, *J. Am. Chem. Soc.* 119 (1997) 4103–4111.
- [7] R. Suedee, W. Naklua, S. Laengchokshoi, K. Thepkaue, P. Pathaburee, Maitri Nuanplub, Investigation of a self-assembling microgel containing an (S)-propranolol molecularly imprinted polymer in a native tissue microenvironment: part I: preparation and characterization, *Process Biochem.* 50 (2015) 517–544.
- [8] S.M. Dymecki, A modular set of Flp, FRT and lacZ fusion vectors for manipulating genes by site-specific recombination, *Gene* 171 (1996) 197–201.
- [9] B. Nilsson, K.N. Ekdahl, T.E. Mollnes, J.D. Lambris, The role of complement in biomaterial-induced inflammation, *Mol. Immunol.* 44 (2007) 83–94.
- [10] S.P. Schwendeman, G.L. Amidon, M.E. Meyerhoff, R.J. Levy, Modulated drug release using iontophoresis through heterogeneous cation exchange membrane: membrane preparation and influence of resin crosslinkage, *Macromolecules* 25 (1992) 2531–2540.
- [11] R. Numano, S. Szobota, A.Y. Lau, P. Gorostiza, M. Volgraf, B. Roux, D. Trauner, E.Y. Isacoff, Nanosculpting reversed wavelength sensitivity into a photoswitchable iGluR, *Proc. Natl. Acad. Sci. U. S. A.* 106 (2009) 6814–6819.
- [12] G.C. Sedvall, P. Karlsson, Pharmacological manipulation of D1-dopamine receptor function in schizophrenia, *Psychopharmacology (Berl.)* 21 (1999) S181–S188.
- [13] C.J. Shatz, MHC class I: an unexpected role in neuronal plasticity, *Neuron* 64 (2009) 40–45.
- [14] G. Dziewczapolski, L.B. Menalled, M.T. Savino, M. Mora, F.J. Stefano, O. Gershanik, Mechanism of action of clozapine-induced modification of motor behavior in an animal model of the super-off phenomena, *Mov. Disord.* 12 (1997) 157–166.
- [15] B.W. Smith, S.R. Starck, R.W. Roberts, E.M. Schuman, Dopaminergic stimulation of local protein synthesis enhances surface expression of GluR1 and synaptic transmission in hippocampal neurons, *Neuron* 45 (2005) 765–779.
- [16] A.E. Hensiek, M.R. Trimble, Relevance of new psychotropic drugs for the neurologist, *J. Neurol. Neurosurg. Psychiatry* 72 (2002) 281–285.
- [17] S. Lambrey, B. Falissard, M.M. -Barrero, C. Bonnefoy, G. Quilici, A. Rosier, O. Guillin, Effectiveness of clozapine for the treatment of aggression in an adolescent with autistic disorder, *J. Child Adolesc. Psychopharmacol.* 20 (2010) 79–80.
- [18] I. Maurer, H.-J. Möller, Inhibition of complex I by neuroleptics in normal human brain cortex parallels the extrapyramidal toxicity of neuroleptics, *Mol. Cell. Biochem.* 21 (1997) 255–259.
- [19] L. Chen, S. Xu, J. Li, Recent advances in molecular imprinting technology: current status, challenges and highlighted applications, *Chem. Soc. Rev.* 40 (2011) 2922–2942.
- [20] R. Suedee, The use of molecularly imprinted polymers for dermal drug delivery, *Pharm. Anal. Acta* 4 (1–23) (2013) 264.
- [21] F. Ning, P. Hailong, J. Li, L. Chen, H. Xiong, Molecularly imprinted polymer on magnetic graphene oxide for fast and selective extraction of 17-estradiol, *J. Agric. Food Chem.* 62 (2014) 7436–7443.
- [22] G.Z. Kyzas, S.G. Nanaki, A. Koltsakidou, M. Papageorgiou, M. Kechagia, D.N. Bikiaris, D.A. Lambropoulou, Effectively designed molecularly imprinted polymers for selective isolation of the antidiabetic drug metformin and its transformation product guanylurea from aqueous media, *Anal. Chim. Acta* 866 (2015) 27–40.
- [23] Y.-T. Tung, C.-C. Chang, Y.-L. Lin, S.-L. Hsieh, G.-J. Wang, Development of double-generation gold nanoparticle chip-based dengue virus detection system combining fluorescence turn-on probes, *Biosens. Bioelectron.* 77 (2016) 90–98.
- [24] Q. Liu, Y. Feng, S. Huang, Q. Wu, J. He, Preparation of ordered macroporous chinchonine molecularly imprinted polymers and comparative study of their structure and binding properties with traditional bulk molecularly imprinted polymers, *Polym. Int.* 64 (2015) 1594–1599.
- [25] W. Naklua, K. Mahesh, P. Aundorn, N. Tanmanee, K. Aenukulpong, S. Sutto, Y.Z. Chen, S. Chen, R. Suedee, An imprinted dopamine receptor for discovery of highly potent and selective D₃ analogues with neuroprotective effects, *Process Biochem.* 50 (2015) 1537–1556.
- [26] T. Nagai, K. Takuma, H. Kamei, Y. Ito, N. Nakamichi, D. Ibi, Y. Nakanishi, Masaaki Murai, H. Mizoguchi, T. Nabeshima, K. Yamada, Dopamine D1 receptor regulate protein synthesis-dependent long-term recognition memory via extracellular signal regulated kinase 1/2 in the prefrontal cortex, *Learn. Mem.* 14 (2007) 117–125.
- [27] J. Walter, P.J. Sherwood, W. Lin, D. Segets, W.F. Stafford, W. Peukert, Simultaneous analysis of hydrodynamic and optical properties using analytical ultracentrifugation equipped with multiwavelength detection, *Anal. Chem.* 87 (2015) 3396–3403.
- [28] J. Svitel, H. Boukari, D.V. Ryk, R.C. Willso, P. Schuck, Probing the functional heterogeneity of surface binding sites by analysis of experimental binding traces and the effect of mass transport limitation, *Biophys. J.* 92 (2007) 1742–1758.
- [29] V. Lobo, A. Patil, A. Phatak, N. Chandra, Free radicals, antioxidants and functional foods: impact on human health, *Pharmacogn. Rev.* 4 (2010) 118–126.
- [30] R. Suedee, V. Seechamnaturakit, B. Banyuk, C. Ovattarnporn, G.P. Martin, Temperature sensitive dopamine-imprinted selective extraction of adrenergic drugs from urine, *J. Chromatogr. A* 1114 (2006) 239–249.
- [31] P. Lulinski, M. Dorota, B.-K. Magdalena, S. Miroslaw, Dopamine-imprinted polymers: template-monomer interactions, analysis of template removal and application to solid phase extraction, *Molecules* 12 (2007) 2434–2449.
- [32] F.L. Dickert, U.P.A. Bäuml, H. Stathopoulos, Mass-sensitive solvent vapor detection with Calix[4] resorcinarenes: tuning sensitivity and predicting sensor effects, *Anal. Chem.* 69 (1997) 1000–1005.
- [33] S.E. Senogles, N. Amlaiky, P. Falardeau, M.G. Caron, Purification and characterization of the D2-dopamine receptor from bovine anterior pituitary, *J. Biol. Chem.* 263 (1988) 18996–19002.
- [34] L. Darwish, H. Abdel-Wadood, N. Abdel-Latif, Validated spectrophotometric and fluorimetric methods for analysis of clozapine in tablets and urine, *Ann. Chim.* 95 (2005) 345–356.
- [35] F.A. Moman, R. Rone, Validation of the general purpose QUANTA[®] force field, *J. Comput. Chem.* 13 (1992) 888–900.
- [36] T. Kamra, T. Zhou, L. Montelius, J. Schnadt, L. Ye, Implementation of molecularly imprinted polymer beads for surface enhanced Raman detection, *Anal. Chem.* 87 (2015) 5056–5061.
- [37] J. Chen, L.-Y. Bai, K.-F. Liu, R.-Q. Liu, Y.-P. Zhang, Atrazine molecular imprinted polymers: comparative analysis by far-infrared and ultraviolet induced polymerization, *Int. J. Mol. Sci.* 15 (2014) 574–587.
- [38] P. Kumar, Y.E. Choonara, L.C.D. Toit, G. Modi, D. Naidoo, V. Pillay, Novel high-viscosity polyacrylamidated chitosan for neural tissue engineering: fabrication of anisotropic neurodurable scaffold via molecular disposition of persulfate-mediated polymer slicing and complexation, *Int. J. Mol. Sci.* 13 (2012) 13966–13984.
- [39] S.L.T. de Souza, A.A. Lima, I.L. Caldas, R.O. Medrano-T, Z.O. Guimarães-Filho, Self-similarities of periodic structures for a discrete model of a two-gene system, *Phys. Lett. A* 376 (2012) 1290–1294.
- [40] M.A. Meyers, P.-Y. Chen, A.Y.-M. Lin, Y. Seki, Biological materials: structure and mechanical properties, *Prog. Mater. Sci.* 53 (2008) 1–206.
- [41] B. Wang, L. You, P. Ren, X. Yin, Y. Peng, B. Xia, L. Wang, X. Yu, S.M. Poh, P. Yang, G. Yuan, L. Chen, A. Rusydi, J. Wang, Oxygen-driven anisotropic transport in ultrathin manganese films, *Nat. Commun.* 4 (2013) 1–7.
- [42] J.S. Yang, S. Perveen, T.J. Ha, S.Y. Kim, S.H. Yoon, Cyanidin-3-glucoside inhibits glutamate-induced Zn²⁺ signaling and neuronal cell death in cultured rat hippocampal neurons by inhibiting Ca²⁺-induced mitochondrial depolarization and formation of reactive oxygen species, *Brain Res.* 1606 (2015) 9–20.
- [43] R. Matsumoto, K. Akama, R. Rakwal, H. Iwashashi, The stress response against denatured proteins in the deletion of cytosolic chaperones SSA1/2 is different from heat shock response in *Saccharomyces cerevisiae*, *BMC Genom.* 6 (2005) 1–15.

- [44] M. Akia, F. Yazdania, E. Motaee, D. Han, H. Arandiyani, A review on conversion of biomass to biofuel by nanocatalysts, *Biofuel Res. J.* 1 (2014) 16–25.
- [45] P. Docampo, A. Ivaturi, R. Gunning, S. Diefenbach, Jame Kirkpatrick, C.M. Palumbiny, V. Sivaram, H. Geaney, L. S.-Mende, M.E. Welland, H.J. Snaith, The influence of 1D, meso and crystal structures on charge transport and recombination in solid-state dye sensitized solar cells, *J. Mater. Chem. A* 1 (2013) 12088–12095.
- [46] I. Tabarean, B. Morrison, M.C. Marcondes, T. Bartfai, B. Conti, Hypothalamus and dietary control of temperature-mediated therapy, *Ageing Res. Rev.* 9 (2010) 1–20.

MANUSCRIPT 3

Dopaminergic Receptor-Ligand Binding Assays based on Molecularly Imprinted
Polymers on Quartz Crystal Microbalance Sensors

(Manuscript submit to *Biosensors and Bioelectronics*)

and Bioelectronics

Elsevier Editorial System(tm) for Biosensors

Manuscript Draft

Manuscript Number:

Title: Dopaminergic Receptor-Ligand Binding Assays based on Molecularly Imprinted Polymers on Quartz Crystal Microbalance Sensors

Article Type: Full Length Article

Section/Category: Synthetic receptors, MIPs, Biofuel cells, Bioelectronics

Keywords: Molecularly imprinted polymer; Dopamine receptor, Quartz Crystal Microbalance, ligand binding assay.

Corresponding Author: Prof. Peter A. Lieberzeit, Dr.

Corresponding Author's Institution: University of Vienna

First Author: Wanpen Naklua

Order of Authors: Wanpen Naklua; Roongnapa Suedee, PhD; Peter A. Lieberzeit, Dr.

Highlights for review

- Design of first MIP for dopaminergic D1R receptor.
- Characterization of binding properties of such MIP in native form as well as in the presence of D1R agonists and antagonists.
- Competitive binding assays of D1R MIP with agonists and antagonists.
- The approach resulted in label-free competitive binding assay leading to similar results as established radioassays.

Dopaminergic Receptor-Ligand Binding Assays based on Molecularly Imprinted Polymers on Quartz Crystal Microbalance Sensors

Wanpen Naklua¹, Roongnapa Suedee¹, Peter A. Lieberzeit^{2*}

¹Molecular Recognition Materials Research Unit, Drug Delivery System Excellence Center, and NANOTEC Center of Excellence, Department of Pharmaceutical Chemistry, Faculty of Pharmaceutical Sciences, Prince of Songkla University, Hatyai, Songkhla 90112, Thailand

²University of Vienna, Department of Analytical Chemistry, Faculty of Chemistry, Währingerstraße 38, A-1090 Vienna, Austria.

*Corresponding author: Tel.: +43 1 4277 52341; Fax: +43 1 4277 9523
E-mail address: Peter.Lieberzeit@univie.ac.at

Abstract

Molecularly imprinted polymers (MIPs) have been successfully applied as selective materials for assessing the binding activity of agonist and antagonist of dopamine D1 receptor (D1R) by using quartz crystal microbalance (QCM). In this study, D1R derived from rat hypothalamus was used as a template and thus self-organized on stamps. Those were pressed into an oligomer film consisting of acrylic acid: *N*-vinylpyrrolidone: *N,N'*-(1,2-dihydroxyethylene) *bis*-acrylamide in a ratio of 2:3:12 spin coated onto a dual electrode QCM. Such we obtained one D1R-MIP-QCM electrode, whereas the other electrode carried the non-imprinted control polymer (NIP) that had remained untreated. Successful imprinting of D1R has been confirmed by AFM. The polymer can re-incorporate D1R leading to frequency responses of 100-1200 Hz in a concentration range of 5.9 to 47.2 μ M. In a further step such frequency changes proved inherently useful for examining the binding properties of test ligands to D1R. The resulting mass-sensitive measurements revealed K_d of dopamine-HCl, haloperidol, and (+)-SCH23390 at 0.874, 25.6, and 0.004 nM, respectively. These results correlate well with the values determined in radio ligand binding assays. Our experiments revealed that D1R-MIP sensors are useful for estimating the strength of ligand binding to the active single site. Therefore, we have developed a biomimetic surface imprinting strategy for QCM studies of D1R-ligand binding and presented a new method to ligand binding assay for D1R.

Keywords: Molecularly imprinted polymer; Dopamine receptor, Quartz Crystal Microbalance, ligand binding assay.

Introduction

D1R is a protein found in different locations in the brain of vertebrates, such as caudate putamen, nucleus accumbens olfactory tubercle, frontal cortex, habenula, amygdala, hypothalamus and thalamus. Previous studies have shown that its molecular mass is 49 to 75 kDa (Huang et al., 1992; Worsley et al., 2000; Diaz et al., 2014). Moreover, D1R is important in the central nervous system and influences motoric control, cognition, neuroendocrine functions, and neuronal differentiation (Blenau et al., 1998; Ricci et al., 2006). The active sites of D1R have become the most important target proteins in the development of anti-psychotic agents or new drug candidates (Guttman, 1992; Goldman-Rakic et al., 2004; Horacek et al., 2006). Anti-psychotic drugs substantially affect most dopaminergic receptors in the prefrontal cortex (Hummel and Unterwald, 2002). The functional affinity of a ligand for D1R is associated with the exact three-dimensional structure of the binding pocket in the protein receptor. The aim of this study has been to establish a molecularly imprinted polymer (MIP) for D1R. By such means it should be possible to assess the biological activity of small molecules – D1R antagonists in this case – via QCM sensors. This is based on the assumption that if binding changes the conformation of D1R, it should be possible to establish a biomimetic ligand binding assay. The basic outline of the approach is given in Fig. 1. The rationale behind the approach is that MIP cavities should more preferably bind pure D1R, than its receptor-ligand complexes. Normally, ligand binding assays are used for finding novel drugs and include radioactive and non-radioactive protocols. Most bioassay technologies thus require labeling of either ligand or receptor (de Jong et al., 2005). The affinity of test compounds for the target can be determined from their ability to displace a marker from the target (Hofner and Wanner, 2003).

[FIGURE 1]

The QCM is the most common mass-sensitive sensor used in biosensor applications (Bunde et al., 1998; O'Sullivan and Guilbault, 1999). Typically, QCM consist of thin quartz discs containing one or more metal electrode pairs on their opposite faces. The change in mass on the quartz surface is related to the change in frequency of the oscillating crystal, as shown by the Sauerbrey equation (1).

$$\Delta f = -\frac{2f^2}{\sqrt{\rho_q u_q}} \Delta m = -C_f \Delta m \quad (1)$$

Here, Δf is the frequency shift, Δm the mass change, f is the intrinsic crystal frequency, ρ_q is the density of the quartz, and u_q is the shear modulus of the quartz film (Baltus et al., 2007). MIPs have been used as selective materials for numerous biosensors (Dickert et al., 1996; Dickert et al., 2000; Apodaca et al., 2011; Sontimuang et al., 2011; Latif et al., 2014). They contain highly selective cavities in a crosslinked polymer. Those are generated during polymerization in the presence of the template and mimic its three-dimensional shape and chemical characteristics. A wide range of templates are possible, including macromolecules, such as proteins (Bonini et al., 2007; Yola et al., 2014). The main advantage of biosensors is the ability to monitor the reaction between bio-selector and analyte in a rapid and sensitive manner (El-Sharif et al., 2015). However, proteins are delicate and sensitive templates. Hence the type of substrate and the procedures used during the polymerization process can strongly affect efficiency of protein recognition in the final MIP. Some successful strategies leading to protein MIP include silica-based materials (Glad et al., 1985; Lee et al., 2007), immobilizations (Shi et al., 1999; Guo et al., 2006; Tan et al., 2008), grafting on surfaces (Li et al., 2008), and surface imprinted polymers (Phan et al., 2014).

Materials and methods

Chemicals and reagents

Acrylic acid (AA) was obtained from Merck (Hohenbrunn, Germany). *N*-vinylpyrrolidone (NVP), acrylamide (ACM) and Coomassie brilliant blue were purchased from Sigma-Aldrich (Steinheim, Germany). Methacrylic acid (MAA), *N,N'*-(1,2-dihydroxyethylene) *bis*-acrylamide (DHEBA), 2,2'-azobisisobutyronitrile (AIBN), bovine serum albumin (BSA), 5-(dimethylamino) naphthalene-1-sulfonyl chloride (or dansyl chloride), dopamine HCl (D) and (+)-SCH23390 (SCH) were obtained from Sigma-Aldrich (St. Louis, MO, USA). Sodium dodecyl sulfate (SDS) and *tris*-HCl were purchased from Aldrich Chemical Company (Milwaukee, WI, USA). Protease inhibitor cocktail was obtained from Sigma-Aldrich (St. Louis, MO, USA). Haloperidol (Ha) is a working standard substance (Ph.Eur/BP, 100%), batch no. LHAP-7/f/150. Biorex-70 resin (batch no. L143-5832) was from Bio-Rad Laboratories Inc. (California, USA) and full-range rainbow molecular weight marker (M_r 12000-225000) was supplied by AmershamTM (Buckinghamshire, UK). Solvents were purchased from Lab Scan Ltd, Dublin, Ireland. All reagents and solvents were of either analytical or HPLC grade.

Preparation of template protein

D1R was isolated from hypothalamus (Wistar rats both sexes, 200–210 g weight) with permission from the Animal Research Ethical Committee at Prince of Songkla University (Ethic Ref no. 30/2014). The protein receptor was removed and homogenized in cold buffer at pH=7.4 (0.32 M sucrose, 50 mM *tris*-HCl, 0.5 mM Na₂EDTA, 0.1% ascorbate and phosphate buffer) containing protease inhibitor (10 μ L mL⁻¹). The homogenate was centrifuged at 1,000 rpm for 10 min to remove rough debris. The supernatant was resuspended in buffer and centrifuged again at 43,000 rpm for 20 min. The obtained pellet was purified with a Biorex-70 resin on the column and eluted with physiological buffer, 0.5 M NaCl and 1 M NaCl in buffer. The resulting solution was freeze-dried to obtain the dopamine receptor (Senogles et al., 1988; Naklua et al., 2015). The isolated D1R receptor

was examined by SDS-PAGE using 3% and 12% polyacrylamide gels under non-reducing conditions after staining with Coomassie brilliant blue. These experiments revealed $M_r \sim 52,000$ observed against a full range of rainbow molecular weight markers. The receptors were kept stabilized by protease inhibitor cocktail and storage at $-20\text{ }^\circ\text{C}$. Moreover, the concentration of D1R was estimated according to Bradford using BSA as the standard.

Synthesis and screening of D1R-imprinted polymers

In the first step we studied the optimal conditions for non-covalent imprinting. Suitable functional monomers, cross-linker, initiator, and solvent were screened and selected. Based on the amino acid pattern of the D1R protein surface, the weight ratios of AA, MAA, ACM, and NVP as functional monomers, respectively, were varied as follows: AA:NVP = 2:3 and 3:2, MAA:NVP = 2:3 and MAA:ACM = 1:1. DHEBA was applied as a cross-linking monomer and AIBN as initiator. The mixed monomer solution was heated at 55°C in a water-bath for pre-polymerization until approaching the gel point (180-300 min). The pre-polymer layer was prepared by spin-coating onto a glass slide at 2,000 rpm for 1 min. The protease inhibitor cocktail necessary for storage was removed by dialysis in PBS buffer leading to pure D1R protein. Template stamps were prepared by coating $5\mu\text{L}$ of a solution containing 8 mg/mL of pure D1R in PBS buffer onto 5×5 mm glass substrates (1.0-1.2 mm thickness, smooth and ground edges with 90 degree shapes, Sail Boat Lab Co., Ltd., China) and keeping at $4\text{ }^\circ\text{C}$ for 20-60 min to sediment. Then, the D1R template stamp was pressed into the pre-polymer layer followed by thermal polymerization at $60\text{ }^\circ\text{C}$ for 14 hours. MIPs were tested for successful washing and the presence of binding sites after each of the following steps, respectively: Before and after rinsing MIP with 10% acetic acid, 1%SDS, and water. UV-Vis photometry was used for assessing protein binding by the layers via so-called xanthoprotein reaction: first, we dropped concentrated nitric acid onto the test sample. HNO_3 reacts with tyrosine and tryptophan present in the template protein and leads to yellow reaction product

as shown in Fig. 2A. Then, samples were heated to 60 °C. In the presence of proteins this protocol yields a yellow product that absorbs at 330-450 nm. The experiments showed that template protein molecules remain in the MIP surface immediately after synthesis and can be removed by rinsing sequentially with 10% acetic acid, 1% SDS, and water. The best monomer for the generating of D1R-MIP was selected for QCM from an optimal formation of binding site on the protein in this screening experiment. Topographic images were obtained on a Veeco Nanoscope 8, (Bruker Instruments, USA) AFM in contact mode.

[FIGURE 2]

QCM manufacturing and measurements

For device manufacturing, commercially available 10 MHz AT-cut quartz plates (diameter 13.8 mm, purchased from Great Microtama Industries, Surabaya, Indonesia) served as basis. Onto those, we screen-printed dual electrode structures on both sides of the quartz substrate with brilliant gold paste, GGP 2093-12%, from Heraeus, Germany. They were burnt at 400°C for 4 hours to obtain QCM with resonance frequencies in the range of 9.90-9.99 MHz with low damping (>-5 dB). Two-electrode QCM were used for comparing MIP and non-imprinted polymer (NIP) signals (Phan et al., 2014)

For measurement, QCM were mounted in a custom-made sandwich cell and contacted to an oscillator circuit read out by a frequency counter (Agilent 53131A, 225 MHz Universal counter, Colorado, USA). Resonance frequency as a function of time was read out to a computer by the means of a Lab View routine. Damping spectra of each QCM were determined by network analyzer (Agilent Technologies E5062A, TX, USA). Affinity of D1R to recognition cavities on D1R-MIP was determined by adding D1R with either stabilizer or BSA solution. These sensor systems were also tested in phosphate buffer to measure dopamine receptor-ligand binding assays at 17-18 °C.

Receptor-ligand binding assay experiments

During receptor-ligand binding assays, we simultaneously exposed D1R MIP-coated QCM to D1R and one of the following test compounds: 47.2 μM of D, Ha and SCH in PBS (from stock solution 0.15 $\mu\text{g}/\text{mL}$). In a next step, both D1R-MIP and NIP electrodes were first exposed to D1R solutions until stable baseline was reached. Then non-binding D1R was removed. For exposure test, each compound, i.e. D, Ha and SCH, respectively, was flushed through the cell. Solutions contained 1.20 to 70.8 $\mu\text{mol}/\text{L}$ of the respective compound in increasing concentrations. Each experiment was repeated three times at $17\pm 1^\circ\text{C}$.

Results and discussion

Synthesis and layer properties of D1R-MIP

D1R contains both polar and non-polar domains: the transmembrane consists of hydrophobic amino acids, such as leucine, methionine, phenylalanine, and valine; The outer surface of the molecule protruding from the cell membrane contains hydrophilic amino acids, such as aspartate, arginine, glutamate, and lysine. Therefore, one can expect that D1R orients itself on the stamp surface in a way that the 7 transmembrane α -helices of D1R preferably point towards the stamp surface as illustrated in Fig. 1. Initial experiments (details not shown) revealed optimal layer composition of 2:3:12 of AA:NVP:DHEBA lead to highly appreciable sensor signals on QCM.

Fig. 2B shows the UV absorption spectra of the optimized MIP following xanthoprotein reaction after different experimental steps, respectively. The results clearly show that D1R-MIP contain observable amount of protein after imprinting. Those protein molecules have obviously detached from the stamp. The results indicate intrinsic stability of the D1R protein during self-organization on the stamp surface followed by stamping and thereafter polymerization. To assess the rebinding ability of MIP, we incubated it with D1R solutions

and detected any protein re-incorporated with the same procedure as before. Obviously, the protein maintained its original conformation and underwent very limited change in structure, if any, because rebinding on D1R-MIP could clearly be observed. It is noteworthy that such MIP can be re-used several times (at least five times per one experiment).

Layer height of D1R-MIP-QCM

Layer height of the polymer could play a role in changing the exact structure of the adsorbed protein during the imprinting and polymerization processes. According to previous experience a frequency shift after coating of $\Delta f=1$ kHz on QCM corresponds to a layer height of 40 nm (Seidler et al., 2009; Iqbal et al., 2010; Kotova et al., 2013). The resulting linear relationship between different volumes of pre-polymer used during coating and corresponding layer height is shown in (Fig. 2C). Both D1R-MIP and reference polymer layer showed similar frequency change on the QCM. However, D1R-MIP layers were slightly thinner than corresponding NIP, which can be traced back to both the stamping procedure and template removal.

AFM studies of D1R MIP

AFM images shown in Fig. 3 depict D1R protein stamp, MIP, and NIP, respectively. The stamp image reveals structures that are roughly 50-100 nm wide and about 125 nm high.

[FIGURE 3]

Comparing this with the size of a single D1R protein molecule of 3.3 x 4.5 x 7.5 nm (protein data bank with PDB ID: 1OZ5), it becomes evident that polymer aggregates form on the surface. However, in terms of imprinting that is no problem. The protein hence has been deposited in almost “brush-like” three-dimensional structures, which increases the surface

area and results in a large number of accessible binding sites in the MIP. This is confirmed by AFM images of MIP that show cavities and ridges in between them that are closely related to the dimensions of the D1R stamp. Finally, NIP shows only minor structures and completely different morphological features, which clearly confirms generation of binding sites in the polymer by the protein. This is also strong indicative that there should be binding cavities once the protein molecules are washed off the surface.

QCM sensor measurements

Fig. 4 summarizes the frequency shift of D1R-MIP on 10 MHz QCM on exposure to different concentrations of D1R, both pure (marked * in the image) and mixed with stabilizer (marked **) or BSA (marked ***). Obviously, the MIP and NIP electrodes react in fundamentally different manner: whereas the MIP-coated electrode shows shifts to lower frequency - the expected Sauerbrey behavior - the NIP-coated electrodes reveal slight frequency increases. First of all, the MIP frequency shifts are caused by analyte-MIP interactions that remain undisturbed even by the presence of BSA in the sample solution. In terms of quantification, the results are very promising: the highest sensor signal of ~ 800 Hz was obtained with $47.2 \mu\text{M}$ D1R in PBS both with and without $10 \mu\text{L/mL}$ stabilizer. Similarly, we observed ~ 420 Hz for $23.6 \mu\text{M}$, ~ 170 Hz for $11.8 \mu\text{M}$ and ~ 100 Hz for $5.9 \mu\text{M}$ in the presence of BSA. These results confirm that neither protease stabilizer, nor BSA had any effect on the MIP sensor signal. Hence, imprinting turned out successful. In contrast to this, the frequency increases observed on the NIP do not depend on concentration, but reveal usual behavior of QCM coated with rather smooth surfaces towards proteins or cells (Wangchareansak et al., 2011). This is further summarized by the sensor characteristics shown in the bottom part of Fig. 4.

[FIGURE 4]

In a next step we tested cross-sensitivity of the system towards the ligands/antagonists of D1R, which is necessary information for receptor-ligand binding assays. When exposing the sensor to 47.2 μM of D, Ha, and SCH, it turned out that haloperidol and SCH lead to only small frequency changes, but dopamine-containing samples (D) still yielded frequency shift of about -250 Hz, as can be seen in Fig. 5. The ligand-target interactions for D1R-MIP can therefore be analyzed on the QCM sensor. The results shows that the potent dopaminergic agonist, D, was significantly adsorbed both MIP and control polymer. Both antagonists, i.e. SCH and D1R display almost no difference in sensor response between the MIP and the NIP indicating only nonspecific binding of those compounds to the sensor layers.

[FIGURE 5]

Because no significant interferences are to be expected, D1R-MIP based-QCM can be utilized for assessing competitive ligand binding between D1R in solution and these ligands: for that purpose D1R solutions in PBS were incubated with, D, Ha, or SCH. As can be seen in Fig. 5, the MIP even yields somewhat higher sensor responses for D1R incubated with dopamine than for pure D1R, though the difference is not statistically significant. This may be assigned to the increase in mass by incorporating dopamine. On the other hand the two antagonists give rise to substantially lower sensor responses indicating that antagonist Ha and SCH bind to D1R outside the dopamine binding pocket and thus change overall morphology or surface chemistry of D1R. These results hence give clear evidence that D1R MIP are actually useful to distinguish between free receptors or D1R containing dopamine and inhibited D1R, respectively. To the best of our knowledge this is the first attempt actually proving this ability. Furthermore it should provide the opportunity to rational process development of anti-psychotic drugs due to its ability to test able to particular target interactions for the binding of ligands and selectivity of receptor conformation.

The protein receptor-ligand interactions by the D1R-MIP-QCM

In a next step towards MIP-QCM ligand binding assays, the sensors were first exposed to D1R until reaching equilibrium. Then, defined amounts of agonist and antagonists, respectively were added step by step until QCM signals reached equilibrium again. Fig. 6 summarizes the QCM frequency responses for these experiments.

[FIGURE 6]

Moreover, EC_{50} values for each compound were calculated by equation (2). Dissociation constants (K_d) and the density of binding sites (B_{max}) were calculated from saturation isotherms of specific binding (3) by the means of non-linear fitting in Sigma plot, frequency shift (on the Y axis) vs. log (test compound) (on the X axis).

$$y = \min + \frac{(max - \min)}{1 + 10^{x - \log EC_{50}}} \quad (2)$$

$$y = \frac{B_{max}x}{K_d + x} \quad (3)$$

Overall, Ha and SCH, which are known antagonist to D1R, lead to similar competition values that correlate well with the values determined in radio ligand binding assay using [3H] SCH 23390, IC_{50} of Ha = 620 nM and K_d of SCH = 0.53 nM (Höfner and Wanner, 2003) and previous studies as presented in Table 1.

[Table 1]

The cavities of D1R-MIP undergo H-bond or other intermolecular interactions between the carboxylic group ($-COOH$) of AA and the carbonyl group ($C=O$) of NVP with amino groups on the surface of the dopamine receptor. Moreover, the crystal structure of dopamine

receptors as shown in protein database have more than two active sites that can bind with ligands, in the stabilization of particular conformation stage leading to greater selectivity of ligands. Therefore, the test compounds can be assumed to bind to various/different sites on immobilized receptor. The QCM data also indicated that D and Ha may bind to the same active site that it is easier for ligand to enter. It is known that D is smaller and more strongly polar than Ha lead to stronger interactions between the H-bond donors and the amino groups of the receptor active site. Therefore as much ligand as possible is directly attached with lower dissociation constant. The results showed that this MIP-QCM sensor can detect ligands that showed affinity to D1R. However, some ligands that have low affinity cannot be detected in lower concentration. The ligand bindings of D1R-MIP-based QCMs that however, they differed from the drug reaction in the vivo due to their transient nature and heterogenous mixture within assembled structure associated with the potency.

Conclusions

Overall D1R-MIP proved highly useful for binding the protein selectively, which leads to corresponding frequency shifts on QCM. In terms of sensing D1R, the approach is merely of theoretical value, because the protein is bound to cell surfaces. However, the MIP has proven useful to distinguish between the free receptor and receptor-dopamine complexes on the one hand and receptor-antagonist complexes on the other hand. Based on those experiments, this work to the best of our knowledge hence represents one of the first attempts to utilize MIP for assessing receptor-ligand binding assays. This in principle allows to mimic processes in the neural signaling pathway and may open up doors to understand the neurophysiology as a result in specific functional regulated on the receptors that facilitate for searching of specific therapeutics.

Acknowledgements

We gratefully acknowledge financial support from: the Office of the Higher Education Commission, Thailand by grant under the program “the Strategic Scholarships Fellowships Frontier Research Networks (Specific for Southern region)”; the National Research University Project of Thailand, Office of the Higher Education Commission; the Thailand Research Fund (Grant No. DBG5480006); Graduate study at PSU, Drug Delivery System Excellence Center at PSU; Nanotechnology Center (NANOTEC), Ministry of Science and Technology, Thailand, through its program of the Center of Excellence Network; the ASEA European Academic University Network (ASEA-UNINET).

References

- Apodaca, D.C., Pernites, R.B., Ponnampati, R., Del Mundo, F.R., Advincula, R.C., 2011. Electropolymerized molecularly imprinted polymer film: EIS sensing of bisphenol A. *Macromolecules*, 44, 6669-6682.
- Baltus, R.E., Carmon, K.S., Luck, L.A., 2007. Quartz crystal microbalance (QCM) with immobilized protein receptors: comparison of response to ligand binding for direct protein immobilization and protein attachment via disulfide linker. *Langmuir*, 23, 3880-3885.
- Blenau, W., Erber, J., Baumann, A., 1998. Characterization of a dopamine D1 receptor from *Apis mellifera*: cloning, functional expression, pharmacology, and mRNA localization in the brain. *J Neurochem*, 70, 15-23.
- Bonini, F., Piletsky, S., Turner, A.P.F., Speghini, A., Bossi, A., 2007. Surface imprinted beads for the recognition of human serum albumin. *Biosensors and Bioelectronics*, 22, 2322-2328.
- Brewster, W.K., Nichols, D.E., Watts, V.J., Riggs, R.M., Mottola, D., Mailman, R.B., 1995. Evaluation of cis- and trans-9- and 11-hydroxy-5,6,6a,7,8,12b-hexahydrobenzo[a]-

- phenanthridines as structurally rigid, selective D1 dopamine receptor ligands. *Journal of medicinal chemistry*, 38, 318-327.
- Bunde, R.L., Jarvi, E.J., Rosentreter, J.J., 1998. Piezoelectric quartz crystal biosensors. *Talanta*, 46, 1223-1236.
- de Jong, L.A.A., Uges, D.R.A., Franke, J.P., Bischoff, R., 2005. Receptor–ligand binding assays: technologies and applications. *Journal of Chromatography B*, 829, 1-25.
- Diaz, M.R., Jotty, K., Locke, J.L., Jones S.R., Valenzuela C.F., 2014. Moderate alcohol exposure during the rat equivalent to the third trimester of human pregnancy alters regulation of GABAA receptor-mediated synaptic transmission by dopamine in the basolateral amygdala. *Frontiers in pediatrics*, 2, 1-12.
- Dickert, F.L., Haunschild, A., Kuschow, V., Reif, M., Stathopoulos, H., 1996. Mass-sensitive detection of solvent vapors. Mechanistic studies on host-guest sensor principles by FT-IR spectroscopy and BET adsorption analysis. *Analytical Chemistry*, 68, 1058-1061.
- Dickert, F.L., Lieberzeit, P., Tortschanoff, M., 2000. Molecular imprints as artificial antibodies-a new generation of chemical sensors. *Sensors and Actuators B: Chemical*, 65, 186-189.
- El-Sharif, H.F., Aizawa, H., Reddy, S.M., 2015. Spectroscopic and quartz crystal microbalance (QCM) characterisation of protein-based MIPs. *Sensors and Actuators B: Chemical*, 206, 239-245.
- Glad, M., Norrlöw, O., Sellergren, B., Siegbahn, N., Mosbach, K., 1985. Use of silane monomers for molecular imprinting and enzyme entrapment in polysiloxane-coated porous silica. *Journal of Chromatography A*, 347, 11-23.
- Goldman-Rakic, P., Castner, S., Svensson, T., Siever, L., Williams, G., 2004. Targeting the dopamine D1 receptor in schizophrenia: insights for cognitive dysfunction. *Psychopharmacology*, 174, 3-16.

- Guo, M.-J., Zhao, Z., Fan, Y.-G., Wang, C.-H., Shi, L.-Q., Xia, J.-J., Long, Y., Mi, H.-F., 2006. Protein-imprinted polymer with immobilized assistant recognition polymer chains. *Biomaterials*, 27, 4381-4387.
- Guttman, M., 1992. Dopamine receptors in Parkinson's disease. *Neurologic clinics*, 10, 377-386.
- Hofner, G., Wanner, K.T., 2003. Competitive binding assays made easy with a native marker and mass spectrometric quantification. *Angew Chem Int Ed Engl*, 42, 5235-5237.
- Horacek, J., Bubenikova-Valesova, V., Kopecek, M., Palenicek, T., Dockery, C., Mohr, P., Höschl, C., 2006. Mechanism of action of atypical antipsychotic drugs and the neurobiology of schizophrenia. *CNS Drugs*, 20, 389-409.
- Huang, Q., Zhou, D., Chase, K., Gusella, J.F., Aronin, N., Difiglia, M., 1992. Immunohistochemical localization of the D1 dopamine receptor in rat brain reveals its axonal transport, pre- and postsynaptic localization, and prevalence in the basal ganglia, limbic system, and thalamic reticular nucleus. *Proc Natl Acad Sci U S A* 89, 11988-11992.
- Hummel, M., Unterwald, E.M., 2002. D1 dopamine receptor: A putative neurochemical and behavioral link to cocaine action. *Journal of Cellular Physiology*, 191, 17-27.
- Iorio, M.A., Reymer, T.P., Frigeni, V., 1987. Combined analgesic/neuroleptic activity in N-butyrophenone prodine-like compounds. *Journal of medicinal chemistry*, 30, 1906-1910.
- Iqbal, N., Mustafa, G., Rehman, A., Biedermann, A., Najafi, B., Lieberzeit, P.A., Dickert, F.L., 2010. QCM-arrays for sensing terpenes in fresh and dried herbs via bio-mimetic MIP layers. *Sensors*, 10, 6361-6376.
- Kotova, K., Hussain, M., Mustafa, G., Lieberzeit, P.A., 2013. MIP sensors on the way to biotech applications: Targeting selectivity. *Sensors and Actuators B: Chemical*, 189, 199-202.

- Latif, U., Qian, J., Can, S., Dickert, F.L., 2014. Biomimetic receptors for bioanalyte detection by quartz crystal microbalances-from molecules to cells. *Sensors*, 14, 23419-23438.
- Lee, K., Itharaju, R.R., Puleo, D.A., 2007. Protein-imprinted polysiloxane scaffolds. *Acta biomaterialia*, 3, 515-522.
- Li, F., Li, J., Zhang, S., 2008. Molecularly imprinted polymer grafted on polysaccharide microsphere surface by the sol-gel process for protein recognition. *Talanta*, 74, 1247-1255.
- Mottola, D.M., Laiter, S., Watts, V.J., Tropsha, A., Wyrick, S.D., Nichols, D.E., Mailman, R.B., 1996. Conformational analysis of D1 dopamine receptor agonists: pharmacophore assessment and receptor mapping. *Journal of medicinal chemistry*, 39, 285-296.
- Naklua, W., Mahesh, K., Aundom, P., Tanmanee, N., Aenukulpong, K., Sutto, S., Chen, Y.Z., Chen, S., Suedee, R., 2015. An imprinted dopamine receptor for discovery of highly potent and selective D3 analogues with neuroprotective effects. *Process Biochemistry*, 50, 1537-1556.
- O'Sullivan, C.K., Guilbault, G.G., 1999. Commercial quartz crystal microbalances-theory and applications. *Biosensors and Bioelectronics*, 14, 663-670.
- Phan, N., Sussitz, H., Lieberzeit, P., 2014. Polymerization parameters influencing the QCM response characteristics of BSA MIP. *Biosensors*, 4, 161-171.
- Ricci, A., Mignini, F., Tomassoni, D., Amenta, F., 2006. Dopamine receptor subtypes in the human pulmonary arterial tree. *Autonomic and Autacoid Pharmacology*, 26, 361-369.
- Risgaard, R., Jensen, M., Jørgensen, M., Bang-Andersen, B., Christoffersen, C.T., Jensen, K.G., Kristensen, J.L., Püschl, A., 2014. Synthesis and SAR study of a novel series of dopamine receptor agonists. *Bioorganic & Medicinal Chemistry*, 22, 381-392.
- Seidler, K., Lieberzeit, P.A., Dickert, F.L., 2009. Application of yeast imprinting in biotechnology and process control. *Analyst*, 134, 361-366.

- Senogles, S.E., Amlaiky, N., Falardeau, P., Caron, M.G., 1988. Purification and characterization of the D2-dopamine receptor from bovine anterior pituitary. *Journal of Biological Chemistry*, 263, 18996-19002.
- Shi, H., Tsai, W.-B., Garrison, M.D., Ferrari, S., Ratner, B.D., 1999. Template-imprinted nanostructured surfaces for protein recognition. *Nature*, 398, 593-597.
- Sontimuang, C., Suedee, R., Canyuk, B., Phadoongsombut, N., Dickert, F.L., 2011. Development of a rubber elongation factor, surface-imprinted polymer-quartz crystal microbalance sensor, for quantitative determination of Hev b1 rubber latex allergens present in natural rubber latex products. *Anal Chim Acta*, 687, 184-192.
- Sun, H., Zhu, L., Yang, H., Qian, W., Guo, L., Zhou, S., Gao, B., Li, Z., Zhou, Y., Jiang, H., Chen, K., Zhen, X., Liu, H., 2013. Asymmetric total synthesis and identification of tetrahydroprotoberberine derivatives as new antipsychotic agents possessing a dopamine D1, D2 and serotonin 5-HT1A multi-action profile. *Bioorganic & Medicinal Chemistry*, 21, 856-868.
- Tan, C.J., Chua, H.G., Ker, K.H., Tong, Y.W., 2008. Preparation of bovine serum albumin surface-imprinted submicrometer particles with magnetic susceptibility through core-shell miniemulsion polymerization. *Analytical Chemistry*, 80, 683-692.
- Wangchareansak, T., Sangma, C., Choowongkamon, K., Dickert, F., Lieberzeit, P., 2011. Surface molecular imprints of WGA lectin as artificial receptors for mass-sensitive binding studies. *Analytical and bioanalytical chemistry*, 400, 2499-2506.
- Worsley, J., Moszczynska, A., Falardeau, P., Kalasinsky, K., Schmunk, G., Guttman, M., Furukawa, Y., Ang, L., Adams V., Reiber G., 2000. Dopamine D1 receptor protein is elevated in nucleus accumbens of human, chronic methamphetamine users. *Molecular psychiatry*, 5, 664-672.

Yola, M.L., Uzun, L., Özalın, N., Denizli, A., 2014. Development of molecular imprinted nanosensor for determination of tobramycin in pharmaceuticals and foods. *Talanta*, 120, 318-324.

Legends

Fig. 1: Schematic synthesis strategy for D1R-MIP and NIP on QCM electrodes.

Fig. 2: Xanthoprotein reaction (A), Rebinding screening via UV-Vis on MIP and NIP (B) and thickness (C) of MIP and NIP materials on gold electrode ($n \geq 3$) as determined by AFM.

Fig. 3: Topographic AFM images of D1R, D1R-MIP and NIP, respectively, on glass slides.

Fig. 4: QCM sensor responses for MIP containing different amounts of D1R in PBS buffer ($n = 3$ for two surface), * D1R, ** D1R+10 $\mu\text{L}/\text{mL}$ stabilizer, and *** D1R+BSA=1:1; the lower part shows the sensor characteristic for D1R on D1R-MIP.

Fig. 5: QCM sensor responses of competitive ligand binding assays based on the D1R-MIP-QCM to, D, Ha, and SCH before incubation with D1R (top) and unbound D1R after incubation with 10% of test compounds (bottom), $n = 3$ and using analysis of variance, ‡ $P < 0.05$ and + $P \geq 0.05$ of the difference between test and D1R.

Fig. 6: QCM response to direct attachment of D1R, followed by exposure to test compounds, D, Ha, and SCH.

Table 1: B_{max} , K_d , and EC_{50} values for test compounds to dopamine D1 receptor from rat hypothalamus using D1R-MIP-QCM and reference value,* dopamine D1 receptor from *Homo sapiens* and + dopamine D1 receptor from *Sus scrofa*.

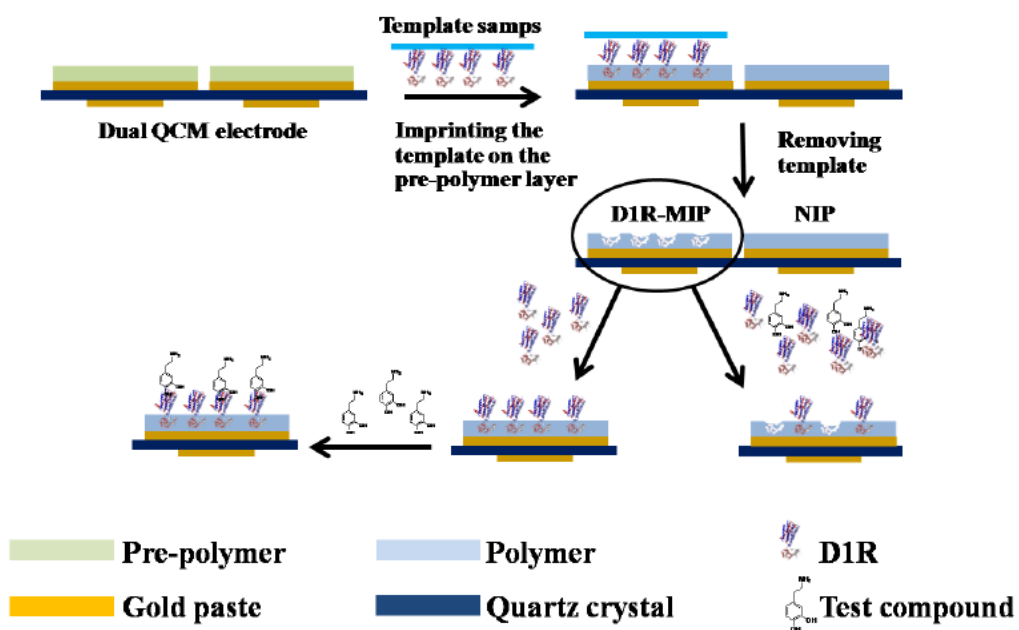


Figure 1: Schematic synthesis strategy for D1R-MIP and NIP on QCM electrodes.

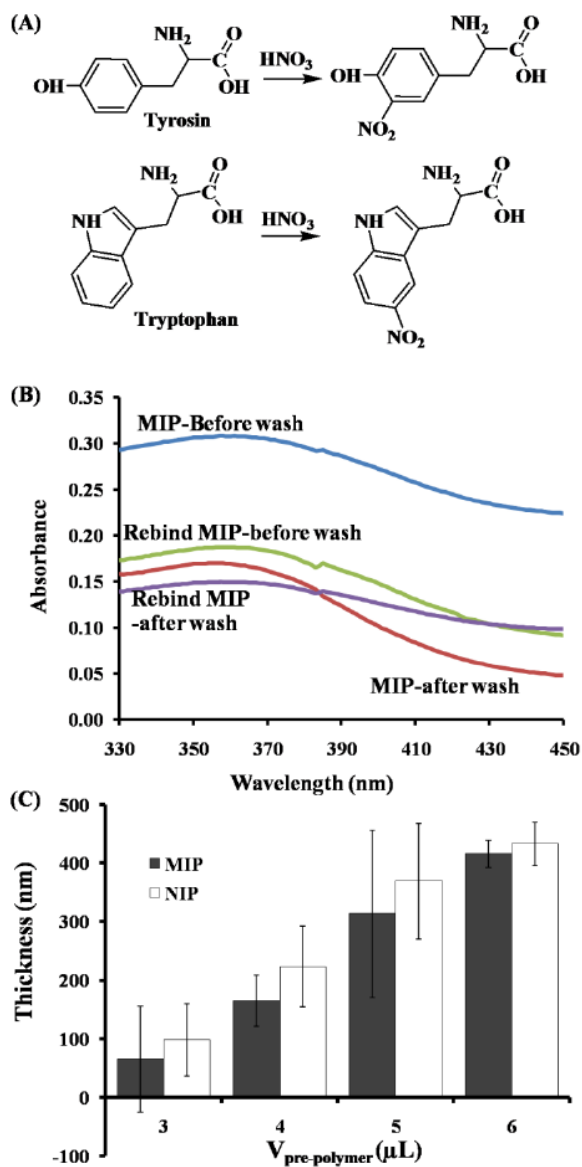


Figure 2 Xanthoprotein reaction (A), Rebinding screening via UV-Vis on MIP and NIP (B) and thickness (C) of MIP and NIP materials on gold electrode ($n \geq 3$) as determined by AFM.

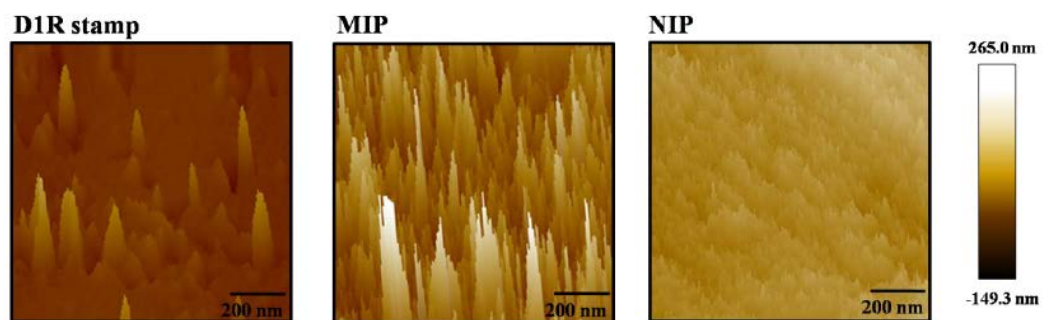


Figure 3: Topographic AFM images of D1R, D1R-MIP and NIP, respectively, on glass slides

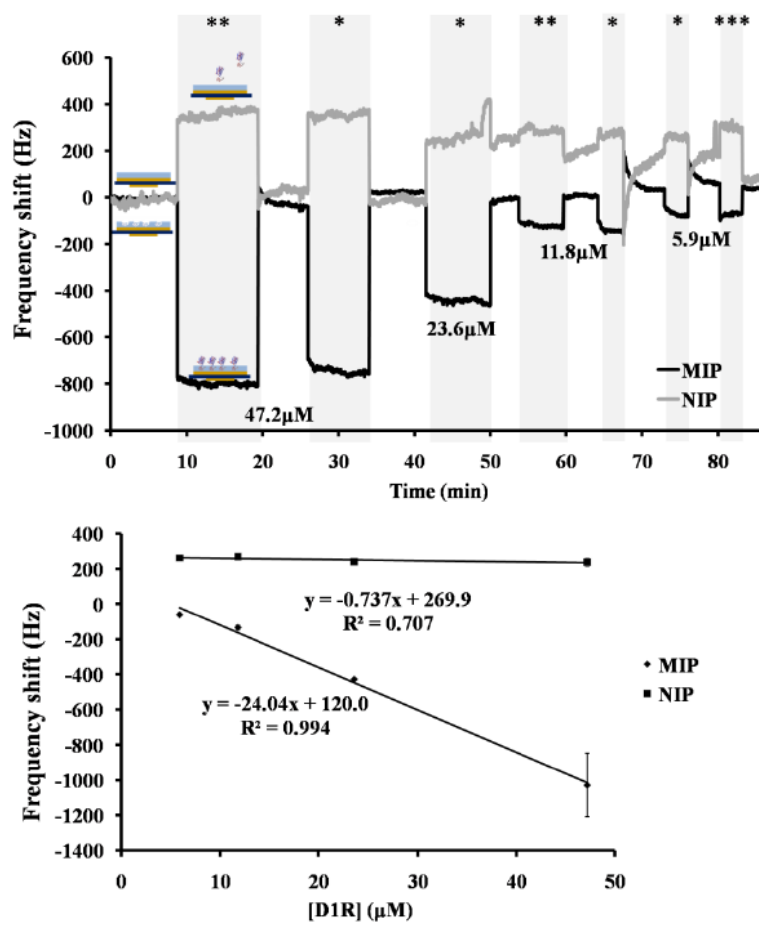


Figure 4: QCM sensor responses for MIP containing different amounts of D1R in PBS buffer ($n = 3$ for two surface), * D1R, ** D1R+10 $\mu\text{L}/\text{mL}$ stabilizer, and *** D1R+BSA=1:1; the lower part shows the sensor characteristic for D1R on D1R-MIP.

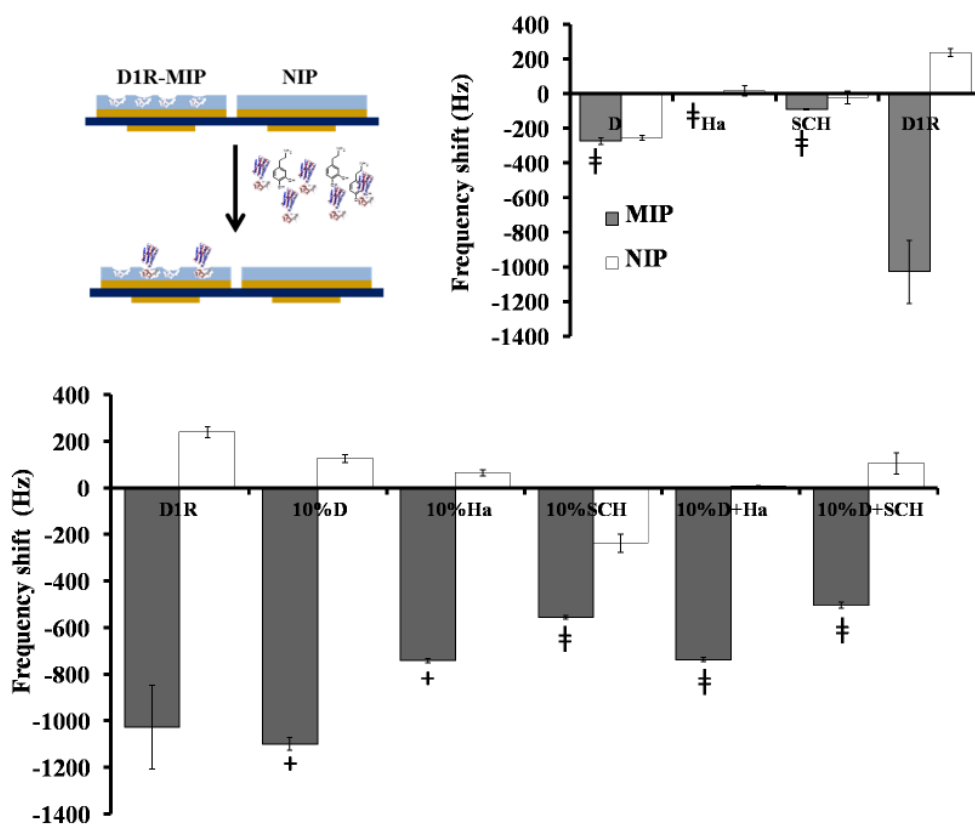


Figure 5: QCM sensor responses of competitive ligand binding assays based on the D1R-MIP-QCM to, D, Ha, and SCH before incubation with D1R (top) and unbound D1R after incubation with 10% of test compounds (bottom), $n = 3$ and using analysis of variance, ‡ $P < 0.05$ and + $P \geq 0.05$ of the difference between test and D1R.

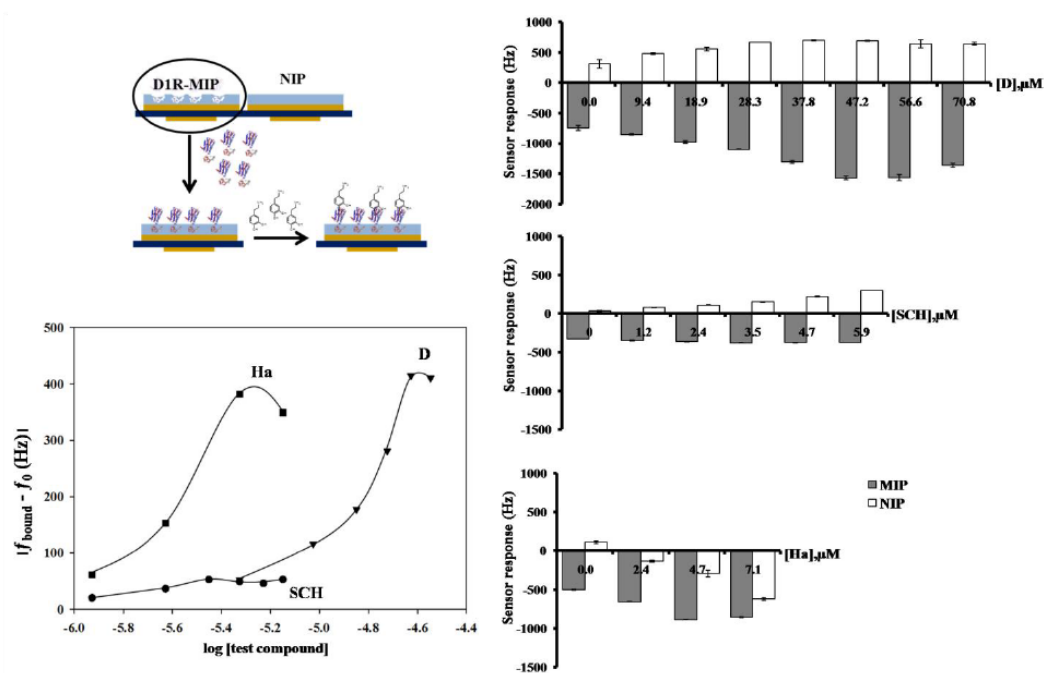


Figure 6 QCM response to direct attachment of D1R, followed by exposure to test compounds, D, Ha, and SCH.

Test compounds	B_{\max}	K_d (nM)	EC_{50} (nM)	IC_{50} or EC_{50} (ref.) (nM)
Dopamine	242	0.874	517×10^{-3}	5000 (Mottola et al., 1996), 39* (Risgaard et al., 2014)
Haloperidol	242	25.7	1904	550 (Iorio et al., 1987), 620 ⁺ (Höfner and Wanner, 2003)
(+)-SCH23390	43.0	0.004	0.283	0.57 (Brewster et al., 1995), 0.60* (Sun et al., 2013)

Table 1: B_{\max} , K_d , and EC_{50} values for test compounds to dopamine D1 receptor from rat hypothalamus using D1R-MIP-QCM and reference value, * dopamine D1 receptor from *Homo sapiens* and + dopamine D1 receptor from *Sus scrofa*.

PROCEEDING 4

Synthesis of the Dopamine Analogs in Molecularly Imprinted Polymer Nanovessel

(Published in *The 2nd Current Drug Development International Conference*)

Synthesis of the dopamine analogs in molecularly imprinted polymer nanovessel

Roongnapa Srichana, Wanpen Naklua

Molecular Recognition Materials Research Unit, Department of Pharmaceutical Chemistry, Faculty of Pharmaceutical Sciences, Prince of Songkla University, Songkla, Thailand.

E-mail address: roongnapa.s@psu.ac.th

Abstract- The purpose of this work was to synthesize the butyrophenone-type ligands in molecularly imprinted polymer (MIP) nanovessel compared among the mould reactions in dual dopamine/serotonin-MIP (DS-MIP) and single template dopamine-MIP (D-MIP) and also the control reactions with nonimprinted polymer (NIP), to study about effect of binding site to the synthesis, by used 1-chloro-(4'-fluorobutyrophenone) reaction with tyramine, benzylamine, phenylethylamine and phenylalanine methyl ester using alkylation of primary amine reaction and characterize dopamine/serotonin receptor ligands by spectroscopic methods. The preparation of MIP was successfully developed to use in this study. The ^1H NMR and m/z together with the data from FT-IR revealed stronger complexation of primary amine and 1-chloro-(4'-fluorobutyrophenone) afforded 4-(4-hydroxyphenethylamino)-1-(4-fluorophenyl)butan-1-one, 4-(2-(6-(4-(4-hydroxyphenethylamino)phenyl)-2*H*-1,2-oxazin-2-yl)ethyl)phenol, 4-(benzylamino)-1-(4-(benzylamino)phenyl)butan-1-one, 1-(4-fluorophenyl)-4-(phenethylamino)-butan-1-one, 4-chloro-1-(4-(phenethylamino)phenyl)butan-1-one and methyl 2-(4-(4-fluorophenyl)-4-oxobutylamino)-3-phenylpropanoate.

Introduction

A number of different approaches in drug discovery and design have been proposed that includes dynamic combinatorial chemistry, stepwise target-guided synthesis and kinetically controlled guided synthesis. Molecular imprinting can be characterized as a synthetic method toward the formation of a polymerizable performed compounds already known to have biological activity [1]. The approach is given by molecularly imprinted polymers via template-guided synthesis in a self-assembly mode they have advantages including easier preparation method and higher physical/chemistry for a wide range of experimental conditions such as pH, temperature and solvent. Only building blocks that adhere to the existing MIP's binding sites react with each other to form bioactivity compounds mimicking the original template that simultaneously access multiple binding sites within the polymer of molecular recognition. These template-guided approaches avoid the classical screening of large compound libraries altogether, and hit identification can be as simple as determining whether a MIP gives combination of building blocks has resulted in a product. The atypical antipsychotic shown to be beneficial for negative symptoms and cognitive function with low extrapyramidal side effects liability has spurred interest of the development of compounds that have high affinity for both dopamine and serotonin receptor. The binding sites of a MIP, are used as molecular-scale reaction vessels to direct the synthesis of multi-acting receptor-targeted compounds [2,3]. In the study, approach with MIP-assisted selective syntheses the imprinted sites consisted of a reactive moiety that could be temporarily linked to a final synthesized compound, leaving the unprotected functional groups to be chemically modified.

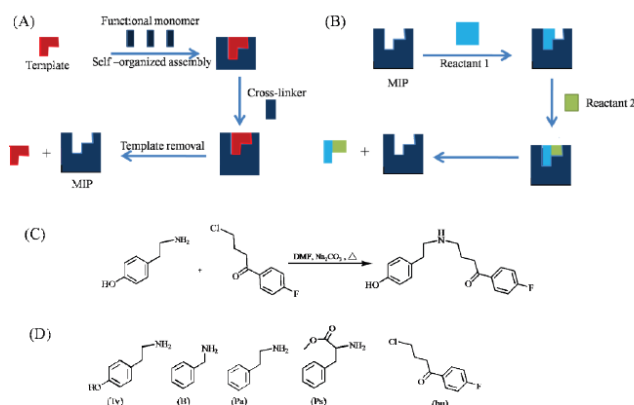
The aim of this work was to synthesize a dopamine/serotonin receptor ligand by use of various amine structures as building blocks similar to dopamine, which is the template for the synthesis of MIP, reaction with 1-chloro-(4'-fluorobutyrophenone) (see Scheme 1). The compounds from the synthesis will have the same or different biological activity from template.

Materials and Methods

1) *Materials:* Dopamine hydrochloride, serotonin hydrochloride, *N,N*-methylenebisacrylamide (MBAA), methacrylic acid (MAA), acrylamide (ACM), 1-chloro-(4'-fluorobutyrophenone), benzylamine, phenylethylamine, tyramine and phenylalanine methyl ester were obtained from the Sigma-Aldrich Chemical Company (Milwaukee, WI, USA). 2,2'-Azobis(isobutyronitrile) (AIBN) was purchased from Janssen Chimica (Geel, Belgium). All solvents were analytical grade and MAA was purified by distillation under reduced pressure before use. IR spectra were obtained by FT-IR spectrometer (Perkin-Elmer system 2000, Perkin-Elmer, Beaconsfield, UK). ^1H NMR spectra were acquired on Fourier Transform NMR 500 MHz spectrometer (Unity Inova, Varian, Germany) and Mass spectra were obtained by using Liquid chromatograph–Mass spectrometer, 2690, LCT, Waters, Micromass, U.K.

2) *Method 1:* The molecularly imprinted polymers (DS-MIP, D-MIP and NIP) were prepared using methacrylic acid (MAA) and acrylamide (ACM) as functional monomers and *N,N*-methylene bisacrylamide (MBAA) as cross-linker, according to the previously described method [4] as shown in Scheme 1(A). Monomeric mixtures dissolved in 80% methanol in water. The mixtures were sonicated to ensure total dissolution of reactants, purged with nitrogen then

sealed and incubated at 60 °C for 24 h. The resultant bulk polymer was ground in a mortar and sieved through a 100 mesh-sieve. The polymers (D-MIP, DS- MIP and NIP) were washed with a mixture of methanol and acetic acid (9:1) on a glass filter and washed with methanol to remove templates from polymer, and finally dried at room temperature.



Scheme 1. (A) Schematic diagram of the preparation of the MIP. (B) Chemical synthesis in molecularly imprinted polymer nanovessel. (C) Typical reaction in the mould reactions (D) Molecular structures of amines used to study the mould reactions.

3) *Method 2*: The butyrophenone-type derivatives were synthesized by the nucleophilic substitution reaction using MIP-nanovessel and amine compounds were dissolved in *N,N*-dimethylformamide (DMF) and incubated at room temperature for 2 h. This solution was added 1-chloro-(4'-fluorobutyrophenone) and Na_2CO_3 . The mixture was kept stirring at 60°C. After 14 h, the suspension was centrifuged at 6000 G for 10 minutes. The polymer particulates were extracted with 0.2%HOAc/MeOH and removed solvent to give the result compound. The synthesis of other substances was prepared in the same way by using different substrates.

Results and discussion

Preparation of MIPs

The MIP material for further synthesis application was successfully produced by imprinting approach. Dopamine and serotonin have a hydroxyl and amine group acts as a hydrogen donor-acceptor interactions with the nitrogen of amine group of ACM and carboxylic acid group of MAA. The template molecules, dopamine and serotonin, forms hydrogen bonds with the amide and amino groups of the templates. The surface morphology of MIP was observed by scanning electron microscopy (SEM) in Figure 1. Imprinted polymers exhibited a rough surface of the particles and the pore diameters were larger than NIP.

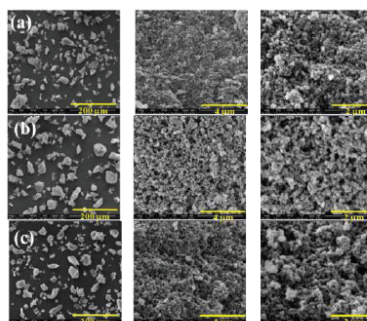
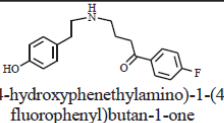
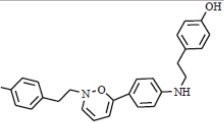
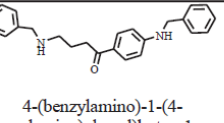
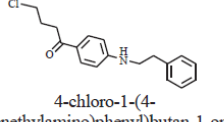
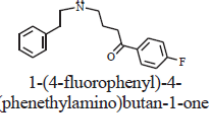
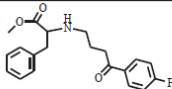


Figure 1. SEM micrograph $\times 300$, $\times 15,000$ and $\times 30,000$ of non-imprinted polymer (a), D-MIP (b) and DS-MIP (c) *Synthesis of dopamine analogs*

The results from chemical synthesis in molecularly imprinted polymer nanovessel were obtained, as all the samples were purified and LC/MS technique with selected ion mass. This analysis extremely easy to perform, allowing crude reaction mixtures to be screened and products to be identified by their molecular weights. After incubating the building blocks 1-chloro-(4'-fluorobutyrophenone) = bu and primary amine (benzylamine=B, phenylethylamine=Pa, tyramine=Ty and phenylalanine methyl ester=Ps), in the in situ screening mode potential hits are identified by looking for significant differences between the chromatograms of the molding reactions. The nucleophilic substitution reaction in D-MIP, DS-MIP and NIP of Ty and Ps with bu by displacing of chlorine atom with amine group but reaction of B, or Pa with bu only in either D-MIP or DS-MIP show attraction of -NH₂ to chlorine atom. However, amine group of the shorter side chain in B appeared to form product by displacing both halogen atoms. Whilst longer phenyl side chain in Pa gave product in the molding reaction by displacing only at chlorine atom, in contrast to coupling of Pa at fluorine group on Bu that was obtained in both the mold reactions and control reaction with NIP. The structure elucidation of synthesized compounds was tested by FT-IR, ¹H-NMR and LC/MS. In the frequency region of 3417-3400 cm⁻¹ (O-H or N-H stretching vibration) 1683-1650 cm⁻¹ was assigned to C=O stretching vibration of ketone in butyrophenone, revealed the presence of one aromatic proton (δ_{H} 6.81- 8.13), methylene proton (δ_{H} 2.00-3.79) and broad peaks of hydroxyl proton or proton of amine. The structure of results was thus assigned in Table 1.

Table 1. Results from chemical synthesis.

Nanovessel	Compound	clogP	ΔG (kJ/mol)	IR(cm ⁻¹)	¹ H-NMR (δ ppm)	m/z
NIP D-MIP DS-MIP	 4-(4-hydroxyphenethylamino)-1-(4-fluorophenyl)butan-1-one	3.19	-73.09	3417, 2481-2823, 1650, 1412, 1348, 1052, 927-653	8.02 (<i>t</i>), 7.09 (<i>t</i>), 7.02 (<i>d</i>), 6.81 (<i>d</i>), 3.79 (<i>t</i>), 3.20 (<i>br</i>), 2.91 (<i>s</i>), 2.85 (<i>s</i>), 2.60 (<i>br</i>), 2.00 (<i>m</i>), 1.30 (<i>s</i>)	301.2 C ₁₈ H ₂₀ FNO ₂
D-MIP	 4-(2-(6-(4-(4-hydroxyphenethylamino)-phenyl)-2H-1,2-oxazin-2-yl)ethyl)phenol	5.49	-	3427, 2935, 1663, 1597, 1560, 1516, 1434, 1490, 1387, 1233, 1155, 1102, 830, 662	-	413.3 C ₂₆ H ₂₆ N ₂ O ₃
D-MIP DS-MIP	 4-(benzylamino)-1-(4-(benzylamino)phenyl)butan-1-one	4.98	528.66	3428, 2934, 1661, 1598, 1459, 1391, 1255, 1158, 1102, 864-560	8.02 (<i>t</i>), 7.09 (<i>t</i>), 7.02 (<i>d</i>), 6.81 (<i>d</i>), 3.79 (<i>t</i>), 3.20 (<i>br</i>), 2.91 (<i>s</i>), 2.85 (<i>s</i>), 2.60 (<i>br</i>), 2.00 (<i>m</i>), 1.30 (<i>s</i>)	358.2 C ₂₄ H ₂₆ N ₂ O
NIP D-MIP DS-MIP	 4-chloro-1-(4-(phenethylamino)phenyl)butan-1-one	4.64	264.41	3406, 1663, 1566, 1410, 1557, 1020, 653	-	301.2 C ₁₈ H ₂₀ ClNO
D-MIP DS-MIP	 1-(4-fluorophenyl)-4-(phenethylamino)butan-1-one	3.86	81.53	3444, 2918, 1667, 1567, 1414, 1231, 1158, 1102, 1053, 1019, 927-666	8.13 (<i>s</i>), 7.33-7.11(<i>m</i>), 5.70 (<i>br</i>), 4.69 (<i>m</i>), 3.74 (<i>t</i>), 3.68 (<i>t</i>), 3.57 (<i>q</i>), 3.48 (<i>q</i>), 3.16 (<i>t</i>), 3.10 (<i>t</i>), 2.96 (<i>s</i>), 2.88 (<i>s</i>), 2.84 (<i>m</i>), 2.24 (<i>m</i>), 2.02 (<i>br</i>)	C ₁₈ H ₂₀ ClNO

Nanovessel	Compound	clogP	ΔG (kJ/mol)	IR(cm^{-1})	$^1\text{H-NMR}$ (δ ppm)	m/z
NIP D-MIP DS-MIP	 methyl 2-(4-(4-fluorophenyl)-4-oxobutylamino)-3-phenylpropanoate	3.60	-214.44	3407, 2924, 2845, 1739, 1683, 1598, 1506, 1409, 1384, 1231, 1156, 1054, 837, 701, 598	8.02 (m), 7.15 (m), 4.84 (br), 3.75 (m), 3.69 (t), 3.45 (br), 3.16 (t), 3.11 (t), 2.96 (s), 2.89 (s), 2.23 (m), 2.08 (br), 2.02 (m), 1.25 (s)	$\text{C}_{20}\text{H}_{22}\text{FNO}_3$

The actual receptor target has been characterized structurally in other a homologous surrogate target has a resolved structure. Accordingly these structures, similar to lead compounds in small molecule design provide templates for drug discovery. Direct moulding leading to a complementary structure of the original molecule can be accomplished utilizing the active site or other preferentially exposed groups of such a molecule. However, the structural constraints imposed by the MIP artificial receptor and the recognition that the ligand itself may induce changes in structure have been elucidated in subsequent investigations of the template.

Acknowledgement

This work was supported by the Thailand Research Fund (ID No. DBG5480006) is gratefully acknowledged.

Reference(s)

- [1] Zhang H, Ye L & Mosbach K (2006) *Journal of Molecular Recognition*, 19: 248-259.
- [2] Mosbach K (2001) *Analytica Chimica Acta*, 435: 3-8.
- [3] Zhang H, Piacham T, Drew M, Patek M, Mosbach K & Ye L (2006) *J. Am. Chem. Soc.*, 128: 4178-4179.
- [4] Suedee R, Seechamnaturakit V, Suksuwan A & Canyuk B (2008) *International Journal of Molecular Sciences*, 9: 2333-2356.

VITAE

Name Miss Wanpen Naklua

Student ID 5410730007

Education Attainment

Degree	Name of Institution	Year of Graduation
Bachelor of Science (Chemistry)	Prince of Songkla University	2004
Master of Science (Organic Chemistry)	Prince of Songkla University	2006

Scholarship Awards during Enrollment

1. Thesis Grant, Education fee and Salary
Strategic Scholarships Fellowships Frontier Research Networks
(Specific for the Southern region)
2. Thesis Grant
The Graduate School, Prince of Songkla University
3. Conference Scholarship
Faculty of Pharmaceutical Science, Prince of Songkla University

Work-Position and Address

Department of Science, Faculty of Science and Technology, Prince of Songkla University (Pattani Campus)

List of Publication and Proceeding

Publication

1. Naklua, W., Mahesh, K., Aundorn, P., Tanmanee, N., Aenukulpong, K., Sutto, S., Chen, Y. Z., Chen, S. and Suedee, R., 2015. An imprinted dopamine receptor for discovery of highly potent and selective D₃ analogues with neuroprotective effects. *Process Biochemistry* 50: 1537-1556.
2. Naklua, W., Mahesh, K., Chen, Y. Z., Chen, S. and Suedee, R., 2016. Molecularly imprinted polymer microprobes for manipulating neurological function by regulating temperature-dependent molecular interactions. *Process Biochemistry* 51: 142-157.
3. Suedee, R., Naklua, W., Laengchokshoi, S., Thepkaue, K., Pathaburee, P. and Nuanplub, M., 2015. Investigation of a self-assembling microgel containing an (*S*)-propranolol molecularly imprinted polymer in a native tissue microenvironment: Part I. Preparation and characterization and Part II. Biological application and testing. *Process Biochemistry* 50: 517-544.

(Remark: This paper is not related to Ph.D. Thesis)

Proceeding

1. Naklua, W. and Suedee, R., 2012. Synthesis of the dopamine analogs in molecularly imprinted polymer nanovessel. The 2nd Current Drug Development International Conference (CDD2012), 2nd - 4th May 2012, Phuket, Thailand.